ALGORITHMS AND PROTOCOLS FOR ENHANCEMENT OF SPECTRUM UTILIZATION IN FUTURE MOBILE NETWORKS

by

PARISHAD KARIMI

A dissertation submitted to the

School of Graduate Studies

Rutgers, The State University of New Jersey

In partial fulfillment of the requirements

For the degree of

Doctor of Philosophy

Graduate Program in Electrical and Computer Engineering

Written under the direction of

Dipankar Raychaudhuri

And approved by

_____

_____

_____

_____

New Brunswick, New Jersey

October, 2019

ABSTRACT OF THE DISSERTATION

Algorithms and Protocols For Enhancement of Spectrum Utilization in Future Mobile Networks

By PARISHAD KARIMI

Dissertation Director:
Dipankar Raychaudhuri

The dramatic growth in mobile Internet services and their diverse requirements motivate the need to significantly improve the design of protocols associated with spectrum use and data transfer over wireless networks. In this thesis, we will examine several algorithms and protocols for improving the spectrum utilization of wireless networks. Specifically, we propose new protocol frameworks and associated algorithms for: (1) multipath routing of data to devices equipped with multiple wireless interfaces such as Wi-Fi and cellular; (2) efficient information-centric multicast over wireless networks; and (3) dynamic spectrum access by wireless networks in both licensed and unlicensed bands. Control and data plane protocol design is examined along with applicable distributed algorithms for each of the above cases, and corresponding performance evaluation results compared with existing solutions are provided. The unifying theme in terms of data transfer protocols is the use of globally unique identifiers derived from a new information centric Internet architecture called MobilityFirst, along with the use of fully distributed algorithms to achieve the desired functionality.

The thesis starts with an investigation of mobile access challenges including device

mobility and multi-interface connectivity and identifies the shortcomings of existing solutions such as transport layer solutions (MPTCP) and dual-connectivity/mobility mechanisms adopted in cellular carriers (5G). To address these challenges, the proposed design uses the concept of named-objects, based on separation of naming and addressing and dynamic binding of connections to identifiers, in the context of a future internet architecture "MobilityFirst". Building on the MobilityFirst architecture, we propose protocols for in-network data splitting based on explicit edge feedback. Detailed performance evaluation of our proposed scheme compared with existing ones is presented using simulations and real-world experiments.

The second chapter presents techniques for extending the usage of named-objects within the cellular network architecture to enable dynamic and efficient wireless multicast while greatly reducing overhead and latency. This novel cross-layer design is important for requirements of emerging services, like large-venue live video streaming applications, autonomous driving assistance and massive IoT. The main idea is to introduce awareness of information centric network (ICN) identifiers at the wireless MAC layer in order to enable efficient multicast services on the wireless channel. To provide a holistic multicast solution, two important aspects are considered: radio resource scheduling and protocol design.

To enable radio resource scheduling, an algorithm for proportional fair resource allocation to a mix of multicast and unicast flows which is deployable in time-slotted systems is proposed. Numerical analysis of the impact of various parameters like total number of UEs/multicast services and grouping of multicast UEs are presented. Finally, comprehensive comparison of ICN multicast with the current wireless multicast standard (eMBMS) is carried out in order to quantify achievable performance gains for the use case of context-based services. The superior performance of ICN multicast in terms of packet delivery time and throughput is illustrated for this use case.

The third chapter considers dynamic spectrum management motivated by the need to share spectrum across the frequency band, including licensed and unlicensed spectrum, more efficiently. We present the case for decentralizing the architecture for dynamic spectrum management as a means to address artificial spectrum scarcity and

overcoming spectrum under-utilization. To this end, we propose SMAP (distributed spectrum management architecture and protocol), which enables coordination of spectrum use among wireless networks and devices through an Internet-based common spectrum control plane. Drawing insight from the success of distributed protocols like BGP in Internet, SMAP facilitates peer exchange of radio usage and control parameters among autonomous wireless network domains. It also provides interfaces to higher level cloud services including spectrum aggregators which facilitate broader cooperation and business relationships between wireless domains in the same area, or to regional spectrum databases such as the SAS (Spectrum Access System). The chapter starts with a technology outline of the architecture, specifying protocols and network entities. Then it establishes three classes of distributed algorithms for optimization of transmission parameters and showcases the feasibility and performance, for a variety of scenarios including coexistence of heterogeneous wireless technologies in the unlicensed band and priority-based spectrum access by bringing all the designed protocols and elements into a single experimental platform on an open-access research testbed. These experimental results are presented to demonstrate significant improvements in system throughput and fairness. We then analyze sample distributed algorithms using large-scale simulations, considering efficiency, scalability, convergence and their adherence to global and local policies.

Acknowledgements

Firstly, I would like to express my gratitude to my PhD adviser, Prof. Dipankar Raychaudhuri, whose patience and encouragement have been my guiding light throughout the years of graduate school. His thought-provoking vision and perseverance have taught me how to tackle research problems in great depth and detail, keeping in mind a path to influence real-world systems and networks. Beyond his technical guidance, I have learned so many life lessons from him and truly aspire to reach his level of patience, compassion, determination, and modesty one day. I am forever thankful for the support of him and his family, Arundhati and Tanika, who have been like a second family for me in the days I really needed it.

I am also thankful to my proposal and thesis committee members, Prof. Roy Yates, Prof. Wade Trappe, Prof. Narayan Mandayam and Dr. Milind Buddhikot, for their guidance and insight and their fruitful suggestions, without which this thesis would not have been complete. I would specifically like to thank Prof. Yates, for all his insightful discussions in MobilityFirst meetings and beyond. Prof. Yates's passion of mathematical problems, while finding their relevance to real-world systems has been a constant inspiration to me. I am grateful to Prof. Trappe, for his unique attitude towards research that goes beyond equations and experiments, and teaches you to examine things from different angles. I would also like to thank Prof. Mandayam, for his mentorship and his great knowledge of wireless technologies which fueled my interest in wireless systems research. Finally, I would like to express my gratitude to Dr. Buddhikot, whose contributions to dynamic spectrum sharing field have paved the way for the research work in this thesis.

Next I would like to thank my collaborators who played a significant role in shaping the research work in this thesis: Prof. William Lehr's guidance on policy aspects of

spectrum sharing and Dr. Ravishankar Ravindran's thorough knowledge of real-wold cellular systems. I would also like to acknowledge the support provided by the Rutgers University staff, the staff at WINLAB, and Department of Electrical and Computer Engineering.

Ivan Seskar deserves a special mention in every WINLAB thesis, and mine is not an exception. The depth of his technical knowledge of wireless systems and networks, from theory to real-world implementation is outstanding. His door is always open, whether you have a question on LTE Wi-Fi coexistence, a bug in some software or you want to see marvelous photos of hummingbirds he had recently taken.

Spending the past 6 years in WINLAB could not have been as much fun without my great lab mates, Shreyasee, Mohammad, Shubham, Francesco, Dragoslav, Shalini and Ali. I feel blessed for our friendships and hope to cross paths with you in future.

I am grateful for my support system, my best friends, Elham, Minoo and Shamim. They were always next to me in all the ups and downs and encouraged me to be my best self.

Finally, I have to thank my amazing family, without whom I would never be where I am today. My mum who is my role model in life with her selflessness, fearlessness and strive for science, learning and adventures; my dad with his perseverance, patience and supportiveness and my siblings, Pegah and Parsa, with their endless encouragement and love.

Dedication

To my parents, for their unconditional love and support.

Table of Contents

List of Tables

List of Figures

Chapter 1

Introduction

There has been dramatic growth in mobile data usage due to proliferation of data-intensive applications like video streaming[1], improved capabilities in devices and increasingly ubiquitous mobile Internet access, and the trend does not seem to diminish soon [2]. According to recent Ericsson mobility report [3], the total mobile traffic will grow by a factor of 5, reaching 136EB/month by the end of 2024, a quarter of which will be carried by new generation of cellular networks. To support this large amount of mobile data, spectrum has to be utilized more efficiently by both the access network providers and end-to-end Internet services. Advancements in physical layer technologies such as 5G-NR [4] and 802.11ax [5], new end-to-end transport and application layer protocols like MPTCP [6] and QUIC [7], and opening up new spectrum bands for multi-technology usage (such as LTE and 5G in unlicensed band[8] and CBRS band [9]) are some of the main proposed solutions.

Efficient data delivery mechanisms will play an important role to fully utilize the wireless capacity provided by new wireless technologies. Two such mechanisms which we focus on are: (i) stitching the capacity of multiple wireless networks through multi-interface connectivity for mobile devices (multihoming) and (ii) simultaneous data transmission to various groups of end-devices (mobile users or IoT devices) on the same radio time and frequency resources, i.e. wireless multicast/broadcast. Multihoming is currently achieved by either transport and application layer protocols or new features added to cellular networks protocols (i.e. dual connectivity [10] and carrier

[1] "Globally, IP video traffic will be 82 percent of all IP traffic (both business and consumer) by 2022, up from 75 percent in 2017" from Cisco VNI [1]

aggregation [11]). Furthermore, cellular multicast has been deployed by means of eMBMS (evolved Multimedia Broadcast Multicast Service) [12], which requires addition of new specialized coordination entities and gateway to the cellular architecture.

In addition, opening up of new frequency bands to mobile operators for licensed or shared use with other incumbent wireless technologies poses spectrum management and coexistence challenges. The current generation of wireless technologies is being designed to incorporate local adaptive mechanisms to address some of these challenges , e.g. LTE/NR-LAA [13] (Licensed-Assisted Access which is based on anchoring the unlicensed link to a licensed one, allowing discontinuous transmission on the unlicensed link), LTE/NR-U [14] (which operates based on incorporating backoff mechanisms, like listen-before-talk, similar to 802.11 CSMA to unlicensed LTE/NR), Multifire [15] (used for stand-alone small cell deployments). However, the mere adoption of these mechanisms on sensing and back-off do not necessarily make efficient use of the newly-opened scarce spectrum. On the other hand, the conventional centralized approach to data-driven spectrum management is exemplified by the Spectrum Access System (SAS) [16] being developed for a new regulatory regime in the 3.5 GHz CBRS band. While the potential benefit of coordinated spectrum allocation can be significant, there are several intrinsic disadvantages to the centralized architecture for a large-scale service of this nature. A centralized approach is inconsistent with the policy goal of transitioning toward greater reliance on market-based spectrum management, suffers from scalability issues and presents a single point of failure.

In summary, efficient data delivery and spectrum management in today's networks are being addressed by incremental addition of new specialized protocols and entities in the access network (5G) or addition of more functionality to end-to-end transport/application layers. While these are crucial to serving the growing volume of mobile data traffic and its bandwidth/latency requirements, they are not sufficient to achieve the required performance of future mobile Internet services. It is thus timely to fundamentally rethink and redesign spectrum-efficient data delivery mechanisms to mobile end-devices, founded on principles such as distributed and autonomous control of radio resources, name-based communication and information-centric networking explored in

this thesis.

1.1 Organization of the thesis

The next chapter starts with network architecture requirements for efficient data delivery using network-assisted multihoming for connectivity to multiple cellular networks. The name-based network architecture which will fulfill these requirements along with the specific protocol design for multihoming are presented. In-network data splitting algorithms are then discussed and a cross-layer feedback mechanism is implemented to provide last hop cellular link quality to routers along the path. The proposed multihoming solution is compared with end-to-end multipath TCP using simulation with real-world traces and experiments on the ORBIT testbed. The results demonstrate the superior performance of network-assisted multihoming compared with multipath TCP both in terms of throughput and latency.

In chapter 3, building upon the name-based network architecture presented in chapter 2, a cellular multicast framework is proposed which enables low-overhead and dynamic multicast transmission of data to devices subscribing to popular content and services. In this architecture, content/service identifiers are utilized at the MAC layer to provide native scheduling of multicast radio resources for the subscribed UEs (referred to as "I-MAC"). This will alleviate the need for specialized core network entities as is proposed in eMBMS. Proportional fair radio resource allocation problem for multiplexed unicast and multicast flows is presented. The formulation is applicable to both I-MAC and an operation mode of eMBMS, namely Single-Cell Point to Multipoint (SC-PTM). To solve it, a per-TTI resource scheduling algorithm is proposed. Finally, considering the use case of context-based services, the performance of I-MAC is compared with existing cellular solutions like SC-PTM. Through packet-level simulation, we demonstrate better performance of I-MAC compared to SC-PTM, mainly in terms of latency and throughput.

Chapter 4 considers the distributed spectrum management challenge with the goal

of achieving high spectral efficiency and robustness without the need for central control. Specifically, we propose the concept of a *wireless domain*, which represents an autonomous network covering a given geographic area and encompassing a number of operating radio devices (base stations, access points, etc). The computation of operating radio parameters within a wireless domain is delegated to the domain's controller. We present a distributed control plane among the wireless domain controllers which facilitates exchange of radio and policy information within the connectivity graph of controllers. We then discuss a number of distributed algorithms which are enabled by SMAP's control plane, and evaluate their performance by conducting proof-of-concept experiments on the ORBIT testbed. To conclude, we conduct large-scale simulations, evaluating various properties of the algorithms like convergence, scalability and adherence to policy.

Chapter 2

Network-Assisted Multihoming

2.1 Introduction

Data delivery to a mobile device through multiple wireless access networks (device multihoming) is motivated by the fact that in contrast to wired networks, a wireless network client can see not just one, but a multiplicity of access networks (perhaps as many as 20-30 in urban areas) using various radio standards including 4G/5G cellular and Wi-Fi [17]. While the wireless medium suffers from various disadvantages in signal quality relative to wired media, the ability to access multiple networks in parallel is an important advantage that should be exploited in the design of future mobile data services. It is interesting to note that parallelization of constrained resources is an important architectural option for evolution of various information technology areas, including processors, storage and cloud computing and there is good reason to believe that the same will be true for wireless networks.

The current generation of mobile phones is usually equipped with both cellular (4G/5G) and Wi-Fi radios, motivating recent work on multi-homing in heterogeneous macro-cell/microcell environments [18, 19]. Google Project Fi [20] is an example of a commercial mobile virtual network operator by Google which adaptively switches between Wi-Fi and multiple cellular carriers for economic and performance improvement purposes. Moreover, dual connectivity of the phone to different base stations operating on different radio technologies has been proposed as initial phase for deployment of 5G (non-stand alone access)[10]. More recently, two major mobile phone vendors, Apple and Samsung, have announced plans for a universal SIM card which is capable of connecting to multiple networks [21, 22]. As the cost/performance of radio hardware continues to improve, it will become increasingly feasible to equip a consumer device

with multiple cellular radios, enabling users to potentially double or triple their bit-rate by using 2-3 cellular networks and available Wi-Fi networks in parallel.

Existing services such as Project Fi and dual-connectivity within one cellular carrier provide some performance gains over conventional cellular network services, but the advantage is limited by the use of a single cellular network at a time (in the case of Project Fi) and the lack of multi-homing support in legacy TCP/IP protocols. Moreover, poor interaction of the end-to-end transport layer protocols like TCP with highly varying cellular channels is a well-known problem [23], due to the inability of TCP's congestion control to adapt to rapid changes in available bandwidth. Multipath TCP (MPTCP) is an extension to TCP which supports striping of data from a single TCP connection across multiple subflows. The various proposals which have been made for congestion control in MPTCP [24] share the same weakness as TCP's congestion control when it comes to agile reactive adjustments of transmission rate to wireless link quality.

In this chapter, we investigate the limitations of the two extremes of end-to-end protocols to dual-connectivity within a single carrier solutions for simultaneous multi-network connectivity of mobile devices. Then we propose a network-assisted multi-homed data delivery service "Network-Assisted MultiHoming" (NAMH). The main contributions of this work are as follows:

- Discussing the fundamental design choices required for network assisted multi-homing that will support simultaneous multi-interface connectivity.
- Designing an end-to-end network-assisted protocol optimized for accessing multiple cellular networks, which leverages cross-layer feedback (radio-link signaling between UE and eNodeB) to perform efficient data splitting.
- Emulating real-world measurements of two commercial cellular carriers to evaluate the performance gains of multihoming and comparing the results with existing solutions like Multipath TCP (MPTCP) using both simulation and testbed experiments.
- Qualitative discussion on deployment of multihoming within a flat mobile core compared with existing cellular architecture.

2.2 Network-Assisted Multihoming in Cellular Networks

In this section we will investigate enabling parallel cellular data transmissions to a single mobile device. With the proliferation of prepaid mobile data bundles from various cellular operators, it will become possible for end-users to boost service quality by blending data across multiple paths, and multiple access technologies. Of course, this is not a common model today mainly due to business model reasons rather than technical limitations of mobile phones, but we do believe that harnessing multiple cellular networks for improved performance will become increasingly feasible in the near future. In fact, a number of recent projects have explored the gains achieved through multi-cellular access in real-world highly mobile scenarios (high speed rails) [25] and considering policy constraints [26].

Similarly, the architecture we consider is based on multi-radio clients each with two or more cellular (LTE) interfaces. The differentiating point in our work compared to the previous projects is how the task of splitting the data flow towards multiple interfaces is handled by network elements such as base stations and routers, removing the need for multi-path scheduling and congestion control at end-points as in MPTCP. In this architecture, network elements cooperate to find a suitable branching point for the data flow to be split towards the two cellular network interfaces. Further, the branching router and base stations will utilize information on radio link quality to determine the right ratio of traffic to be sent along each path. The notion of *network-assisted multi-path delivery* in our work has many advantages compared with approaches which delegate the task of scheduling and splitting the flows to the end hosts [19, 27–29]. The advantages stem from having more fine-grained control over network resources, complete information regarding routing path quality and load conditions, and more adaptive response to congestion/loss. An overview of building blocks of network architecture for existing end-to-end and single carrier solutions compared to proposed NAMH is shown in Fig.2.1.

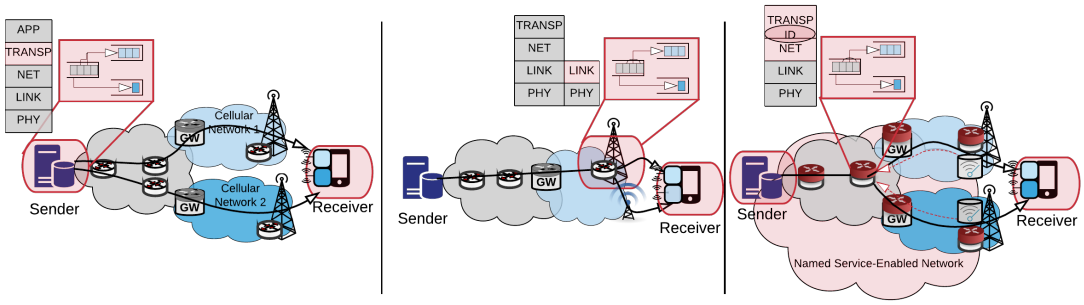

Figure 2.1: Overview of device multihoming solutions: *left:* end-to-end transport protocol; *middle:* edge dual-connectivity in next generation cellular networks; *right:* network-assisted multihoming

2.2.1 System Design

In this section the design of a reliable, multi-homed (NAMH) data delivery mechanism for future cellular networks is discussed. To present a complete solution, the proposed design should cover required functionalities both in the *core network* and the *access network*, which are explained in the following subsections along with the design principles addressing them.

Network Architecture Requirements

The main functionalities of the core network for the delivery of packets from a server to a host with multiple interfaces are as follows: Firstly, the server should be able to detect the existence of multiple interfaces bound to a single host. Secondly, multi-homing requires protocol support to identify the bifurcation point which will conduct the flow splitting mechanism to schedule the packets along the various paths based on some path quality criteria. In the following paragraphs, we discuss how our core network design handles these issues.

1. **Naming:** The TCP/IP design is not capable of addressing the naming issues which rise with multi-homing. By assigning an IP address to a device, the connection is bound to that IP address which is overloaded to both represent the identification and addressing of the device. Currently deployed multihoming protocols like MPTCP suggest detours to avoid problems caused by combining the

roles of names and addresses. For example, in MPTCP the endpoints should inform one another about their MPTCP-capability in the 3-way handshake process using the options field of TCP [30]. The solution we adopted in our design is to alleviate the connection from being bound to source and destinattion $< IP\ Address, Port\ Number >$ tuple through unique identifier assignment to objects. The network addresses are then dynamically bound to the objects' points of connection to the network.

2. **Bifurcation router:** We believe that future mobile networks should consist of more capable in-network elements which can be programmed to perform more complex tasks than just simple forwarding of packets, like data splitting to various routes or bitrate monitoring of bottlenecks (wireless edge) links. This can be achieved as follows: A router is identified as a bifurcation point when it receives a packet destined to a host with multiple network addresses, and detects different next-hops for each network address. This bifurcation router can then enforce reliability and congestion control for multiple subflows belonging to a single data stream instead of end hosts.

3. **Data Splitting:** Existing end-to-end data splitting mechanisms like the one adopted in MPTCP tend to underutilize scarce wireless bandwidth due to their end-to-end nature, which results in out-dated visibility of the network conditions and inability to differentiate between packet losses and in-network congestion. The bifurcation router will request wireless link quality from either the associated edge routers at the base stations or an aggregated controller (in case of SDN cellular network architecture) and then schedule the sub-flows towards multiple interfaces accordingly. This process is explained in detail in the next section.

Realization of Cellular Multihoming in MobilityFirst

The above-mentioned requirements can be supported in networks in various ways. Extensions to current protocols such as IP or setting up overlay protocols through network entities like proxies are examples of backward-compatible solutions. It is also possible to

integrate functions like naming and multi-path support into clean-slate protocols now being considered in various future Internet architecture projects. Some of the proposed FIA proposals such as "MobilityFirst"[31] (MF) support the concept of name-address separation and are thus suitable frameworks for building network-assisted multihoming services under consideration here. Hence in this study, we adopt the MobilityFirst principles due to its native support of aforementioned features as follows:

1. **Naming:** In MobilityFirst, each host is assigned a long-lasting public-key based flat globally unique identifiers (GUIDs) and short-lasting network addresses (NA) depending on the points of connection of the host to the network. The entity which provides the mapping between GUID and NAs is the Global Name Resolution Service (GNRS) that gets updated by hosts regarding current network addresses. The host can inject an optional service identifier (SID) in the GNRS update (similar to ToS in IP header), which expresses the host's policy preferences, for example stripe across all available cellular links.

2. **Bifurcation router:** After the data packets destined to a multihomed device get resolved through GNRS to multiple network addresses corresponding to device's multiple cellular interfaces, those network addresses will be inserted to the packet's routing header by the edge router. The routers detecting multiple network addresses in a packet header perform routing algorithms to find the next hop. MobilityFirst's intra-domain routing is handled by Generalized Storage Aware Routing protocol (GSTAR)[32], which takes care of neighbor discovery, link quality estimation and link- and storage-state dissemination. The router which finds different next hops for the network addresses, will be the designated router acting as a proxy in charge of scheduling different subflows and maintaining reliability on different paths. Since the routes towards multiple cellular interfaces of a device might diverge and converge at multiple points in the network, only the last bifurcation router can be considered. Having GSTAR in place, the MobilityFirst's control path can potentially comprise of multiple independent protocol

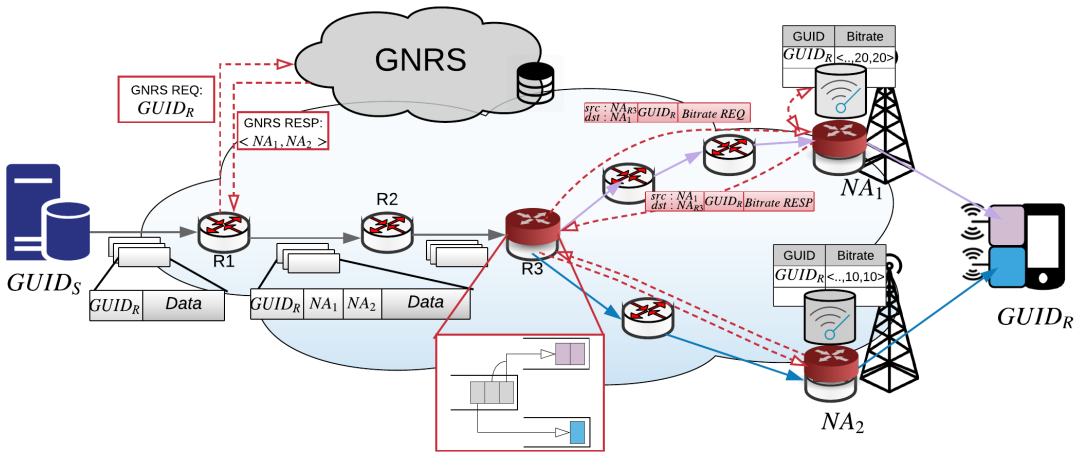

Figure 2.2: Overview of network-assisted multihoming in MobilityFirst using path quality metric for data splitting

implementations, complementing forwarding decisions made by GSTAR. We propose enhancements to routing logic of bifurcation router by adding an explicit link quality feedback from the edge wireless routers.

3. **Data Splitting:** The Hop protocol in MobilityFirst [33] provides hop-by-hop reliable data transfer and has been shown effective in previous multihoming studies when incorporating an ack-withholding backpressure mechanism for hop-by-hop congestion control [18]. Moreover the GSTAR routing protocol in MobilityFirst provides link quality measurements (short-term and long-term estimated transmission time) through link state announcements. In addition to these link quality measurements which can be used by the bifurcation router for data splitting, we extend routing at the bifurcation router to take into account wireless link quality measurements for data splitting. This is achieved by running a bitrate provision service at the edge routers (collocated with base stations). More details on protocol design is outlined in the following section.

2.2.2 Protocol Building Blocks

In this section we describe all the necessary protocol components for network-assisted multi-carrier cellular data transmission.

Bitrate Provision Service

In this section we introduce a cross-layer mechanism and the suitable metrics that leverage the radio layer information denoting the cellular link quality for in-network data splitting. Based on the radio signaling standards defined for high-speed cellular networks using LTE and 5G technologies [34], each User Equipment (UE) periodically observes and quantifies the downlink channel conditions and sends channel condition indicator (CQI) feedback to the Evolved Node B (eNB). After receiving these control messages, the eNB decides which UEs it will serve and how to divide the Physical Downlink Shared Channel (PDSCH) between the UEs. The data is carried in form of transport blocks which are passed to the physical layer from MAC layer every Transmission Time Interval (TTI). The transport block size (TBS) is the metric we will exploit to directly obtain the available bandwidth to the UE instead of passively inferring it through reactive approaches. This metric is suitable because it takes into account the MCS index (modulation and coding index which is based on the CQI reported by the UE) and number of resource blocks assigned to the UE (based on the load conditions). The bitrate service which runs on top of routing layer has an interface to the eNB's MAC scheduler, mapping UEs' MAC addresses to their GUIDs using the association table for the edge router and stores the GUID to TBS mapping in the bitrate cache.

In-Network Data Scheduling

Having the necessary core and access network functionalities in place, we aim to design a lightweight protocol which leverages the cross-layer cooperation of the routing layer and last-hop radio layer. The main active components in addition to legacy Mobility-First entities (GNRS, core and edge router) are the MF-enabled eNBs, the bifurcation router and the multi-homed UE as shown in Fig.2.2. Once a router identifies itself to be a bifurcation router (router R3 in Fig.2.2) as described earlier, it will initiate a control message requesting wireless link quality information from the corresponding edge routers (at NA1 and NA2). This can also be deployed as a subscription service, where the edge routers' link quality report will be automatic. Prior to the receipt of the

response the router will perform round-robin scheduling of the packets. On receipt of the request message, the edge router consults the bitrate cache and sends link quality response for receiver's GUID ($GUID_R$).

As mentioned before, Hop protocol in MobilityFirst utilizes a back-pressure mechanism to perform hop-by-hop congestion control. Upon transmission of a chunk, the router would send a *CSYNC* to its downstream router which will trigger a *CSYNC ACK* with a bitmap of packets received within the chunk from it. The backpressure mechanism works as follows: the downstream router will retain from sending *CSYNC ACK* to its upstream router if the corresponding flow's queue exceeds a value H. This procedure has been shown effective to throttle the rate to the bottleneck along each path from the bifurcation point in previous work [18].

Low values for H will result in under-utilization of the resources by leaving routers along each path idle waiting for upstream routers when sporadic transmission opportunities at the edge become available. On the other hand, large values for H might result in unnecessary buffering of data on the routers along the path and as a result long reaction times to highly varying wireless link quality. Despite the crucial role the value of H plays in the performance of the data splitting, it has been chosen to be static upon configuration in previous projects [18, 33]. In this work, we eliminate the need for this arbitrary threshold, and set it to be a variable just depending on the buffer size and queue management policy on the router, e.g. max-min fair share queuing. Instead, the bifurcation router will maintain reliability and congestion control to the edge routers as follows.

After receiving the cellular link quality for each path (R_i), the bifurcation router will schedule packets to subflows in a weighted round robin fashion to minimize reordering overhead at the receiver buffer, with the ratio of R_is determining the scheduling weights. In order to set bounds on the number of sent and not acknowledged (by the last hop routers) bytes for each subflow, the bifurcation router will set a threshold for the Transmission Window for each subflow (TW_i). By setting this threshold relative to the

product of RTT[1] and R_i for each path, TW_i is guaranteed to be large enough to avoid under-utilization of costly and scarce LTE network resources, and yet small enough not to overfill the buffers at base stations and cause bufferbloat-like [35] congestion in the network. If TW_i exceeds the threshold corresponding to its subflow, the transmission will be halted until the TW_i falls behind the continuously updating threshold. This will happen when either (i) new data gets acknowledge or (ii) the wireless link quality improves.

2.2.3 Simulation Model & Evaluation

After discussing the key design elements, we now implement the proposed network-assisted multihoming using discrete event simulator ns-3 [36] in conjunction with LENA LTE module [37]. This module incorporates necessary components including LTE radio protocol stack and EPC interfaces, entities and protocols (some modifications on these models were required to support multihoming). In order to conduct a comprehensive comparison between NAMH and MPTCP, Direct Code Execution (DCE) [38] was used, which enables ns-3 to execute the Linux kernel space implementation of MPTCP (stable release of the MPTCP Kernel implementation version v0.9). The parameters used in the LTE model for both cases are summarized in Fig.2.3(a). In the rest of the paper the other parameters are set to default, the buffers are set to be very large (including the send and receive socket memory for TCP) to make sure the performance is not limited by the lack of sufficient memory.

Bandwidth Estimation Algorithm

Due to rapid fluctuations of the radio link quality over milliseconds (small-scale fading) and larger variations in LTE signal strength over seconds (large-scale fading), an adaptive bandwidth estimation algorithm is needed. Resource allocation at the eNBs is done on millisecond basis, but due to small scale fading specially in mobile scenarios, it

[1]measured from ACKs, estimated similar to TCP RTT calculation

Parameter	Value
DL & UL Resource Blocks	50 & 25
DL & UL Tx Power(dBm)	30 & 10
MAC scheduler	Proportional Fair
RLC Type	Unacknowledged mode
TCP Version	Cubic

(a) Simulation details.

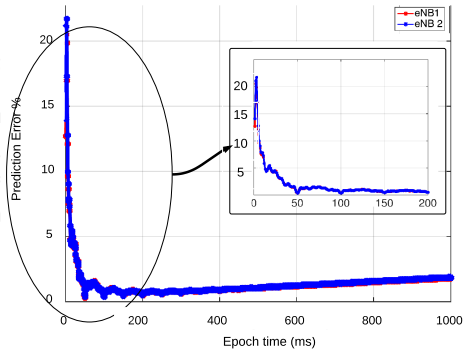

(b) Tuning epoch interval

Figure 2.3: Simulation Parameters

is both unnecessary and high overhead inducing to report the rate values every millisecond. In order to examine the effect of this epoch interval, we run a simple simulation with the setup depicted in Fig. 2.4(a). Moreover, ns-3's built-in "log-distance" path-loss model and pre-calculated trace-driven fading model have been used. By sweeping the value of the epoch interval through the window [0-1000] milliseconds, the prediction error is measured. As can be seen from Fig.2.3(b), the error is minimum, when the epoch interval is set to be around 50 ms. We use this in the rest of our simulations. This parameter depends highly on the mobility of the UE, channel conditions, the delay between the eNodeB and the scheduling router, etc. The base stations can perform some analysis like the following to obtain an adaptive value for the epoch time. Each base station keeps a queue for the packets destined to each UE. The length of this queue at each time step T_0 for interface i on the UE ($Q_i(T_0)$) is determined by

$$Q_i(T_0) = Q_i(T_0 - T_i) + \overline{R}_i(T_0) \times T_i - \overline{B}_i(T_0) \times T_i \tag{2.1}$$

where $\overline{R}_i(T_0)$ is the average incoming rate to the base station's queue i, $\overline{B}_i(T_0)$ is the average outgoing rate of queue i and T_i is the epoch interval. Depending on the delay from the eNB to the router (queueing and processing delay in EPC components like PGW, SGW and MME) $\overline{R}_i(T_0)$ is related to previous $\overline{B}_i(T_j)$. Equation 2.1 can be rewritten as

$$\frac{Q_i(T_0) - Q_i(T_0 - T_i)}{T_i} = \overline{B}_i(T_j) - \overline{B}_i(T_0) \tag{2.2}$$

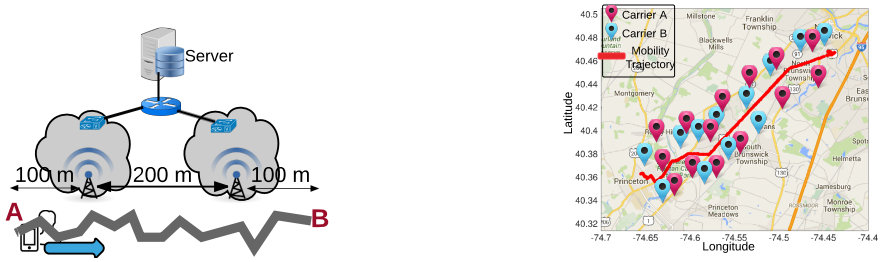

(a) UE moves according to a random way-point mobility model. The UE is connected to both cellular networks.

(b) Mobility trajectory along which the RSSI measurements were made with arbitrary base-station distribution

Figure 2.4: Mobility Scenarios

The aim is to keep the length of the queue bounded for each UE at the base station (after the connection becomes stable). This will avoid overflowing the large buffers at LTE base stations, which are believed to cause large packet delays [35]. By taking periodic samples of the queue size and computing the queue occupancy rate (left side of Eq. 2.2), and given the RTT from the router to the base station and average bandwidth available (right side of Eq. 2.2), T_i can be chosen to maintain the balance between queue occupancy rate, and available bandwidth.

Baseline Evaluation

The baseline scenario in Fig. 2.4(a), provides us with a benchmark to evaluate our proposed network-assisted multihoming scheme. To evaluate the performance of network-assisted multihoming in comparison with MPTCP in terms of throughput and latency, we investigate the infinite backlog file transfer during which a huge file is retrieved in the rest of the paper (unless stated otherwise). The results are depicted in Fig.2.5. By comparing the NAMH and MPTCP throughput curves from Fig.2.5, it is observed that NAMH utilizes the channel capacity more efficiently. By defining a parameter called *bandwidth underutilization %* as

$$U(i) = \frac{|C(i) - T(i)|}{C(i)} \tag{2.3}$$

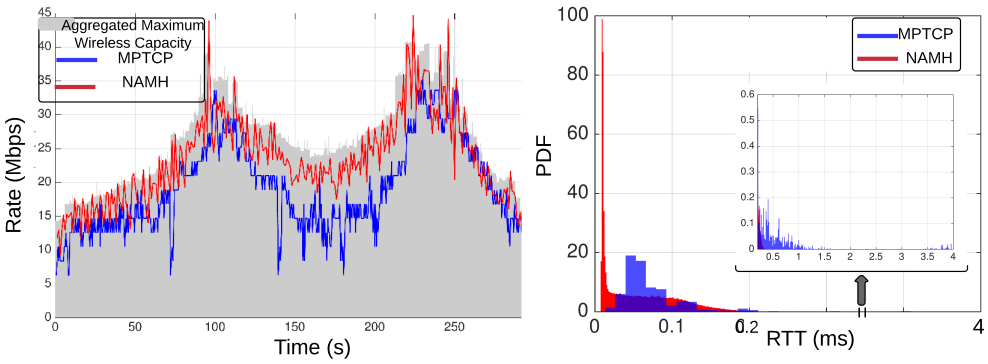

Figure 2.5: Baseline scenario throughput and RTT evaluation

where $C(i)$ is the maximum channel capacity and $T(i)$ is the achieved throughput. MPTCP underutilizes the resources by 30% on average whereas NAMH's underutilization is 9%. It should be taken into account that MPTCP's underutilization problem exacerbates with increase in the number of end-to-end hops, and hence the end-to-end delay (investigated in subsection 2.2.3). In order to evaluate the round-trip time (RTT), the PDF of RTTs experienced by packets are demonstrated in Fig.2.5. Unlike MPTCP which fills up the buffers in the network and will back-off only after congestion, the per-subflow bound on the congestion windows in our method will ensure smooth delivery of packets. Evidently, from Fig.2.5 we can see that the NAMH RTTs are bounded, whereas MPTCP RTTs have a long-tailed distribution with values up to 4000 ms. These values will contribute to undesirable conditions like bufferbloat, poor quality of experience, etc.

Best interface vs. Multi interface: Another method of multi-interface connectivity which is already in use by projects like Google Fi [20] or iCellular [27] is to utilize only the best interface at any time. This is a reasonable first step to make use of multiple available networks within the current structure of mobile and IP networks. In order to examine the gains achieved through best-interface selection, a simulation using baseline setup has been conducted and the results are compared with MPTCP and NAMH. In the simulation, selecting the interface is done based on the achievable rates reported by eNodeBs. Throughput and latency results (95-th percentile) are presented in Fig. 2.6. In terms of throughput, it can be seen that choosing the best interface is

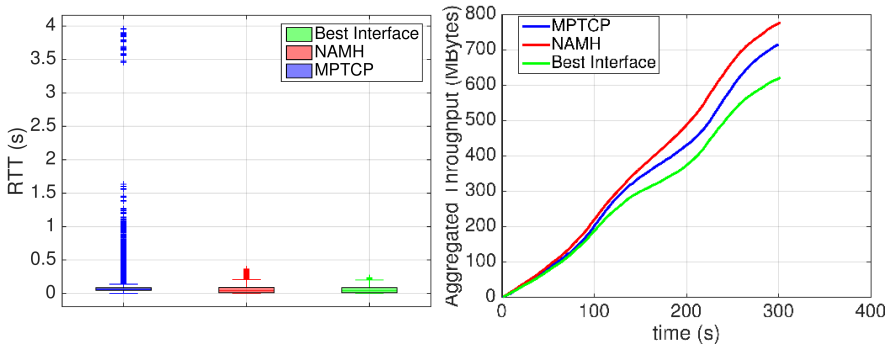

Figure 2.6: Baseline scenario, Best-interface vs. Multi-interface

at a level similar to multi-path TCP in performance. Moreover, from the RTT plot it can be seen that similar to NAMH behavior, best-interface also has bounded RTT. The median of RTT for MPTCP is around 60 ms, whereas for NAMH and best interface it is around 40 ms. Although MPTCP has comparable median RTT to NAMH, the 5-percentile very large RTTs can significantly degrade the quality of data connection.

Trace-Driven Evaluation

In this section, the goal is to evaluate the throughput and delay characteristics of NAMH in comparison with MPTCP based on real world measurements.

Data collection: We developed "NetMobilityTracker", an application using the android telephony API in order to capture wireless connectivity information from smartphones. This application performs both passive and active measurements in the background. For passive measurements, it periodically logs the following information: (i) the current timestamp, (ii) cell-ID and local area code (LAC) of the cellular basestation the phone is connected to, (iii) the cellular technology used, such as LTE, UMTS, HSPA+, 3G, etc., (iv) the received signal strength indicator (RSSI) of the cellular connection, (v) the service set identifiers (SSIDs) of available Wi-Fi access points, and, (vi) the RSSI of each of the Wi-Fi APs. For active measurements (an optional feature), the app periodically tries to download the ORBIT webpage and logs the latency and throughput it observes. NetMobilityTracker was installed on two phones (Samsung Galaxy S3 and S5) with different cellular carriers (Net-A & Net-B) and they monitored the wireless

channel conditions over a predefined vehicular commuter route (see Fig.2.4(b)) twice a day (morning and night). The two phones were always co-located and collected the measurements simultaneously to record spatially correlated channel conditions.

The passive measurements, which demonstrate the collocated channel conditions for two carriers, are replayed in the ns-3 simulation model described earlier. To ensure the consistency of data, only the measurements with "LTE" network type (which was 10 of them) are used in the simulation. In Sec.2.3, we describe how all the data is used to emulate mobility in ORBIT testbed for further evaluation of mobility and multihoming sevices.

Due to different receiver sensitivity (governed by the noise floor for different devices) and different technologies, the raw signal strength data cannot be directly injected into the ns-3 simulation environment. In order to address this issue, the measurements need to be mapped to ns-3's operating range. The mapping between this range and the data rate assigned to the UE with the parameters in Fig.2.3(a), and RSSI-to-rate mapping for a sample of data is shown in Fig.2.7. Another issue with the reported signal strength is the fact that the small scale fluctuations have been averaged out, causing inaccuracies in the evaluation of mobile scenarios. To overcome this, we used the built-in Rayleigh fading model of ns-3 which is based on pre-calculated traces for vehicular scenario (TraceFadingLossModel class is used). Based on the combination of large scale fading governed by signal strength measurements and ns-3's Rayleigh small time-scale fading model, the signal strength traces are utilized in the simulation. Injecting these traces into the simulation will provide us with an upper-bound on the performance of the system. This is due to the fact that the methodology used in trace collection does not provide information on base station loading or scheduler state, so that our use of signal strength values corresponds to the lightly loaded network case which is an upper bound of achievable performance.

In order to investigate the performance gains of NAMH, the download performance of MPTCP, single TCP for each carrier, best-interface and NAMH for all the traces is compared. A total of 10 series of measurements (total of 217 minutes of measurements) of each carrier have been fed into the LTE physical layer module modeling the retrieval

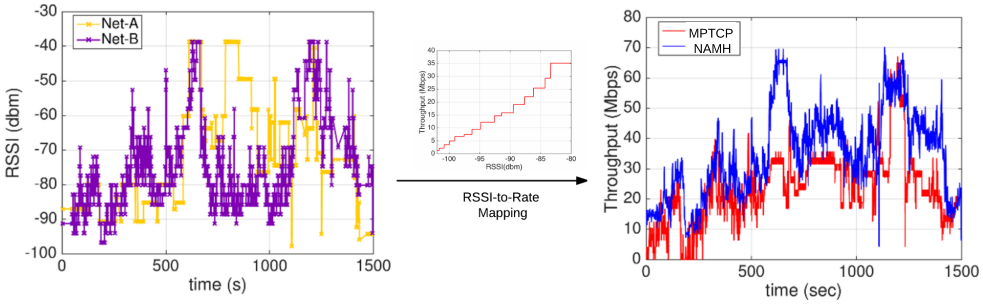

Figure 2.7: *left:* Mapping between the measurements and ns3's operating range.*right:* Throughput achieved replaying this sample, the RSSI-to-rate mapping in ns-3 determines the rate by each eNB

of a large file from a server.

Fig.2.8(a) shows the average throughput vs. average RTT for the large file download scenario across each of the traces (for better visualization of tail the x-axis is shown in log scale). In terms of throughput, the NAMH average throughput outperforms MPTCP by 30-80 % (on average $\times$1.4 increase), while MPTCP and best interface method perform relatively similar (MPTCP $\times$1.15 better) and better than single TCP connections (MPTCP $\times$1.4 better). In terms of RTT, NAMH exhibits 12-80% smaller values compared with MPTCP (on average $\times$2.3 reduction). Single TCP connections show the largest values for RTT (only 5-9% larger than MPTCP).

The improvements in performance achieved through network-assisted multihoming are a result of overcoming underutilization in MPTCP caused by indirectly inferring the link capacity. Also the MPTCP user suffers from complete disconnections (zero throughput) for total of 353.3 seconds, whereas NAMH is able to maintain nonzero throughput throughout the simulation.

Effect of In-Network Delay on Performance

In the scenarios we investigated so far, the in-network delay is fairly small compared with wireless link delay (1ms vs. 20ms). By varying the in-network delay, we show that as the in-network delay increases, the throughput gains of network-assisted approaches like NAMH tend to improve even further. To show this, we replay one of the traces and on each round of simulation, steadily vary the in-network delay in steps of 5 milliseconds.

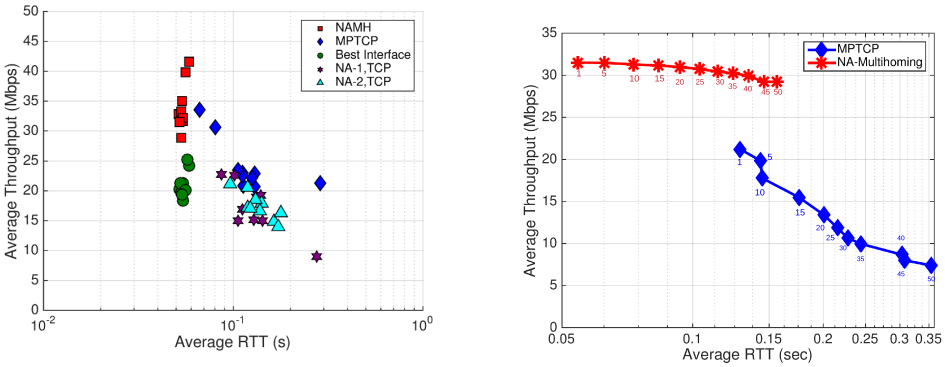

(a) Average throughput vs. Delay for all the traces

(b) Average Throughput vs. Delay, The numbers on the markers show the in-network delay in ms.

Figure 2.8: Performance Evaluation

The average throughput vs. RTT result is shown in Fig.2.8(b). Our simulation results confirm that adaptation of MPTCP to fluctuating wireless link quality degrades as the in-network delay increases. Consequently, self-inflicted delays in MPTCP which are a result of inaccurate estimation of bandwidth will result in order of magnitude decrease in average throughput (20 Mbps to 5 Mbps) and increase in average RTT (100 ms to 350 ms).

2.3 ORBIT Mobility and Multihoming Experiments

In this section, through experiments on the ORBIT testbed, we aim to evaluate how using network-assisted multihoming protocol in MobilityFirst, which utilizes network elements for scheduling the traffic, will perform in comparison with delegating scheduling and data-splitting to the end hosts in MPTCP. Further details of a mobility-emulation framework on ORBIT testbed, which can be used for testing various mobility-centric protocols, is given in Appendix.B.

2.3.1 WiFi and LTE Multihoming

In our experimental evaluation we aim to deploy a baseline device multihoming scenario in ORBIT testbed, in which the client will receive data on its both interfaces, Wi-Fi and LTE. As MF routers need a L2 connection between them, we connect the LTE

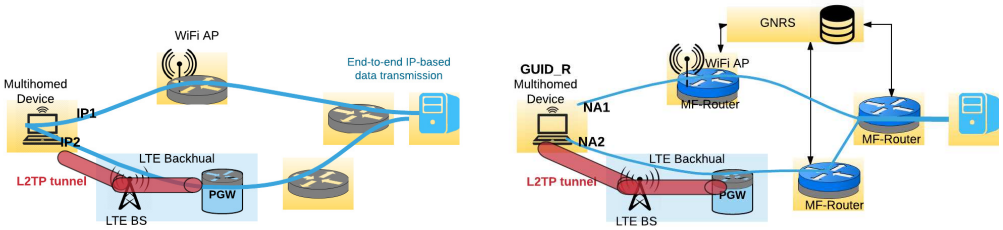

(a) MPTCP-based setup: data splitting on an end-to-end basis

(b) MobilityFirst-based setup: GNRS service and MF-software routers enable network assisted multihoming

Figure 2.9: Benchmark experimental setup

Client, and LTE MF router via an L2TP tunnel. This enables us to swap out the underlying LTE implementation transparently to the MF configuration. The Wi-Fi link is using 802.11g technology (Atheros AR928X wireless network adapter) [39] and hostapd daemon[40] is used for Wi-Fi AP implementation and management.

In order to evaluate the throughput gains achieved due to network-assisted multihoming compared with MPTCP two scenarios are deployed. An overview of the baseline setup for both the cases of MPTCP-based multihoming and MF-based multihoming is depicted in Fig.2.9. The underlying L2 connectivity is the same for both cases, except for the additional GNRS node in MF setup which provides the name-to-address mapping to the MF-enabled routers.

MPTCP v0.90 is installed on the end points (sender and receiver) [41] and for traffic generation in the MPTCP-based scenario, *iperf* has been used to measure the downlink application level performance. In order to measure the downlink throughput for MF-based scenario, *mfperf* is used, which is a modified version of iperf adopting MF API calls [42] to transmit and receive data. We ran 20-second data transmission, 10 times for each of the scenarios. For the sake of comparison, the same set of experiments are conducted for single LTE and single WiFi link connectivity, using iperf. The result of the average throughput at the client is shown in Fig.2.10.

As can be seen from Fig.2.10, single LTE and single WiFi have comparable throughput. However, performing ping test on each of the technologies revealed high disparity in the latency on each link (WiFi has latency of average 2 ms, whereas LTE's latency averages 40 ms). The higher latency in LTE is a result of the L2TP tunnel and the LTE's

core network delay. The default scheduler in MPTCP is based on RTT of each path; it will firstly fill up the congestion window on the subflow with lowest RTT, and sequentially transmit on next-higher RTT. Previous work has shown that the latency disparity on links causes under-utilization of available resources due to reordering overheads[18]. This is also backed up by our experimental evaluation, which shows MPTCP can barely perform better than the best of single link data transmission.

On the other hand, Mobilityfirst is capable of better utilization of available resources due to features such as storage aware routers capable of temporarily caching in-transit chunks, along with the bifurcation router assigning chunks to each path based on their quality. This is validated through our experimentation which shows multihoming will achieve higher throughput gain compared with MPTCP.

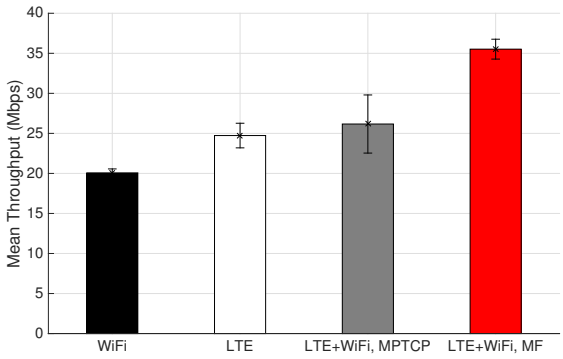

Figure 2.10: Achieved downlink throughput at the client for 4 different scenarios: Single WiFi, Single LTE, MPTCP (LTE+WiFi), Moblityfirst(LTE+WiFi)

2.4 Multihoming in Next-Generation Wireless Networks (5G)

Multihoming (connectivity of an end-device to multiple BSs and access points (APs)) improves user throughput and enables load balancing and connectivity robustness in the case of mobility or disparate channel conditions. Multihoming is an important technology considered within 5G architecture for interworking of heterogeneous wireless access technologies, i.e. Wi-Fi, LTE and NR. Dual connectivity (DC) has been proposed as the first phase in deployment of 5G, allowing for a user to be served simultaneously by an LTE BS and a NR BS [43]. As a natural progression and generalization to this first

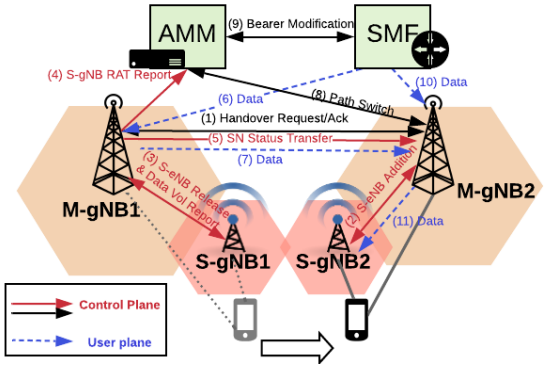

Figure 2.11: Mobility and multihoming in 5G

phase, in [10], multi-rat dual connectivity is discussed. Another example of enabling multihoming within 5G network is LTE/NR aggregation with Wi-Fi. An overview of the overall architecture and signaling for a baseline mobility/multihoming scenario in the current cellular network is depicted in Fig. 2.11 and using MobilityFirst in Fig. 2.12. As seen in Fig. 2.11 the Master eNB (M-eNB) can be LTE or NR BS with control plane interface to MME, while the control signaling related to Secondary eNB (S-eNB) (which can be LTE/NR in unlicensed band or Wi-Fi) has to be maintained by the M-eNB. This approach of anchoring a secondary RAN to a master RAN has

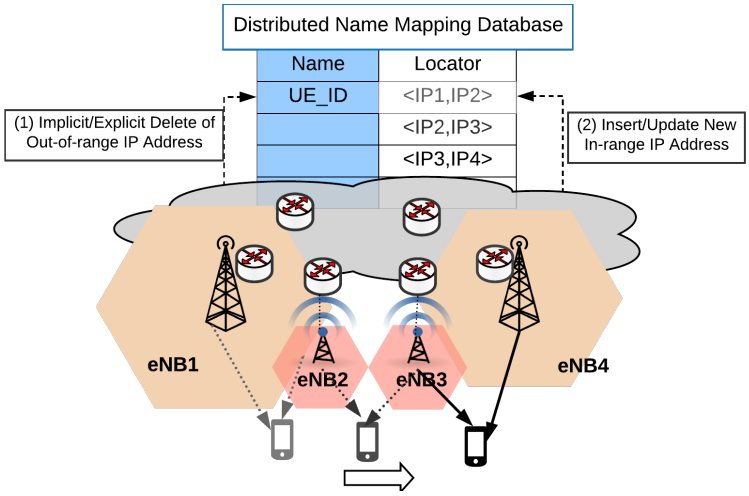

Figure 2.12: Mobility and mutihoming in a distributed flat core

limitations for support of dynamic mobility and session continuity. The signaling needed for a multihomed device handover is shown in Fig. 2.11, with extra signaling overhead needed due to the S-eNB's control interface being anchored on the M-eNB shown in red. As can be seen from the figure, the overhead is 2X more than a typical handover

scenario (shown with black arrows). Moreover, since small cell deployments will have smaller coverage area, handovers will be very frequent in future mobility scenarios. As a result, exploiting all the wireless capacity will require a scalable and dynamic architecture for support of multihoming. The flat name-based architecture will natively support multihoming by eliminating the need for anchors and triangular routing, and all the RAN components interfacing with the distributed name-to-address mapping service to provide seamless mobility and service continuity while minimizing the control overhead, and hence latency. As can be seen from Fig. 2.12, the proposed architecture greatly reduces signaling overhead, while maintaining the session/service continuity by providing uninterrupted coverage and intermittent connectivity while moving from one macro-cell to the other.

2.5 Related Work

Accessing the Internet through multiple interfaces available on wireless devices has gained considerable attention in recent years [19]. Various solutions have been proposed, mostly at the transport layer. Multipath TCP [24] is the most prominent example with significant gains [25]. Despite proposals to modify MPTCP by using cross-layer information [28], MPTCP's performance suffers because of the end-to-end design and relatively slow estimation of channel quality. To address this, we have presented a network-layer solution which has the advantage of providing transparency at the end-points along with more direct routing and path quality information.

Splitting a connection across multiple WiFi APs has been achieved by means of a virtualized driver [29, 44] or MPTCP[45]. Our project is one of the first which attempts to propose network-assisted solutions to aggregate capacities of multiple cellular networks for better services to users. Network-assisted approaches like [18, 46] show results of performance improvement with multihoming across heterogeneous networks, either by use of back-pressure algorithms on routers [18] or delay/bandwidth of wireless links [46]. The focus in our work is on LTE networks based on available predictions eNodeBs can make about link quality.

The cross-layer mechanism proposed in this work has been adapted from some recent projects [47, 48] which attempt to improve the quality of services over cellular networks by leveraging information from lower layers in phones. Our work takes the natural next step, by exploiting the more complete information available at the basestations and proposing the necessary network architecture and techniques to support cross-layer feedbacks.

One of the important issues regarding clean-slate mobility and multihoming solutions is their deploy-ability on testbeds and in real-world scale networks. The clean-slate nature of these architecture proposals necessitates the study of approaches to deploy and evaluate them on today's networks along with 4G/5G technologies available on testbed and real-world scale. In [49], authors describe the framework they implemented within GENI to test vertical handover between heterogeneous wireless networks. Our work focuses on deploying more general services within MobilityFirst architecture in the context of cellular technologies available within ORBIT testbed.

Deploying multi-interface connectivity has also been the subject of study in a couple of projects [19, 50]. There have been efforts focusing on micro-scale deployment of MPTCP and its interaction with diverse wireless access technologies like WiFi, LTE, etc. [51–53]. In [54], a control and measurement SDN-based framework has been built on top of two testbeds to enable large-scale deployment, testing and evaluation of MPTCP.

2.6 Conclusion

In this chapter, multi-network access has been proposed for achieving improved mobile data performance in wireless access networks. An architecture for network-assisted multi-homing in cellular networks was described and compared with the transport-layer alternative MPTCP. Ns-3 based simulation models are used to evaluate achievable performance, and significant gains are demonstrated in comparison with single network access and with MP-TCP over multiple networks. The simulation study is supplemented with a trace driven emulation which uses measured signal strength data from

two commercial networks over a 10 mile trajectory in central New Jersey. The results show that average throughput with multi-network access increases from about 18 Mbps to 34 Mbps, corresponding to a gain of $\times 1.9$. The proposed in-network design also provides significant improvements over the transport layer alternative, MP-TCP, with gains of about $\times 1.4$ in achievable throughput. In the end, the results are further validated with experimental evaluations using a MobilityFirst based network running on the ORBIT wireless testbed [55].

Chapter 3

Cellular Multicast

3.1 Introduction

Simultaneous delivery of identical content to a group of mobile users or smart devices is an important requirement for future cellular services. Techniques for efficient multicasting over cellular networks can help to significantly reduce radio resource consumption and increase spectrum efficiency. To address wireless multicast within 3GPP standards, the Multimedia Broadcast/Multicast Service (MBMS) was originally proposed more than a decade ago for optimized video broadcasting services over large pre-planned areas over multiple cells. Evolved-MBMS (eMBMS) currently defined in Rel 14 3GPP specification [56] has improved performance compared to MBMS by incorporating new features like single frequency network (SFN) and carrier configuration flexibility applicable to media broadcasting. Moreover, single-cell point-to-multipoint (SC-PTM) has been proposed in Rel 12 of 3GPP specification to extend MBMS for IoT (Internet of Things) and mission critical communication [57]. Switching dynamically between unicast and multicast/broadcast transmission (mixed-mode broadcast) is essential to the following new mobile services [58] [1]:

- *IoT:* Enhancement to SC-PTM can be applied for efficient over-the-air (OTA) upgrade of devices and group messaging.
- *Cellular vehicle-to-everything (C-V2X):* Vehicular-to-network (V2N) can utilize eMBMS for delivery of real-time information (e.g. traffic) to vehicles and autonomous driving assistance.

[1] Another use case of eMBMS is terrestrial broadcasting for next-generation digital TV, with radio access and system layer enhancements specified in Rel 14 [59]. This use-case is out of the scope of this thesis.

- *Public safety:* Real-time emergency notifications can efficiently be delivered by leveraging eMBMS.

- *Venue broadcast:* In high-density deployments like stadiums, video and multimedia traffic can take advantage of eMBMS.

Despite all the advancements of eMBMS, it still lacks support for low latency, low overhead and more dynamic multicast scenarios that is required to fulfill the latency and bandwidth requirements of these 5G services.

The emerging information centric network (ICN) paradigm has been used to enable efficient multicast in wired networks and the same principles can potentially be applied to the cellular wireless scenario as well. In ICN architectures, the use of identifiers rather than addresses makes it possible to dynamically route data to groups of objects such as a number of geographically co-located sensors or mobile devices. These use cases require fine-grained and dynamic support of multicast within the core network, as almost any ICN packet can be addressed to a group object with continuously changing membership [60].

In this chapter, we propose extending ICN support of group objects via identifiers to support dynamic and efficient multicast to cellular access networks. We propose an ICN enabled architecture, "I-MAC" control and data planes, as necessary for support of fine-grained dynamic multicast services and seamless integration with identifier-based core network routing associated with ICN. The proposed I-MAC design eliminates the need for service gateways or specialized control plane and makes it possible to directly interface with the base stations (eNB) to a flat ICN-based mobile core network. Multicast service is realized via lightweight control that uses ICN identifiers to set up "multicast virtual channels" between the eNB and UEs. MAC layer services are tied to the name/identifier associated with an ICN packet, making it possible to use any cellular radio such as 5G-NR or 4G data slots for both unicast and multicast transmission modes. In this mode, multicast is the norm for any transmitted packet rather than a special communication mode in the radio access.

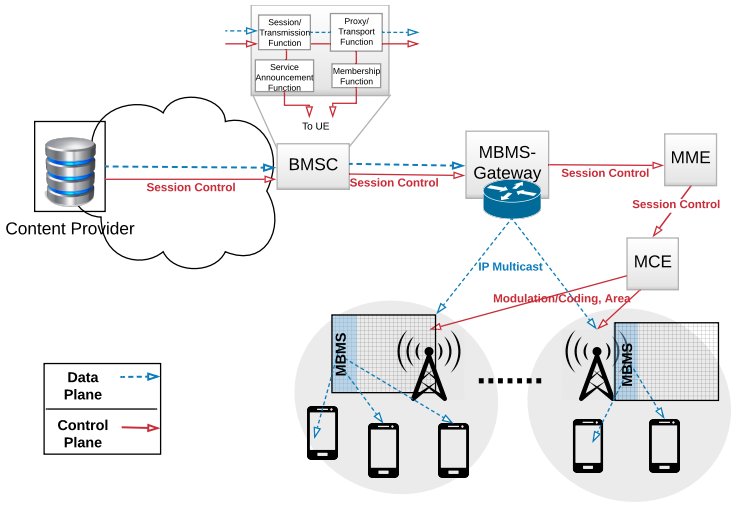

Figure 3.1: LTE eMBMS architecture

3.2 Evolved Multimedia Broadcast Multicast Service (eMBMS)

The currently available eMBMS specification [12] is based on addition of channels (logical, transport and physical) to eNB's radio stack and network entities including an MBMS gateway (MBMS-GW), multicast coordination entity (MCE) and a broadcast multicast service center (BM-SC) as shown Fig.3.1. The BM-SC interfaces with the content provider to set up preplanned multicast sessions by performing announcement of MBMS services to the UEs subscribed and delivery of MBMS content into the core network through the MBMS-GW. The MBMS-GW is in charge of distributing session control signalling via mobile management entity (MME) to the eNBs and handling the establishment and release of user plane bearers using IP multicast traffic. On receipt of session control signalling, MME further uses a signaling protocol to communicate the setup information to the MCE which in turn will deal with session control and setting up radio resources. The MCE performs radio resource configuration (e.g. MCS selection) to ensure that all eNBs participating in an MBMS transmission within a semi-statically configured area use exactly the same configuration and also handles admission control. The signaling required to setup eMBMS multicast transmission is shown in Fig.3.2. There have been a number of trials in the past few years to demonstrate the capability of eMBMS for high-density stadium scenarios [61]. The inefficiencies of eMBMS

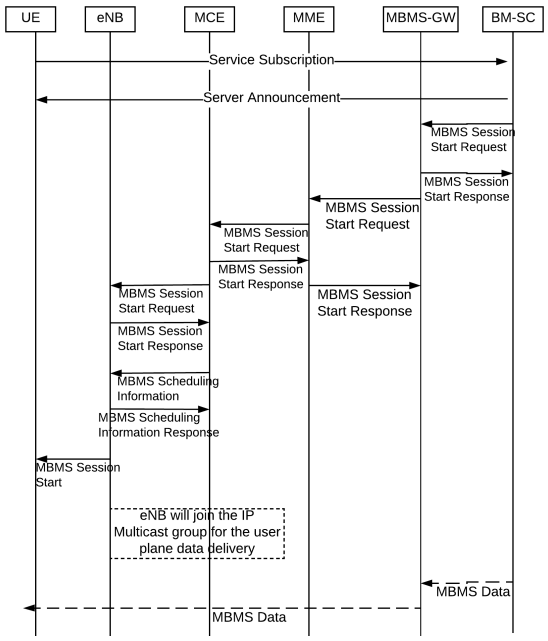

Figure 3.2: eMBMS signalling overhead

considering video as a use case as it consumes significant portion of the spectrum resources today have been reported [62]. EMBMS was designed for linear video content consumption and for it to adapt resources to the current user behavior would require significant re-engineering [63]. For instance, additional functional components such as a centralized controller would be required to track the current demand and predict the future demand and reprogram the broadcast resources that map to the set of contents at the BM-SC to cover the majority set of users within a given geography.

This has been observed to result in inefficiencies in the eMBMS system [63], for instance Rel-14 contains enhancements addressing the simpler case of switching a UE from broadcast to unicast mode, which improved the switching time from 5s to 10ms. However, this latency is expected to be worse when re-programmable broadcast network and control functions are involved. Alternately, ICN architectures have shown their usefulness of leveraging receiver-oriented communication paradigm to dynamically allow the forwarding plane to adapt to user requirements rather than using out-of-band control plane components that is required in a sender-oriented communication paradigm. We exploit this design principle to propose a cellular multicast architecture that allows radio resources to dynamically adapt to user requirements in the forwarding plane in

real time than having it orchestrated using out of band control plane functions.

3.3 I-MAC Architecture

The goal of I-MAC is to integrate ICN semantics which make multicast dynamic and efficient into MAC layer design. A baseline scenario is shown in Fig.3.3, in which multiple users subscribe/request for the same content (same interest packet in NDN[64], GUID in the Get/Subscribe API in MobilityFirst[65]). The main challenge addressed by I-MAC design is in identifying a technique for incorporating this identifier along with its semantics to the MAC layer. The goal of the design is to avoid unicast transmissions to multiple end points interested in the same content, reducing to a single multicast transmission tagged with the ICN identifier. To this end, the I-MAC design should account for the following:

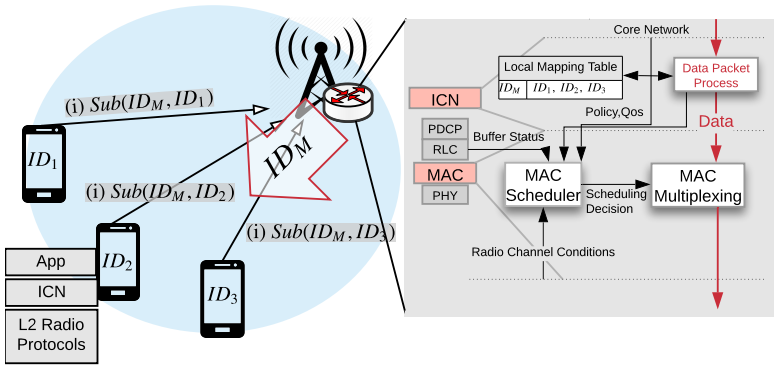

Figure 3.3: ICN-enabled MAC; mapping of requested content ID (ID_M) to an identifier used by MAC layer, and resource blocks

- It should integrate seamlessly with an ICN network which uses names (identifiers) to route data through the network. It is recognized that ICN's name-based routing inherently enables multicast, with unicast being a special case with group size N=1. Unlike eMBMS, this also allows the time, frequency and spatial resource units to be shared between the unicast and multicast flows.

- Group membership is expected to be very dynamic due to mobility, changes in context, changing content interest, etc. The multicast protocol should thus support the ability to easily add or delete group members without requiring a complex control

setup procedure.

- The design should be general enough to handle the full range of named objects including multicast user groups and named content. This implies the need to support both push and pull modes of multicast communication.
- The MAC layer design should enable service differentiation to support heterogeneous types of multicast flows over the radio interface so as to satisfy different reliability, latency and bandwidth requirements.

With these goals in mind, we discuss the I-MAC architecture for a hybrid ICN architecture, MobilityFirst, which as described in Sec.2.2.1 at its core is based on an identifier-based service layer [66]. Though the following discussion is presented in the context of MobilityFirst, it can be easily adapted to the CCN/NDN architecture over a cellular radio system. In this architecture, identifiers can be assigned to network-attached objects like mobile end-users, groups of end-users, static servers, network entities or all principals like contents, services and even context. To push these functionalities to the edge wireless access network, the ICN-enabled base stations will maintain local mapping tables for the services/contents. The local mapping table will store mappings of IDs of services/contents which the users have prior subscription to (push-based multicast).

The I-MAC architecture overview is depicted in Fig.3.4. The new idea here is to push the use of ICN identifiers to the MAC layer and set up a multicast virtual channel (MVC), which aggregates unicast virtual links into a single logical multicast group denoted by the common ID. The multicast service module will tag each MAC allocation request sent to the radio's control API with the ID, and slot scheduling will be done based on ID rather than based on device's MAC address. Multiple UEs can then listen to the same time/frequency resource block associated with a given ID, thus making it possible to use regular data slots for both unicast and multicast modes.

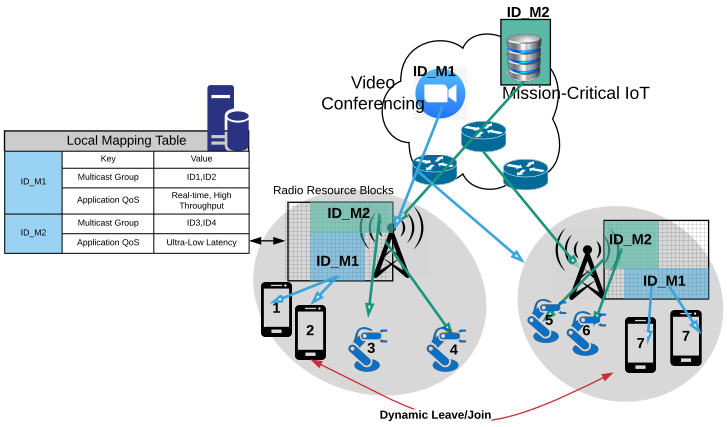

Figure 3.4: ICN-enabled MAC architecture overview.

3.4 Multicast Protocol Design

Next we consider example scenarios which will require simultaneous transmission of data to a group of end-devices. In this section, the signaling and protocol message exchange in I-MAC which is built on top of MobilityFirst multicast[60] are discussed.

Multicast in the core network has been realized using ICN architectures and publish-subscribe systems [60, 67] and has many applications. For example, a server running an application for controlling IoT devices would send a single message to request content or actuate resources in all of them. For sensors/machine-to-machine communication scenarios, there is a high probability that many devices will be under the same eNB. Geo-based applications like navigation or traffic control via vehicle-to-infrastructure (V2I) and live video broadcasting are other examples that would benefit from multicast. It is shown in Fig.3.5 how multicast can be extended to a wireless access network using the I-MAC architecture. In this scenario, multiple UEs will subscribe to a specific service with ID_M. Using the Local Mapping Table (LMT), the subscribed UE IDs will be inserted to ID_M mapping entry at the eNB, and then triggering insertion of this subscription to GNRS by the edge router.[2] Later whenever the server wants to push data to the subscribed UEs, after querying GNRS it will send data destined to the set of eNBs serving those UEs (at R1 and R2 in Fig.3.5). When the data arrives

[2]Here we are considering the most basic multicast scenario with no multicast tree creation. Details on multicast tree creation can be found in [60]

at the edge routers collocated with the eNBs, since it is destined to the routers, they will decapsulate the packet and look up the LMT for ID_M. After getting the MAC addresses for the subscribed UEs, the forwarding engine will trigger the creation of MVC at the MAC layer, which will be used to multicast the data. The details of opening ID-tagged VC are discussed further in the next section.

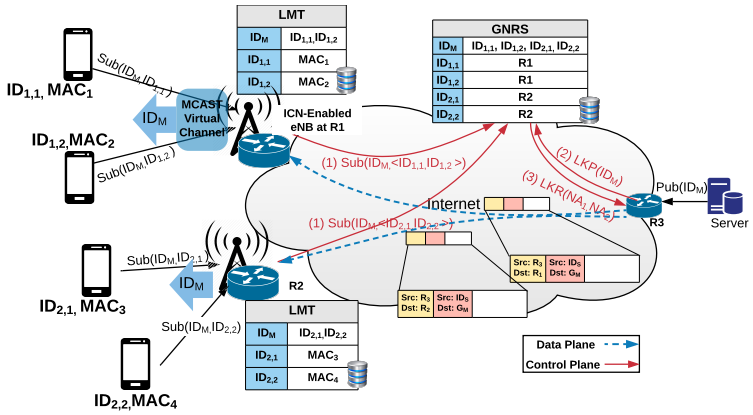

Figure 3.5: Multicast protocol design diagram

3.4.1 Radio Signaling Protocol

In this section we present an overview of radio signaling for setting up multicast RBs in SC-PTM. We then propose a mechanism for generation and integration of I-RNTI in the LTE attach process in I-MAC, which reuses the existing process for unicast flows. This is merely enabled by mapping of multicast service identifiers to I-RNTIs. The performance of I-MAC in terms of service start delay is then compared with SC-PTM in Section. 3.6.

SC-PTM Access Protocol

Each LTE/5G radio subframe is divided into 2 parts: the first few symbols are reserved for control channels and the remaining ones are used for data transmission. The control channels (with different formats called Downlink Control Information - DCI) carry some information common to all UEs (like system bandwidth, HARQ channel structure, etc) and some informing specific UEs of upcoming data transmission (called PDCCH). The

DCI for each UE is only decodable by that UE, since its CRC is scrambled by the C-RNTI of the UE, assigned to the UE in the attach process. The common information to all UEs are coded by RNTIs which are predetermined and known by all UEs, like paging RNTI (P-RNTI) or System Information RNTI (SI-RNTI). An example of a subframe PDCCH and PDSCH is given in Fig.3.6(a).

Two new logical channels are introduced for SC-PTM; the single cell multicast control channel (SC-MCCH) and the single cell multicast transport channel (SC-MTCH). SC-MCCH includes necessary scheduling information on the multicast session i.e. MCS value, scheduling period, scheduling window, start offset of the sessions and a mapping between a temporary identifier associated with the SC-PTM session (Temporary Mobile Group Identity - TMGI) and Group RNTI (G-RNTI) which will be used to decode SC-MTCH. In order to decode the SC-MCCH itself the UEs subscribed to the SC-PTM service will use SC-RNTI (which is broadcasted in SIB20). SC-MCCH is periodic with configurable period, with the maximum repetition period of 256 frames (2.56 seconds). An overview of the frame structure with presence of SC-PTM is shown in Fig.3.6(b).

One main issue with SC-PTM access protocol is the trade-off between the transmission period of SC-MCCH and battery usage of UEs. At the presence of SC-PTM the UEs need to wake up at every SC-MCCH transmission in addition to their normal DRX (*Discontinuous Reception*) cycles [3]. As a result having a short interval between consecutive SC-MCCH transmissions will incur high battery usage to UEs. On the other hand, SC-MCCH needs to be short enough to assign proper MCS value to the multicast session considering the mobility of the UEs and dynamic wireless links. Also shorter SC-MCCH period will cater to new subscribed UEs in a more timely manner.

I-MAC Access Protocol

In I-MAC, since the eNB stores the mapping between the multicast ID and the MAC addresses of UEs subscribed to it in LMT, it can use the typical LTE attach process

[3]DRX is a mechanism to reduce the power consumption of UEs, it means that the UE can switch off its receiver to preserve battery power and only wake up at predetermined times to check for incoming data.

to inform the UEs about the I-RNTI which will be used to mark the multicast data in PDSCH, as shown in Fig.3.6(c).

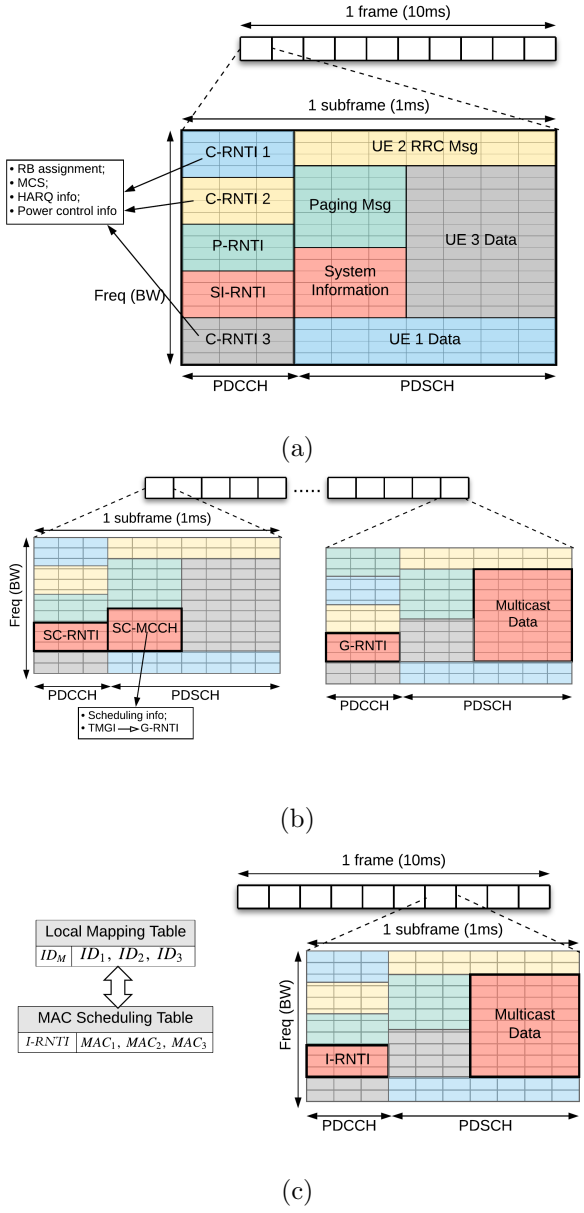

Figure 3.6: The resource block scheduling for (a) legacy cellular systems transmitting unicast traffic; (b) SC-PTM system, which uses a fixed RNTI (SC-RNTI) for control information for multicast data scheduling; (c) I-MAC system utilizing a common RNTI (I-RNTI), which is the map of the multicast service ID the UEs are subscribed to.

In the following, an overview of the LTE attach process along with integration of I-RNTI in it is given. In LTE systems (similar to 5G), UEs are either in *RRC_idle* or *RRC_connected* mode. When in *RRC_idle* mode, the UEs apply DRX (Discontinuous

reception) and would wake up to check the paging message periodically. If the UE finds its identity in the paging message, meaning that there is data available for it, it will initiate the random access procedure by sending a *Random Access Request* using a random access preamble (RA-RNTI). The eNB responds by sending a *Random Access Response* including a temporary RNTI (Temporary Cell RNTI - TC-RNTI). At the success of the random access process, the eNB can use the same TC-RNTI as the Cell RNTI (C-RNTI) which will be in effect for the lifetime of the connection (as long as the UE is in *RRC_connected* mode). In I-MAC we use the same process, and will use the same TC-RNTI (and subsequently same C-RNTI) for all the UEs in the multicast group. An overview of this process compared with SC-PTM is shown in Fig. 3.7

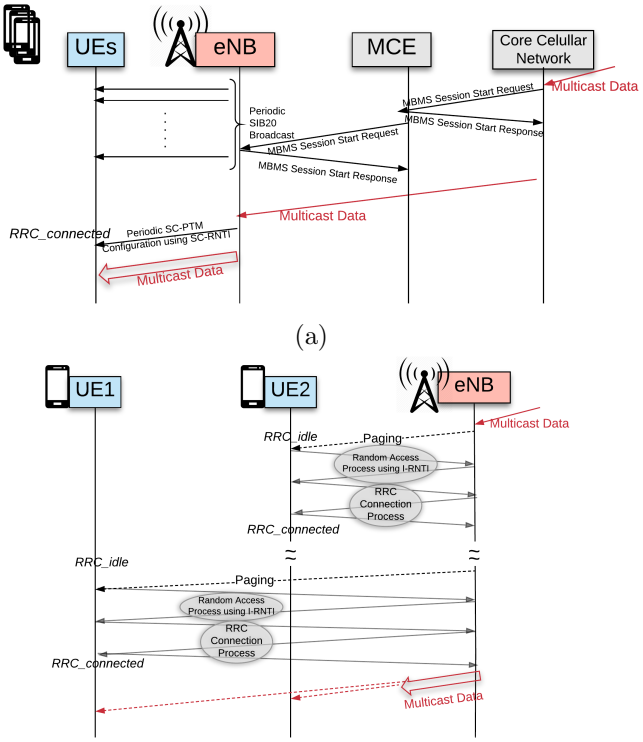

Figure 3.7: The process of notifying UEs of the incoming multicast data and necessary scheduling information in (a) SC-PTM system; (b) I-MAC system

One issue with this process is the different paging occasions for the UEs in the multicast group, which might cause an initial delay for the start of the service. However, considering the fact that the typical interval between paging occasions is 1.28 seconds

for UEs, and they will stay in *RRC_connected* mode for 11.576 seconds before going back to *RRC_idle* mode [68], the service start time of I-MAC is guaranteed to be the same as SC-PTM in the worst case. In Section. 3.6, we evaluate the performance of I-MAC compared with SC-PTM for service delivery time of bursty multicast traffic.

3.5 I-MAC Scheduling

One of the main technical challenges of the I-MAC architecture is to design a scalable and low-overhead MAC scheduling algorithm which natively detects the potential for multicast transmission and assigns resources to multicast groups in a dynamic manner. We propose a scheduling algorithm based on dynamic MAC scheduling at the eNB. The discussion considers MAC and PHY layer control and frame formats similar to LTE [69]. This can also be extended to 5G-NR [70] specification too, considering its similarity to LTE, but with more flexibility offering better efficiency, for instance various OFDM numerology, etc.

Typically, MAC scheduling in a cellular base station is done based on mapping of MAC addresses of the UEs to a Radio Network Temporary Identifier (RNTI), and allocating resource blocks to various RNTI agreed upon in control message exchanges. In I-MAC scheduling, the service/content ID is mapped to I-RNTI (shared by multiple UEs) and the eNodeB (eNB) performs centralized scheduling based on I-RNTI. Similar to current LTE operation UEs have to be updated about the PHY channel allocations and then receive multicast content. The difference between unicast and multicast scheduling here is that for unicast transmission, the UEs are informed about the assigned resource blocks and other control information through individual LTE physical downlink (DL) control channel (PDCCH) decoded using each UE's individual C-RNTI. However, in our design in the setup procedure the same I-RNTI is assigned to UEs belonging to the same multicast group. More details on I-MAC and SC-PTM signaling to setup multicast sessions is given in Section. 3.4.1

In this section the resource allocation for mixed unicast and multicast traffic at the eNB to enable efficient delivery of multicast packets to corresponding UEs are described.

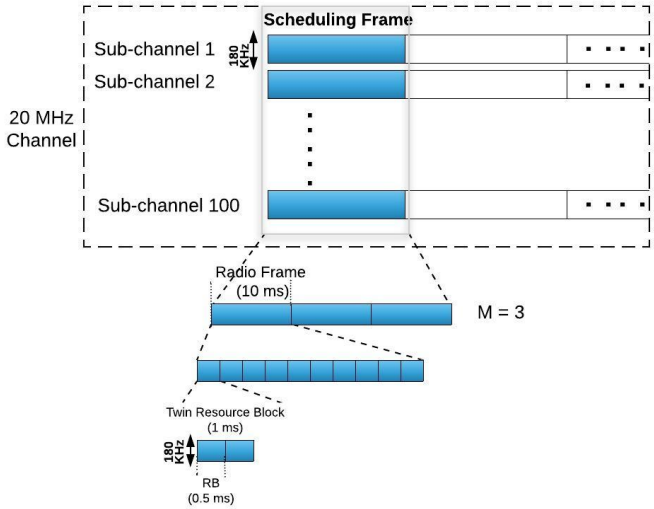

Figure 3.8: Radio resource allocation in cellular networks

3.5.1 Radio Resource Allocation

Radio resource allocation in cellular systems is performed based on OFDMA radio frames which will be divided in frequency and time into scheduling units called *Resource Blocks (RBs)*. In the frequency domain bandwidth is divided into a number of subcarriers (15, 30, 60, 120 KHz in 5G NR) and in time domain to 10 ms frames, each of which divided into 1 ms subframes which are in turn 2 slots (same for LTE and 5G NR). Each RB consists of 12 subcarriers and 1 slot, as shown in Fig.3.8. Resource allocation is done at intervals called *transmission time interval (TTI)*, which can range from multiple radio frames (3 as shown in Fig.3.8) to few slots or even 1 slot. The choice of TTI depends on a number of parameters including channel coherence time and mobility of UEs.

Resource allocation for unicast UEs has long been investigated in the literature [71–73]. More recently, resource allocation considering multicast transmission has been considered in [74] for video multcast in OFDMA-based systems (LTE and WiMax). Since the introduction of cellular multicast in 3GPP release 9, eMBMS has been initially used in MBSFN (Multicast-broadcast single-frequency network) mode, where multicast data is transmitted in a synchronized manner through multiple cells [75]. Proportional fair resource allocation for the MBSFN mode has been considered in [76]. MBSFN mode operates in a semi-static multi-cell area, which cannot be dynamically adjusted

without re-instantiation of the services. Moreover, this mode requires the same frame configuration for all the eNBs in one MBSFN area through MCE. In this mode, specific subframes are fully allocated for MBSFN transmission. Hence multicast and unicast data cannot be multiplexed within one subframe and only one multicast session can utilize the MBSFN resources at a time.

In order to improve eMBMS to support more dynamic scenarios, SC-PTM (Single Cell - Point To Multipoint) has been proposed. Similar to I-MAC, SC-PTM enables utilization of PDSCH (Physical Downlink Shared Channel) for mixed transmission of unicast and multiple multicast sessions within the same subframe. In MBSFN the scheduling of the single multicast session happens at the MCE, and then the eNB performs unicast scheduling taking into account the resource allocation from the MCE, whereas in SC-PTM and I-MAC the joint resource allocation of unicast and multicast sessions happen at the eNB on a more fine-grained time scale. Moreover, due to the division of the task of resource allocation for unicast and multicast flows between the MCE and eNBs in MBSFN mode, the percentage of multicast traffic has to be limited to a fixed value by the MCE (60% in current eMBMS specification), which in turn would make scheduling in this mode less adaptive to system traffic load. Fig. 3.9 presents the resource allocation for MBSFN mode of eMBMS compared with I-MAC and SC-PTM resource allocation. In the rest of our discussion we formulate the resource allocation problem for I-MAC which can also be applied to SC-PTM.

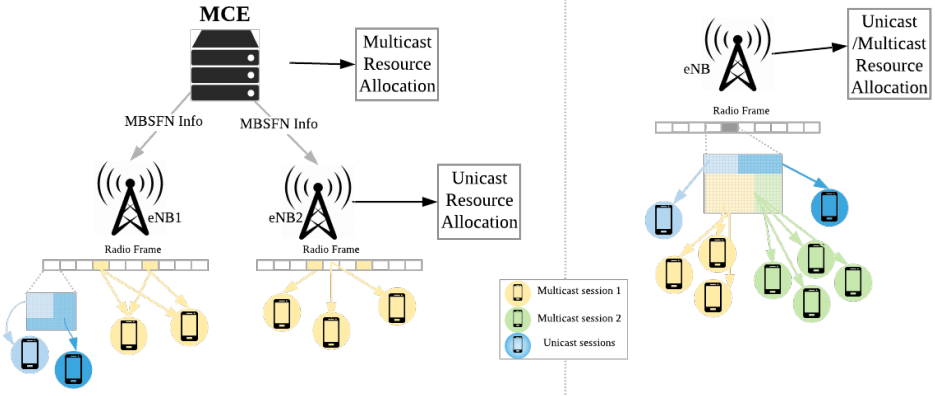

Figure 3.9: Radio resource allocation cellular multicast, MBSFN mode *the left figure* and SC-PTM/I-MAC mode on the right *the right figure*

Proportional fair resource scheduling problem

The problem of resource allocation boils down to assigning two parameters to each unicast/multicast session. One is the *Modulation and Coding Scheme (MCS)*, which is determined by the eNB based on the feedback from UEs regarding their channel condition (Channel Quality Indicator- CQI). The second parameter is the number of RBs assigned to each session. For the unicast sessions, all the RBs are modulated with the same MCS (determining the number of bits transmitted per RB). All the RBs assigned to the multicast sessions have to be modulated to the lowest MCS of the UEs in the multicast group, since transmitting at higher MCS will cause the low MCS UEs to suffer high bit error rates and possible data loss.

One important issue when considering a mix of multicast and unicast traffic is to allow for different groupings among the multicast UEs, as each group will be served with the lowest MCS in that group. Previous work for eMBMS in MBSFN mode has shown the gain achieved through grouping to achieve higher PF utility [76]. However, eMBMS in MBSFN mode does not support this and SC-PTM requires high signaling with core network entities (BM-SC) to support it. In Section.3.4.1, we describe how I-MAC will inherently support this.

In order to achieve a balance between fairness (avoiding starvation of UEs with poor channel conditions while ensuring good quality of experience for UEs with good channel conditions) and total throughput of the system, we adopt the widely used *proportional fair* (PF) metric[77–79]. A commonly used PF objective function is to maximize the aggregated log of long-term throughput of UEs. Combining the two objectives of (1) optimizing the grouping of multicast UEs and (2) maintaining fairness among unicast UEs and groups of multicast sessions will result in the following problem formulation. The notation used is summarized in Table. 3.1.

Problem 1. *Long-term resource allocation*

$$\text{maximize} \sum_{n=1}^{N} log(\overline{R_n}(t)) + \sum_{m=1}^{M} \sum_{k=1}^{K_m(t)} |G_{m,k}(t)| log(\overline{R_{m,k}}(t)) \tag{3.1}$$

Table 3.1: Notation Table

Input	
$\mathbb{M}$	Set of multicast sessions with total number of M
$\mathbb{U}_m$	Set of UEs subscribed to multicast session $m \in \mathbb{M}$
$\mathbb{N}$	Set of unicast UEs with total number of N
$d_n(t)$	Instantaneous MCS for unicast user $n \in \mathbb{N}$ at TTI t $(bits/RB)$
$\overline{d_n}(t)$	Average MCS for unicast user $n \in \mathbb{N}$ up to TTI t
$\mathbb{B}$	Set of resource blocks (RBs) with total number of N_B
$\overline{R_n}(t)$	Average rate for unicast user $n \in \mathbb{N}$ at TTI t
$\overline{R_m}(t)$	Average rate for multicast session $m \in \mathbb{M}$ at TTI t
Output	
$r_{i,k}^b(t)$	Binary variable indicating whether RB $b \in \mathbb{B}$ is allocated to group k of user or session $i \in \mathbb{M} \cup \mathbb{N}$ at TTI t
$y_n(t)$	Number of RBs for unicast UE $n \in \mathbb{N}$ at TTI t
$x_{m,k}(t)$	Number of RBs for group k of multicast session $m \in \mathbb{M}$ at TTI t
$G_{m,k}(t)$	k_{th} group of multicast session $m \in \mathbb{M}$ at TTI t
$c_{m,k}(t)$	MCS for group k of multicast session $m \in \mathbb{M}$ at TTI t $(bits/RB)$
$K_m(t)$	Number of groups for multicast session m at TTI t

$$\text{s.t.} \qquad \sum_{n=1}^{N} y_n + \sum_{m=1}^{M} \sum_{k=1}^{K_m(t)} x_{m,k} \leqslant N_B \tag{3.2}$$

$$G_{m,k}(t) \cap G_{m,l}(t) = \emptyset \qquad \forall m, k \neq l \tag{3.3}$$

$$G_{m,1}(t) \cup \cdots \cup G_{m,K_m}(t) = \{1, \cdots, |U_m|\} \qquad \forall m \in \mathbb{M} \tag{3.4}$$

$$\text{variables: } \{y_n\}, \{x_{m,k}\}, \{G_{m,k}\}, K_m$$

In Eq. 3.1, $\overline{R_n}(t)$, which is the average rate for unicast user $n \in \mathbb{N}$ is defined as follows:

$$R_n(t) = \overline{d_n}(t) \times y_n(t) \qquad \forall n \in \mathbb{N} \tag{3.5}$$

Similarly in Eq. 3.1, $\overline{R_{m,k}}(t)$ (average multicast session rate) is defined as follows:

$$\overline{R_{m,k}}(t) = c_{m,k}(t) \times x_{m,k}(t) \tag{3.6}$$

where $x_{m,k}(t)$ is the number of RBs assigned to group k of multicast session m, modulated with the minimum MCS of the UEs in the group:

$$c_{m,k}(t) = min\{\overline{d_i}(t)\} \qquad \forall i \in G_{m,k} \tag{3.7}$$

Constraint.3.2 limits the total number of RBs assigned to unicast and multicast sessions. Constraints 3.16 and 3.17 ensure the grouping covers all the UEs belonging to a multicast session with no overlap among the groups.

Considering the long term throughput in the PF utility function, fractional values can be achieved for the number of RBs assigned to unicast/multicast sessions. Hence, the problem is a mixed integer optimization problem consisting of two parts: 1) enumerating only a subset of grouping of UEs subscribed to a multicast session as explained later 2) considering each grouping as input solving Prob.1, which is a convex optimization problem.[4]

Solution to Problem. 1

- Resource allocation

  As previously mentioned, in Problem. 1 given the grouping, the problem will be a convex optimization problem with parameters $\{y_n\}$ and $\{x_{m,k}\}$. The solution to the problem is as follows and the proof is given in Appendix-6.

  Proposition 1. *For fixed grouping of multicast UEs, the optimal values for y_n and $x_{m,k}$ are as follows:*

$$y_n^* = \frac{N_B}{\sum_{m=1}^{M} |\mathbb{U}_m| + N} \qquad \forall n \tag{3.8}$$

$$x_{m,k}^* = \frac{|G_{m,k}|}{\sum_{m=1}^{M} |\mathbb{U}_m| + N} \times N_B \qquad \forall m, k \tag{3.9}$$

- Group partitioning

[4]Similar approach of separation of problem to two parts (grouping and resource allocation) is taken in [76] for different formulation of the problem in MBSFN mode

Although the resource allocation given the grouping of multicast UEs results in optimal solutions, enumerating all the possible groupings to find the maximum utility based on optimal values will result in the following total number of groupings to consider:

$$\prod_{m=1}^{M} B_{|U_m|} \tag{3.10}$$

Here $B_{|U_m|}$ is the bell number, which counts the possible partitions of the set U_m [80]. It has been shown in [76] that an optimal solution to Problem.1 exists without any unordered grouping[5]. This will reduce the number of groupings considered to:

$$\prod_{m=1}^{M} 2^{|U_m|} \tag{3.11}$$

We prove the following in Appendix.6 that:

Theorem 1. *All the UEs with the same MCS should always be placed in the same group.*

This will reduce the number of groupings considered further to:

$$\prod_{m=1}^{M} 2^{min(T_{mcs},|U'_m|)} \tag{3.12}$$

Where T_{mcs} is total MCS levels and $|U'_m|$ is the set of unique MCS values in U_m.

Per-TTI resource scheduling

A common approach to perform PF resource allocation per TTI (instead of doing long-term resource allocation and allowing for fractional values for resources) is to approximate $\sum log(\overline{R})$ with $\sum R(t)/\overline{R}(t-1)$ [77–79]. This approximation maximizes the ratio of user's instantaneous throughput to the long-term average throughput. The following shows a reformulation of the long-term resource allocation problem to reflect

[5]For users sorted in the ascending order based on their MCS, and unordered grouping is one that contains user i and $i+j$ but not user $i+k$ where $1 < k < j$ [76]

the *log* approximation:

Problem 2. *Per-TTI resource allocation*

$$\text{maximize} \sum_{n=1}^{N} \frac{R_n(t)}{\overline{R_n}(t)} + \sum_{m=1}^{M} \frac{1}{\overline{R_m}(t)} \sum_{k=1}^{K_m(t)} |G_{m,k}(t)| R_{m,k}(t) \tag{3.13}$$

$$\text{s.t.} \quad \sum_{i \in \mathbb{N} \cup \mathbb{M}} \sum_{k=1}^{K_i} r_{i,k}^{b}(t) \leqslant 1 \qquad \forall b \in \mathbb{B} \tag{3.14}$$

$$r_{i,k}^{b}(t) \in \{0,1\} \quad b \in \mathbb{B}, i \in \mathbb{M} \cup \mathbb{N}, k \in \mathbb{K}_i \tag{3.15}$$

$$G_{m,k}(t) \cap G_{m,l}(t) = \emptyset \qquad \forall m, k \neq l \tag{3.16}$$

$$G_{m,1}(t) \cup \cdots \cup G_{m,K_m}(t) = \{1, \cdots, |U_m|\} \qquad \forall m \in \mathbb{M} \tag{3.17}$$

$$\text{variables: } \{r_{i,k}^{b}\}, G_{m,k}, K_m$$

In Eq. 3.13, $R_n(t)$ is the instantaneous rate to be assigned to unicast UEs in TTI t and defined as follows:

$$R_n(t) = d_n(t) \times y_n(t) \qquad \forall n \in \mathbb{N} \tag{3.18}$$

where $y_n(t)$ is the total number of RBs to be assigned to the unicast UE $n \in \mathbb{N}$ defined as:

$$y_n(t) = \sum_{b \in \mathbb{B}} r_{n,1}^{b}(t) \quad \forall n \in \mathbb{N} \tag{3.19}$$

Same holds for $R_m(t)$, the instantaneous rate to be assigned to a multicast UE in TTI t:

$$R_m(t) = c_{m,k}(t) \times x_{m,k}(t) \tag{3.20}$$

where $x_{m,k}(t)$ is the total number of RBs to be assigned to the multicast session.

$$x_{m,k}(t) = \sum_{b \in \mathbb{B}} r_{m,k}^{b}(t) \quad \forall m, k \in G_{m,k} \tag{3.21}$$

Moreover, in Eq. 3.13, $\overline{R_n}(t)$ and $\overline{R_m}(t)$ correspond to exponential moving average of throughput. For fixed grouping, Problem. 2 is an Integer Linear Program (ILP), the optimal solution of which is obtained using commercial optimizers like IBM CPLEX. It has been shown that the approximation we adopted for Problem. 2 will result in assignment of all resources to 1 UE/multicast session at each TTI, which is not ideal for multi-slot OFDMA systems which allow for both time and frequency sharing [81].

In order to address this, we use the idea of *virtual partial update* to the average throughput [82]. Within each TTI, instead of solving Problem.2 for all RBs ($\{r_{i,k}^b\}$), the problem is solved for each RB with average throughputs in Eq. 3.13 going through virtual partial update, denoted as $\widetilde{R_n}(t)$ and $\widetilde{R_m}(t)$. These average throughput values are only used within each TTI to make decisions about allocation of each RB and at the end of each TTI $\overline{R_n}(t)$ and $\overline{R_m}(t)$ are updated based on the total RBs assigned to each unicast UE or multicast session. At the beginning of the next TTI $\widetilde{R_n}(t)$ and $\widetilde{R_m}(t)$ are initialized to $\overline{R_n}(t)$ and $\overline{R_m}(t)$, and then will go through partial updates.

3.5.2 Resource Allocation Evaluation

In this section we evaluate the performance of the per-TTI scheduling algorithm proposed for I-MAC. We firstly consider the impact of number of UEs and multicast sessions on the total throughput achieved. Then we present the effect of considering grouping and how it is realized in I-MAC when applying per-TTI resource allocation.

Impact of the total number of UEs and multicast %

In this evaluation scenario we consider 1 eNB, and vary the total number of UEs (N) and the percentage of UEs which are subscribed to 1 multicast session (P). We use synthetically generated MCS traces using NS-3 simulation as the input to the per-TTI resource allocation algorithm and map the MCS values to spectral efficiency using Table 5.1.3.1-1 of 3GPP standard 38.214 [83]. The details of the simulation are listed in Table. 3.2. In the rest of this chapter, unless otherwise stated, this trace is used as the input to the simulations. We also consider an infinitely backlogged model in which for each user there will always be data available for service. Figure. 3.10 shows the result of the

Attribute	Value
Transmit Power	46 dBm
Bandwidth	20 MHz
Minimum Outdoor Speed	25 mph
Maximum Outdoor Speed	60 mph
Shadowing	Log Normal
Mobility Model	Steady State Random Waypoint

Table 3.2: NS-3 simulation parameters for MCS generation

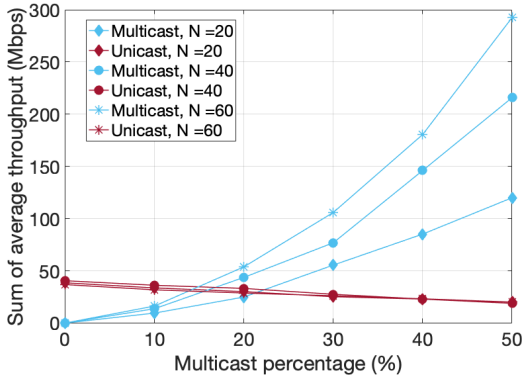

Figure 3.10: The effect of varying the total number of UEs (N) and percentage of UEs subscribed to multicast session (Multicast percentage) on sum of average throughput

sum of average throughput when performing resource allocation for 400 TTIs.

The results are consistent with the optimal values obtained from the solution to the convex problem, Eq. 3.8 and 3.9. Since the sum of unicast throughput is shown in Fig. 3.10, it is independent of the number of UEs and will be proportional to the percentage of unicast UEs. As the percentage of unicast UEs drops to 50%, the sum of average throughput also drops to the 50% of the all-unicast scenario. For the multicast throughput, the aggregated average throughput [6] is shown. Considering Eq. 3.9 it is expected that the aggregated multicast throughput will be proportional to NP^2. This trend is maintained in Fig.3.10.

Impact of grouping the multicast UEs

As previously mentioned, grouping the multicast UEs has been shown to be effective in maximizing the PF utility for the long-term resource allocation. In this section we

[6] defined as follows: if the rate of the multicast session is R_{m1} and $M1$ UEs are receiving the multicast session, the aggregated throughput is $M1 \times R_{m1}$

aim to evaluate the effect of grouping on the per-TTI resource allocation algorithm. Considering the virtual partial update method, at each TTI the RBs assigned to the multicast session will be assigned to only 1 group, and few of the UEs with low MCS values will be left out of the multicast session. This is dictated by the trade-off between having more UEs in the multicast session (which on average will result in assignment of more RBs to the multicast session) and the MCS value of the UEs (since the minimum MCS will determine the rate of the multicast session).

As an example, the average throughput of 20 UEs, 50% of which subscribed to a multicast session is shown in Fig. 3.11 for 2 scenarios: 1) putting all the UEs always in one group; 2) optimizing the grouping to maximize PF utility. As can be seen from Fig. 3.11, optimized grouping will on average penalize UEs with lowest MCS values by not including them in the multicast session (UEs with indices 11 to 14). However, this will in turn increase the total average throughput of the system. At TTIs which the low MCS UEs are not served by the multicast session, they can receive the data through D2D mechanisms from the served UEs [84].

In order to see the effect of percentage of multicast UEs on the gain achieved through grouping, we run the resource allocation algorithm for $N = 40$ UEs, while increasing the multicast percentage from 10% to 50%. The ratio of average sum throughput for optimized grouping to 1-group scenario ($\frac{\sum \overline{R}_{opt}}{\sum \overline{R}_{1group}}$) for both multicast and unicast UEs averaged over 5 rounds of simulation is summarized in table. 3.3. As expected, grouping has an insignificant impact on unicast throughput. However, 50% gain in average multicast throughput is achieved for higher number of UEs subscribed to the multicast session. This can be explained considering the fact that grouping will be beneficial if the MCS values for multicast UEs have high dispersion, which is likely to be the case for larger percentage of multicast UEs. In fact the lowest gain achieved, which corresponds to 20% scenario, has the lowest standard deviation for MCS values.

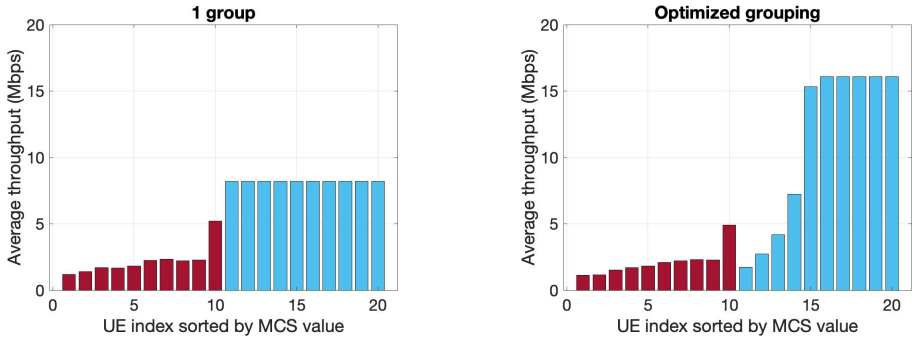

Figure 3.11: The effect of grouping multicast UEs on the average throughput (the UE indices are sorted based on their MCS values)

Percentage Multicast	$\frac{\sum \overline{R}_m^{opt}}{\sum \overline{R}_m^{1group}}$	$\frac{\sum \overline{R}_u^{opt}}{\sum \overline{R}_u^{1group}}$
10 %	1.348	0.997
20%	1.179	1.0011
30%	1.515	0.965
40%	1.526	0.95
50%	1.502	0.94

Table 3.3: Ratio of sum average throughput for optimized grouping to 1 multicast group

3.6 I-MAC use case

In this section we investigate the performance of I-MAC and SC-PTM for a realistic use case. In this use case, context-based services are examined, which can natively be supported by I-MAC but not handled by SC-PTM. The following gives a description of this use case along with results from a custom packet level simulator.

3.6.1 Context-based services

One of the main advantages of using I-MAC compared to eMBMS is the native support for aggregating requests for the same service/content identifier, and then serving those with a single multicast transmission on the radio channel. EMBMS has no means of supporting these *context-based* services. Examples of such types of services are geographically-correlated requests in vehicular scenarios or machine-type communication (MTC). For instance, consider a smart-city scenario, where the self-driving vehicles reaching a turn in a highway would all request to join an ongoing live video stream of traffic ahead. Using I-MAC, the new vehicles wishing to join the ongoing

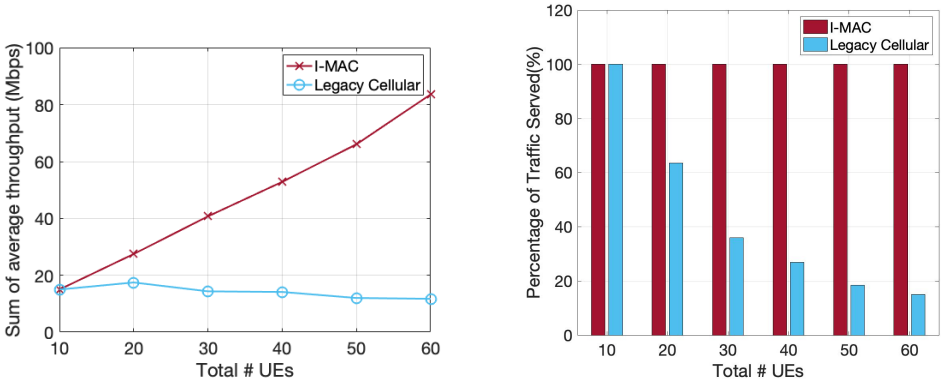

Figure 3.12: The effect of varying the total number of UEs on (a) Throughput and (b) Percentage of requests for potentially-multicast traffic served

session would dynamically be added to it, hence receiving the data from the existing multicast channel.

In order to evaluate the performance of I-MAC, we consider a scenario with total of N UEs, 50% of which are the vehicles whose traffic has the potential to be served using I-MAC, and the rest are UEs with unicast data. We assume that each unicast UE's rate is 2 Mbps and the potentially-multicast traffic's rate is 5 Mbps. By varying N from 10 to 60, we look into the aggregate throughput of the potentially-multicast traffic in I-MAC and legacy cellular systems (which do not have a means to aggregate the context-based requests and will serve them by unicast transmissions). We also investigate the percentage of the requests to receive the multicast traffic that can be served as N increases. The results are shown in Fig.3.12. When the number of UEs is small, $N = 10$, the sum of traffic is below the capacity of the system. Therefore, both systems can serve all the traffic. As the total number of UEs increases, I-MAC would still only require radio resources to serve one 5 Mbps flow, whereas serving the UEs using unicast transmission would lead to inefficient utilization of the spectrum for transmitting the same traffic on multiple channels. As the number of UEs, hence the total traffic demand increases, the systems gets overloaded beyond its capacity and results in decrease in the percentage of traffic served, as can be seen in Fig.3.12 (b).

3.7 Related Work

Realizing ICN multicast in the core of network has been investigated in a number previous projects, like NOMA in MobilityFirst [65] architecture or COPSS in pub-sub based architectures [60, 85]. However, there has been less focus on extending multicast support to the wireless access network. In [86], the authors propose using information obtained from interest packets in ICN to increase security and energy efficiency for IoT link layer protocols. One of the recent papers focusing on incorporating ICN semantics to the link-layer is [87]. This project addresses the issue of link layer being agnostic to ICN packets, hence causing local resources (CPU and battery usage) of the end devices to be sacrificed. In [88, 89] the authors discuss deployment of NDN within WiFi networks by using an NDN-based cross-layer approach. In contrast, our work focuses on enabling dynamic ICN-based multicast in cellular networks via interfaces from ICN layer to the MAC layer scheduling.

3.8 Conclusion

In this chapter we proposed ICN-based cellular multicast and presented the protocol design necessary to enable it. We also presented an overview of the existing cellular multicast standard (eMBMS), and its shortcomings to support the growing dynamic mobile traffic. We then formulated the resource allocation problem and proposed a per-TTI resource scheduling algorithm. We then put forward a use case scenario which will benefit from cellular multicast, namely context-based services and evaluated the performance gains achieved by incorporating ICN awareness to cellular MAC layer for supporting multicast in comparison with existing eMBMS solutions.

Chapter 4

Distributed Dynamic Spectrum Management

4.1 Introduction

Advances in wireless technology, markets, and regulatory policies are enabling dynamic spectrum management on a more granular basis in time, geo, and frequency-space [90]. Advances in LTE and Wi-Fi [91] expand opportunities for these technologies to be both complements and substitutes, creating mixed incentives for both cooperation and competition among heterogeneous networks. Dynamic spectrum sharing is also a key requirement in emerging 5G NR systems which include spectrum aggregation, vertical/horizontal band sharing and multi-band radio capabilities [92]. A data-driven architecture for dynamic spectrum management among heterogeneous networks is needed to manage such sharing [93].

While both centralized and fully-decentralized schemes for managing the co-existence of LTE and Wi-Fi in the same frequency band have been proposed, recent work [94, 95] demonstrates that additional system efficiency (measured in terms of increased throughput) may be realized with the addition of a control plane for facilitating the exchange of spectrum use data among independently operated radio networks. Moreover, such a control plane offers significant benefits in terms of supporting the policy and economic developments that are needed to facilitate the transition toward more dynamic spectrum management architectures for wireless and the emergence of robust spectrum sharing markets [96].

The conventional centralized approach to data-driven spectrum management is exemplified by the Spectrum Access System (SAS) being developed for a new regulatory regime in the 3.5 GHz CBRS band [9, 16]. While the potential benefit of coordinated spectrum allocation can be significant, there are several intrinsic disadvantages to the

centralized architecture for a large-scale service of this nature. Even if the required scale could be achieved through state-of-the-art data center and cloud replication technologies, there are fundamental economic and policy arguments against centralizing spectrum allocation authority. A centralized approach is inconsistent with the policy goal of transitioning toward greater reliance on market-based spectrum management, suffers from scalability issues and presents a single point of failure for a critical national resource. Moreover, a centralized management authority would lead to excessive concentration of market power, insufficient local autonomy and would provide less scope for innovation in technical and business models.

In contrast, the Internet offers an example of a fully distributed architecture which works well without any central point of control from a technical perspective; and from a business/market perspective, supports vibrant innovation and competition. The border gateway protocol (BGP) underpinning the global Internet uses the Bellman-Ford path vector algorithm to distribute consistent network reachability information in a decentralized manner, while also providing for a degree of local control over routing policies [97, 98].

In this chapter we present the technical architecture for SMAP (distributed spectrum management architecture and protocol), which helps address incentive issues for both spectrum users and policymakers grappling with how to better reconcile the co-existence of wireless users with diverse access needs and business models. The control plane for data exchange between peer networks in SMAP can facilitate the management of market-based contracts for dynamic spectrum sharing, or to borrow a term from the data networking industry, Service Level Agreements (SLAs). For such a control plane to adequately take advantage of the opportunities for granular spectrum management and to be incentive compatible with market-based approaches for spectrum sharing (as opposed to Command and Control), the control plane needs to be distributed. To provide a rich platform for spectrum users with diverse requirements for access rights and diverse business/ usage contexts (e.g., accommodating ad hoc demand, managing spectrum access in stadiums or other venues, or providing more flexible integration of end-user and service provider wireless infrastructures), the control plane should support

the exchange of and processing of rich data on the local wireless environment needed to design, implement a range of distributed and logically centralized algorithms for spectrum coordination and for enforcement of service level agreements between colocated networks.

4.2 Spectrum Management Requirements

In this section we briefly discuss spectrum management requirements from economics points of view, and how SMAP's architecture can meet these requirements[1]. The goal of spectrum management is to efficiently accommodate the growing usage needs of heterogeneous wireless networks. To achieve this goal, perfect information about value of the heterogeneous uses, spectrum requirements of users and the load/costs on networks supporting the uses should be available [99].

Due to lack of perfect information on range of users and networks in the real world, no single entity knows all that is needed to compute a globally efficient allocation of spectrum resources, and partial information that would need to be shared to compute a globally optimal allocation is asymmetrically distributed. Moreover, many of the actors with partial information have strategic incentives to keep the information private. In such situations, economists have long recognized the benefits of decentralizing the resource allocation challenge to competitive markets [100, 101]. For spectrum management, this means enabling market-based dynamic sharing of spectrum among heterogeneous wireless networks. For this to be feasible, those with excess spectrum resources need to be able to contract with those seeking additional spectrum resources.

Existing models of market-based spectrum sharing, like roaming agreements amongst cellular operators or coordination of heterogeneous Wi-Fi networks for joint optimization of their resources [102], are limited and dependent on relatively high-cost and indirect contract arrangements to enforce.The shift toward smaller cells and advances in both cellular and Wi-Fi technologies are expanding opportunities for better coordinated and non-coordinated (competitive) sharing among cellular and Wi-Fi network

[1]This section includes material from discussions with our collaborator Prof. William Lehr of MIT

users within the same band [103]. Prospects for unlicensed use in 5G in the same bands shared by Wi-Fi and potentially other users of the spectrum expands opportunities for a richer set of sharing options and an enhanced need for more flexible contract mechanisms, or a generalized SLA [104].

The SLAs should enable the capability of the contracting parties to specify and communicate the spectrum resources to be exchanged and the terms under which the spectrum is to be shared. First, the SLA will need to provide a technical description (which is a "RadioMap"[2] of the wireless domain in question, as described later in Sec. 4.3) of the spectrum resources, which at a minimum will include a specification of the frequencies, power levels, locations, and times for which the spectrum may be used.

Second, the SLA will need to identify the contracting parties and the business terms governing their shared usage. Implicitly, the rules for unlicensed access define a form of open access SLA, while the terms of the lease agreement negotiated between the holder of a license to exclusive-use spectrum and a lessee provides an example of another type of SLA. Note that each wireless network domain is viewed as an autonomous entity which is free to establish SLAs with peers or merely announce adherence to a given licensed or unlicensed spectrum use regime.

Third, for the SLA to serve as an effective contract, there has to be an enforcement mechanism. The control plane will provide crucial infrastructure for collecting and communicating the requisite information. Enforcement mechanisms have been investigated in [106–108] and are out of the scope of this thesis.

Some examples of a range of potential SLAs to support different contexts may include:

- *Ad hoc*: A need for ad hoc spectrum to meet on-demand needs (i.e., not previously anticipated at that location or time) may be satisfied by an SLA that specifies take-it-or-leave-it access terms for potential users.

- *Public Safety*: A special kind of ad hoc spectrum demand may arise in the context

[2]There is an ongoing parallel effort within the IEEE DySPAN-SC P1900.5.2 group to standardize a technology-agnostic model for spectrum access, called Spectrum Consumption Model (SCM) [105].

of public safety users in need of spectrum wherever unpredictable emergencies may occur. In such situations, an SLA may define the rights and terms under which a public safety user may preempt other users [96]. Another use of this may be by unlicensed users who offer to delay their usage (allowing other users to preempt their usage) to reduce potential congestion for higher-value uses. In this way, the SLA might be used to coordinate voluntary sharing among users.

- *High-Traffic Venues*: An important scenario for coordinated spectrum management arises in the context of a stadium, mall, or other high-traffic local area where it is reasonable to expect a large number of diverse wireless devices to congregate. In such environments, spectrum resource capacity constraints are likely to be very important determinants of individual and aggregate wireless performance. A local spectrum manager with authority to centrally manage the spectrum usage of the myriad devices in the local area could significantly improve the performance realized by all users in the locally managed area. A local spectrum manager with local infrastructure (e.g., distributed antennas or small cells, potentially with wired backhaul) and its own spectrum resources may offer differential SLAs to wireless radios in the stadium to induce them to cooperate with the spectrum managers terms and conditions. The control plane would allow radios to express their requirements and capabilities, providing the spectrum manager with the information needed to compute globally optimal spectrum allocations.

- *Service Provider-Customer Infrastructure Sharing*: Today, much of the traffic from smartphones is off-loaded from cellular LTE spectrum to Wi-Fi provided by customer-owned APs connected to wired broadband services. This is a form of infrastructure sharing between heterogeneous network operators. With the growing densification of Wi-Fi APs and LTE base stations and radio devices, there is a growing potential for sharing spectrum and other network capacity (e.g., backhaul, power, computing or storage resources, etc.) among these diverse wireless networks. A control plane could support the design and implementation of flexible SLAs to enable such sharing scenarios.

The Spectrum Access System (SAS) model that is being used for sharing spectrum in the Citizens Broadband Radio Service (CBRS) band at 3.5GHz represents an important step forward to creating a framework that may eventually evolve into a platform for generalized SLA-based sharing. The SAS takes advantage of a database engine to manage sharing among the three tiers of spectrum users that are expected to co-exist in the spectrum: the incumbent users that include satellite and military radar systems and the two tiers of commercial users: the Priority Access License (PAL) and the General Authorized Access (GAA) users. The precise architecture of the SAS is still evolving, but the plan is for there to be multiple SAS managers, administering access across license territories [9]. Precisely how these managers may overlap, the size of the PAL territories, and how PAL and GAA network operators may interact is being developed. What is especially noteworthy about the CBRS tiered usage rights model is that it embraces the potential for multiple classes of users. Although the CBRS identifies three-classes of users, it demonstrates the plausibility of defining additional user classes, further enabling expanded options for distributed spectrum sharing.

4.3 Distributed Spectrum Management Architecture

The proposed dynamic spectrum management architecture (SMAP) is built on a set of standardized APIs and protocol interfaces for wireless devices or networks to report and/or set radio resource parameters over a common control plane for spectrum. The architecture supports exchange of radio usage and control parameters between multiple autonomous wireless domains operating in the same geographic region, thus providing a level of local visibility that enables a range of distributed (and possibly competing) algorithms for mitigating interference. For example, a map of frequencies in use by neighboring systems can be built from control plane information and then used by a newly entering network to implement an autonomous interference avoidance procedure. Further, given the right incentives, networks in a given region can actively collaborate by participating in a cooperative optimization algorithm that sets operating radio parameters over multiple networks to achieve efficiency and fairness while adhering to both global and local policies. In addition to supporting the technical management of

spectrum, these capabilities will also need to support the commercial contracting and regulatory rules that will jointly govern how resources are shared and arrangements are enforced within the SMAP architecture. The architecture also provides a well-defined interface to higher-level cloud services including regional spectrum aggregators/brokers and global spectrum databases (such as Spectrum Observatory [109], SharedSpectrum [110], SpecNet [111] and SAS spectrum assignment server [16]) and policy repositories.

The first design challenge in architecting the SMAP system is that of specifying and instrumenting a control plane for spectrum that harnesses actual spectrum use information and makes it available for interference management at participating wireless networks. Second, once the control plane has been defined, a set of distributed protocols and algorithms is needed to enable fully decentralized yet consistent allocation of radio resources across networks and geographic regions. The third design problem is that of defining collaborative or competitive market mechanisms enabled by cloud-based spectrum aggregators on the control plane. Some of the key technical requirements of the architecture can be summarized as follows:

- *Scalability*, in terms of number of wireless devices (10B today to 100B in 2020), frequency bands to be served (10 GHz), and geographic area to be covered (US land area 10^7 km^2).

- *Decentralization*, allowing for each network entity to make autonomous decisions and/or collaborate without the requirement for a global central controller or database.

- *Hierarchical structure*, with support for mobile devices, base stations or access points, wireless network controllers and cloud-based aggregate spectrum management entities.

- *Radio technology neutrality*, i.e. a uniform set of protocol and API specs that work across multiple radio access technologies such as Wi-Fi, LTE, Bluetooth, Zigbee, and future 5G standards.

- *Support for flexible local and regional policies*, reflecting differences in spectrum

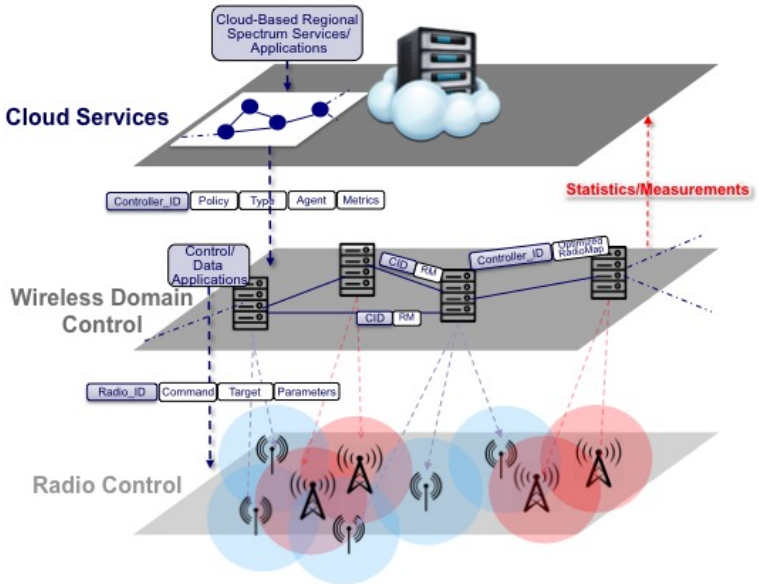

Figure 4.1: Overview of proposed decentralized spectrum management architecture (SMAP)

access rules and optimization criteria by frequency band, geographic region, or network operator.

- *Robustness and security*, providing a degree of immunity against failures in the network or malicious end users or network operators.

Considering the above requirements, we have developed the system concept for SMAP based on the notion of a 3-tier hierarchy corresponding to radio-device level, regional network level, and global cloud-services level distribution of spectrum information, shown in Fig. 5.2. At the lowest level, there is an interface for each radio device to express its current spectrum usage and set its radio operating parameters. The spectrum use information can be made available to neighboring radios via beacons or dedicated wireless control channels where available or can be propagated upward to radio network operators who use a second control interface to express aggregate radio system parameters (also called "RadioMap"). RadioMap information from individual wireless networks is further aggregated at the domain controller level (typically one per autonomous wireless domain (WD), but other mappings such as one per region or group of WDs are also possible). The WD controller is envisioned as a software-defined entity similar in spirit to wired network SDN controllers but with syntax extensions

for handling radio-specific parameters [112–114]. A protocol interface for exchange of RadioMap information between WD controllers and for inter-network policy negotiation (corresponding to the SLAs discussed earlier in Sec.4.2) is also provided at the network peering level as shown. Finally, an additional SLA interface is provided to the cloud-service level which serves roles such as regional spectrum aggregator/broker across multiple domains or as a repository for regional and global policies. As shown in the figure, the information exchanged over these protocol interfaces can be used to run spectrum coordination algorithms and/or market mechanisms either at the individual spectrum controllers or at the cloud servers.

The architecture outlined above enables network owners/operators to obtain an improved view of spectrum use in their region, and then execute either autonomous or cooperative algorithms intended to improve spectrum use and avoid mutual interference. This functionality also supports the commercial and regulatory rule enforcement mechanisms that induce users to comply with the management framework. Various levels of control information described earlier enable devices and networks to respond at whatever level is supported by local policy. For example, radio-level information may be used to directly control frequency or power selection at a neighboring node, while aggregate RadioMap information shared between adjacent networks could be used to run a cooperative optimization algorithm involving multiple networks. The cloud services level can include multiple "spectrum as a service (SpAAS)" offerings including regional spectrum aggregators whose role is to form regional coalitions of wireless domains and perform logically centralized optimization to improve spectrum efficiency and provide participants with improved performance metrics. The SAS [16] is another example of a cloud service which provides a relatively long-term database for spectrum use in shared bands such as the 3.5 GHz "innovation band" or mmWave bands now under consideration by the FCC. In that sense, the SMAP architecture proposed here for enabling distributed spectrum coordination in local regions is complementary and backwards compatible with the centralized SAS database intended to support global coordination at coarser geographic granularity and slower time-scales.

4.3.1 Realizing Local Spectrum Policy in SMAP

Policymakers at the FCC and in regulatory bodies around the world are actively considering a number of shared spectrum bands, including the 3.5GHz, television broadcast, and millimeter wave bands. For economic and technical efficiency, policymakers are seeking to enable mechanisms which can support more fine-grained and dynamic allocation of spectrum resources (in frequency, time, space, etc.) and provide improved support for spectrum secondary markets [115–117]. This includes enabling new business models and new ways to configure, change, and enforce portfolios of spectrum rights, including usage rights. In addition to the technical work to design appropriate metrics for characterizing spectrum usage and information sharing mechanisms to aggregate and share data, the architecture enables sharing of information on non-technical (business/policy-relevant) spectrum characteristics, including the rights bundles associated with the spectrum to be managed. The design of the architecture requires jointly addressing engineering (RF and Internet-related) and economic (business/policy) issues.

Analogous to local policies for BGP path selection in the Internet [97], each participating network in SMAP may have certain local policies corresponding to preferences in frequencies used, technology constraints (power limits, time coordination capability, etc.), multi-homing access technology choices if any, cooperating networks based on business relationships, type of optimization algorithm to be used and so on. At the regional level, each cooperative regional cluster may also express policies such as scope (in terms of area coverage, access technologies, frequency bands, etc.) and type of optimization algorithm used (in terms of metric to be maximized and fairness constraints). There could also be policies related to the data plane, e.g., multi-network access where networks agree to let users migrate across networks during times of congestion. At the same time, there will be a set of top-down global policies as specified by regulatory agencies and spectrum owners, specifying which bands can be used for what purpose and with what radio parameters.

4.4 Use Case Studies

In the following we present a number of use case scenarios which will benefit from SMAP architecture and algorithms.

4.4.1 Cellular/5G Pooling

In this scenario, we have multiple MNOs (e.g., Verizon, AT&T, and Sprint) that each have different portfolios of spectrum resources. For example, each operator has different amounts of exclusively-licensed spectrum in different frequency bands, as well as the right to use unlicensed spectrum in the IS-LM bands and PRI and GAA spectrum in the CBRS band. Their spectrum assets vary by location and their needs for capacity vary with time and by location, due in part to both MNO-specific factors (behavior of their customers, state of their network investment) and external factors impacting all MNOs (aggregate demand shifts, technical innovations).

Traditional models for addressing the need to share wireless network capacity include cellular roaming and sub-leasing arrangements. With traditional cellular roaming, a customer of MNO A is connected to MNO B's network. Such arrangements are common where coverage is lacking (i.e., driven by the need to provide universal access coverage as key feature of the service), but are less common when coverage is available but capacity is lacking (e.g., to sustain QoS for customers when own-resources are insufficient). With sub-leasing arrangements, MNOs may enter into long term contracts for access to spectrum or other infrastructure components. Such sub-leasing arrangements are quite flexible/customizable but are not readily adaptable to (near) real-time capacity needs and are likely to have relatively high transaction costs.

SMAP creates a new way to share peak capacity investments efficiently by allowing spectrum resources to be pooled directly via a (near) real-time market. This expands options for unbundling wireless network infrastructure investments and allowing easier and lower cost matching of aggregate spectrum resources and MNO-specific infrastructure investments and traffic needs. The goal is to allocate the spectrum resource to maximize aggregate spectrum availability.

The model for sharing may draw on the model of peering and paid peering in the Internet: those with resources to share may participate in a revenue-neutral peering whereas those without resources to contribute may need to pay for peering rights. Wireless networks seeking a "transit" type of service may opt for a virtualized roaming service. The fundamental economic thesis is that by pooling peak spectrum capacity to allow optimal assignment, the aggregate scarcity costs associated with spectrum resources are minimized. If the sharing does not shift strategic competitive advantages, then the aggregate benefits create an opportunity for Pareto improving allocation of those scarcity costs. Features of SMAP needed to realize this use case (see Fig. 4.2) are the inter-WD RadioMap exchange, the RNO algorithm for regional optimization between peers, SLA's for supporting agreements between WD peers, local policy for specifying constraints (such as operator preference for use of certain bands), global policies to enable regulatory enforcement (e.g., for antitrust protection), and the optional spectrum broker for computing the logically centralized optimization (LCO). The SLA for supporting this aggregate management of the spectrum resources would reflect an arrangement akin to Tier 1 peering. Each MNO would be modeled as participating in multiple local (but spectrally distant) markets. In each local market, the MNO is represented by a Wireless Domain (WD) controller that would announce its spectrum requirements and capacity via "BGP-like" announcements akin to routing announcements. This would signal the WDs willingness to "sell" and "buy" spectrum resources. A regional controller would optimize the assignment of resources from the pool to the WDs, and with feedback from a cloud-based spectrum broker that would ensure that congestion (scarcity) costs were being fairly allocated across the multiple local areas.

4.4.2 Public Safety Sharing

Communication systems for emergency response require assembling significant capacity in a location on an ad hoc basis citep20. The ability to pool and share resources more flexibly offers numerous potential benefits in terms of enhanced capacity and capabilities, faster response times, and reduced costs. Traditional methods for integrating communications capabilities for first-responders are to establish a Network Operations

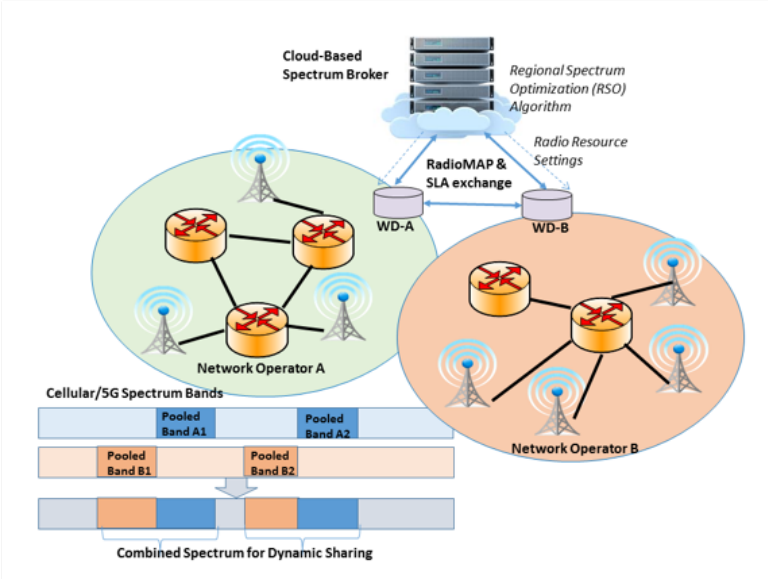

Figure 4.2: Cellular/5G Pooling Scenario

Center (NOC) and to tie together communications infrastructure via gateways. This approach limits options for capacity sharing and consumes scarce resources in enabling the gateways (e.g., bridging voice channels for emergency radio communications).

SMAP provides a platform for flexibly re-assigning spectrum resources among first-responders. Although the need for shared resources may be local and ad hoc in nature (i.e. coordination between WD peers representing locally deployed networks), the management of the interoperability among the different mutual-aid first-responders may also benefit from optional cloud-based coordination. The implementation of SMAP in this context is logically analogous to the case above, but provides more scope for demonstrating the capabilities of SMAP to provide layered local, regional, and global policies (e.g., pre-emption etc.). In the context of a coordinated first-responder situation, there are reduced concerns that competitive interests may lower incentives to cooperate (e.g., regulations may mandate participation), but there are still advantages to allowing local autonomy to enable flexible use of local information for on-site adaptability. The design of the SLAs may focus less on incentive issues, and more on how to structure policies and their enforcement in real-time and on an ad hoc basis.

Features of SMAP useful for the emergency response scenario include (see Fig.

4.3): the inter-WD RadioMap exchange, simple neighbor exchange protocols for ad-hoc coordination between independent first responder networks deployed in the same area, SLA's for supporting agreements between WD peers, local policy for specifying constraints (such as technology constraints and preemptive priority for certain services), and optionally the cloud-based spectrum broker to facilitate interoperability.

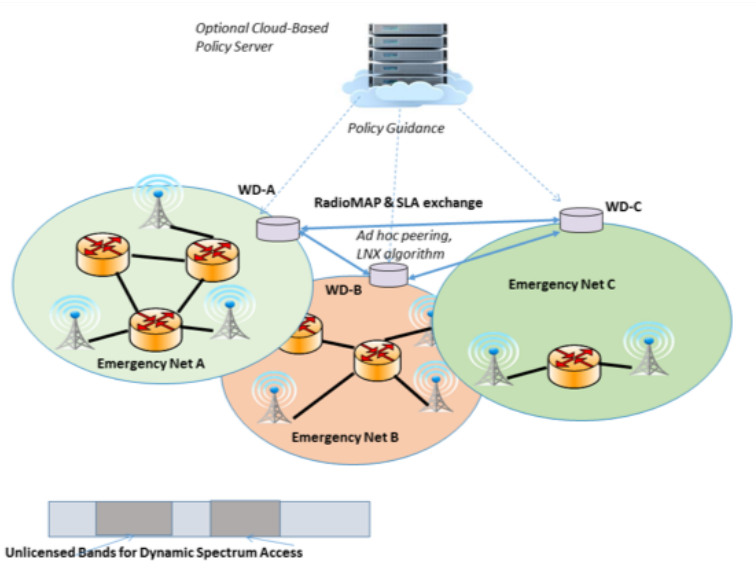

Figure 4.3: Public Safety Scenario

4.4.3 Venue Sharing

In many future wireless scenarios there will be a high density of multiple heterogeneous networks with correlated peak capacity needs in a specific local area where significant elements of the local infrastructure must be shared and may be controlled by the local venue operator. A significant economic motivation for such sharing is to reduce the costs of deploying 5G networks. Examples include stadiums, theaters, malls, and multi-tenant buildings (offices and residences). Today, cooperative sharing across networks is relatively limited in both exclusive-use licensed and unlicensed spectrum.

SMAP allows the venue operator to assume role of local spectrum manager, across multiple bands. Traditional models for band managers have tended to focus on spectrum management within a specific, limited set of spectrum resources. In this case, the

vision is to enable much more flexible options for enabling SpaaS (Spectrum as a Service) and local infrastructure sharing capabilities to be offered by the venue operator. When coupled with SDN capabilities, the SMAP architecture facilitates the implementation of "turn-key" spectrum/local communication resource management "in-a-box" solutions.

The venue serves as a regional coordinator of the multiple WDs (one for each wireless network operator) that wish to operate in the venue. The venue operator offers local coordination/spectrum management capabilities to WDs in the venue. This might involve coordinating and interfacing with multiple (band-specific) band managers (or cloud-based aggregators such as those described in the cellular roaming case study). The SLAs would govern how the local band manager connects logically to different spectrum usage authorities. The coordination service would also deal with multiple radio technologies such as WiFi and LTE operating in the same unlicensed bands.

Features of SMAP that are applicable for this scenario (as shown in Fig. 4.4) are: the cloud-based aggregator for joint control and optimization of local networks, protocol for exchange of RadioMap information and radio resource settings between WD controllers and cloud-based aggregator, the logically centralized optimization service provided by the cloud aggregator, and local policy constraints such as technology or band preferences specified by each operator.

4.4.4 Spectrum Coordination Algorithms

The three-tier architecture of SMAP enables dynamic and distributed spectrum management with functionality split at different hierarchy levels. These range from simple local heuristics at WD controllers to collaborative optimizations across a regional cluster of WD controllers optionally assisted by cloud-based aggregators. The first step in setting up a distributed algorithm in SMAP is the connectivity graph formation and clustering of radio devices. Geographical proximity of radio devices (i.e. access points (APs) or base stations (BSs)) is considered when aggregating APs to a single WD controller. Fig. 4.5 shows the data and control planes associated with the SMAP architecture for a sample of Wi-Fi APs, obtained from an open-access, crowd-sourced

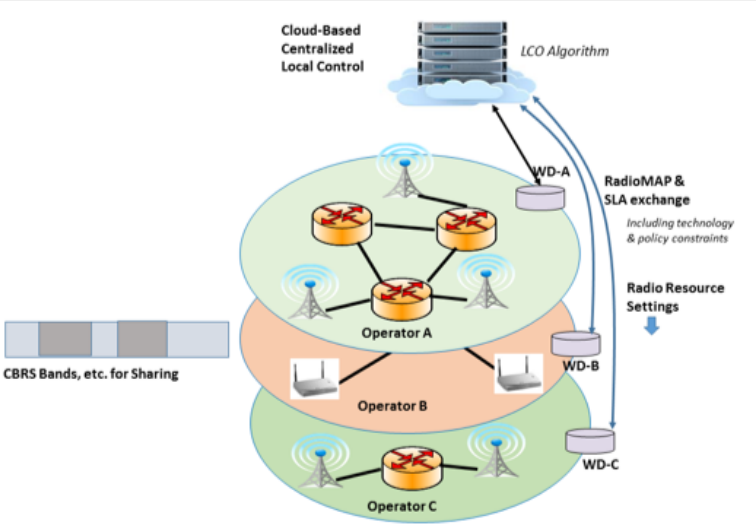

Figure 4.4: Venue Sharing Scenario

dataset "WIGLE" [118]. The lower plane in the diagram shows coverage regions for APs in a given region of the city. The plot is obtained by aggregating an average of 10 APs into each WD represented by a controller on the control plane shown on top. The connectivity graph G = (V,E), defined as a graph with WDs as its vertices and an edge existing between 2 WDs if they have APs within transmission/interference range of one another.

At the simplest level of distributed algorithms, adjacent nodes exchange RadioMap information with neighboring WDs to iteratively assign radio parameters and allocate resources. This class of "local neighbor exchange (LNX)" algorithms has been investigated in the graph theory literature in terms of how closely it can approach centralized algorithms for minimum span graph coloring [119, 120], providing bounds on time complexity of various distributed algorithms[121].

Alternatively, the architecture also supports "regional network optimization (RNO)" in which WDs in a region disseminate RadioMap information over a larger region and use that data to jointly execute more complex distributed algorithms which are formulated to optimize a global utility function such as throughput or fairness. A variety of RNO algorithms are enabled by the SMAP architecture, ranging from iterative optimizations across a hierarchical ordering of WD controllers in the graph to global

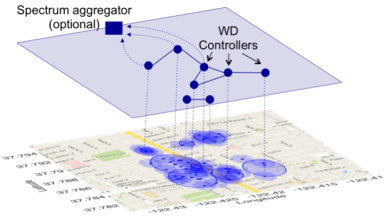

(a) Data Plane Geographic Coverage Area and Control Plane Topology for San Francisco WiFi Access Points Example

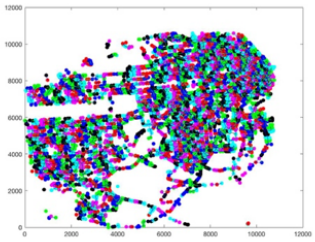

(b) Sample Frequency Assignment

Figure 4.5: WD graph formation

optimization based on full broadcast of topology and RadioMap information to all the nodes, or through the use of a centralized spectrum broker. This centralized case of the RNO algorithm is would be evaluated separately under the "Logically Centralized Optimization (LCO)" algorithms. A description and evaluation of these different classes of algorithms (LNX, RNO and LCO) using experiments and simulation are given as follows.

Local Neighbor Exchange (LNX):

In this algorithm each WD controller exchanges RadioMaps with its immediate one-hop neighbors in the control plane and uses this information to periodically run a local interference avoidance algorithm which sets radio parameters (e.g. frequency, time and power) at radio devices in this domain. After setting the new RadioMap parameters, the WD informs its directly connected neighbors about the new values and this may trigger the iterative computation at these adjacent nodes.

Regional Network Optimization (RNO):

SMAP's flexible interfaces among the cloud services and WD controllers enable more advanced spectrum sharing algorithms, potentially improving on simple one-hop coordination among the neighboring graph nodes. Utilizing the information about the connectivity graph structure provided by a cloud service, like unique identifiers of WD controllers, visibility of node degrees in subgraphs of interest to each node, etc., can

improve the time complexity and convergence of the distributed algorithms. Designing the specific information to be distributed across the network and quantifying the improvement due to this additional information are important aspects to be studied for regional spectrum allocation. An example of the RNO class of algorithms without central coordination is considered next. Firstly since the connectivity graph [3] of WD controllers is not available at each node, a bootstrapping step is required during which each node will construct partial hierarchical ordering of its 1-hop neighbors based on their vertex degree exchanged in initial messaging state. This bootstrapping step can be done either in a fully distributed vertex grouping algorithm or with assistance from a cloud controller with access to the network topology graph. Afterwards, the global function we aim to optimize, whether it is interference avoidance, transmission power, fairness, throughput, etc, will be approximated by a sequence of local optimizations at each individual node interacting with neighboring nodes based on the partial ordering created in the initial bootstrapping step. An overview of the algorithm for the general case of optimizing the global function $F^{glob}(x)$, by partial order execution of optimizing local functions $F^{local}(x)$ is given in Algorithm1.

Algorithm 1 Partial order of execution of coordination algorithm at distributed controllers

1: **procedure** At Master node i
2: Runs optimization algorithm $F_i^{local}(x)$ for its WD
3: Sets optimized radio access parameters
4: Notify updated radio parameters through RadioMaps with neighboring controllers with lower order index
5: Share the list of controllers to whom updated radio state is shared with other neighboring controllers
6: **procedure** At Slave node k
7: Receives update message and its list(neighboring controllers) from higher order controller i
8: If list contains any common neighboring controller with index higher than k, k waits until receives update message from them
9: Runs optimization algorithm $F_k^{local}(x)$, considering the effect of radio parameters at higher order neighboring WD
10: Send update message and list (neighboring lower order controllers at k) to neighboring lower order controllers

[3] defined by a graph with WDs as its vertices and an edge existing between 2 WDs if they have base stations within transmission/interference range of one another

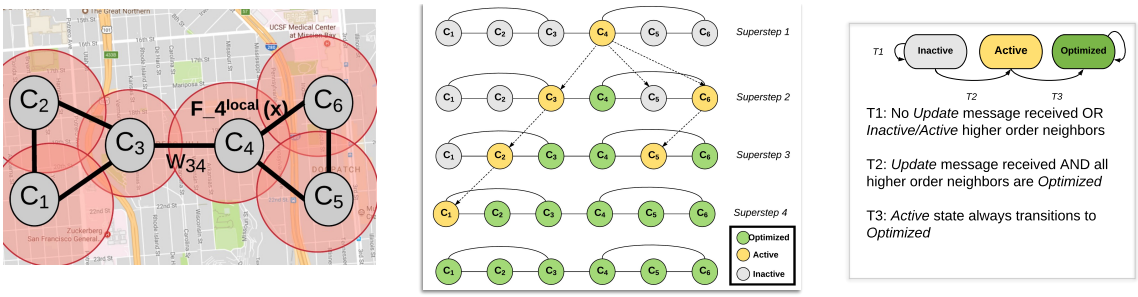

Figure 4.6: Example of execution of the distributed algorithm based on partial ordering. C_i corresponds to controller within WD_i (a) sample topology, (b) supersteps for the sample topology, (c) state machine for WDs

As an example, following is the execution of Algorithm1 with regards to topology given in Fig.4.6 The partial ordering at each node determines the supersteps, during which a group of nodes within the connectivity graph can simultaneously run the local optimization. Fig.4.6 shows the sequence of supersteps for the given topology. During each superstep S each node will be master or slave node based on the partial ordering and the Update message (shown as dotted line) it has received during superstep S-1. During each superstep the master nodes will be at either active or optimized state and the slave nodes will be at inactive state. The vertex state machine along with transition actions is shown in Fig.4.6.

In order to experimentally evaluate the baseline scenario shown in Fig.4.6, we have deployed the graph topology on Sandbox 4 (SB4) in the ORBIT radio testbed [122, 123] for 2 scenarios: 1) homogeneous scenario with all the WDs consisting of one Wi-Fi AP, 2) heterogeneous scenarios as shown in Fig.4.7 There exist tight control of attenuation between each pair of nodes in SB4, allowing for -33 to -96 dB of attenuation, resulting in arbitrary graph topologies [124]. For simplicity each WD only contains one base station/access point. The Wi-Fi link uses 802.11g technology, implemented with Atheros AR928X wireless network adapters (2.4/5 GHz). The eNB-UE pair are equipped with RF front-ends based on Ettus USRP B205mini [125]. For LTE, OpenAirInterface [126] is used, which is an LTE open-source software implementation. The experiments were conducted in the 2.4 GHz unlicensed band, with 20 MHz bandwidth for both Wi-Fi bandwidth and LTE. For traffic generation in all the experiments, *iperf* has been used to measure the downlink TCP application level performance for both Wi-Fi and LTE.

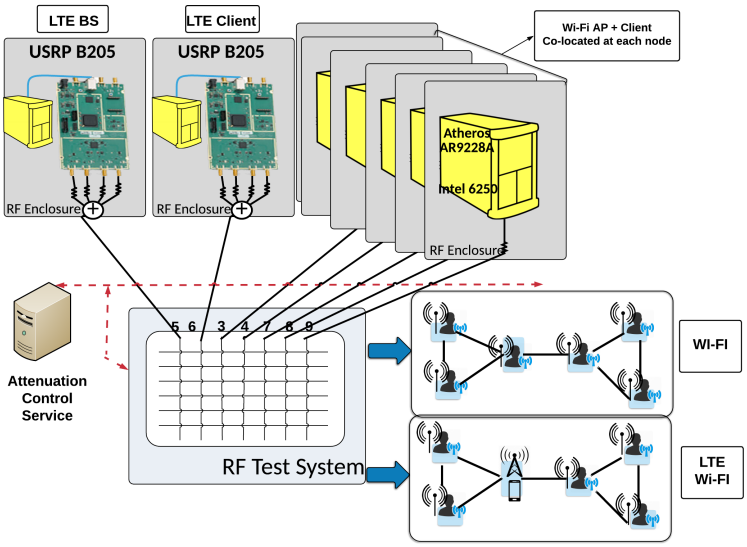

Figure 4.7: Experimental setup in Sandbox 4 of ORBIT testbed, which allows for arbitrary graph topologies between different wireless technologies; Wi-Fi only and Wi-Fi/LTE scenarios.

Fully-Distributed Channel Assignment for Wi-Fi WDs

In this scenario, each WD consists of 1 AP and 1 station (STA) attached to it. The partial order execution of a channel assignment algorithm at each super step is conducted. In the fully-distributed case demonstrated here, each WD controller is in control of AP-STA pair. The distributed algorithm shown in Fig.4.6 is followed and the throughput results for each AP are shown Fig.4.8. In step 1, all the APs are on the same channel. In step 2, WD 4 will select another channel for the AP under its control from the 3 orthogonal channels available to improve its performance. As is seen, in step 2 C4's throughput increases greatly. In this step, C4 announces its operating channels to its neighbors and among its neighbors due to partial ordering, C3 and C6 run their local channel assignment algorithm. Following the same pattern, after step 4, the performance of all the nodes improve significantly.

Distributed channel Assignment for LTE/Wi-Fi WDs

In this benchmark scenario, there are 2 WDs, WD-1 consists of one eNB-UE pair and 2 AP-STA pairs and WD-2 consists of 3 AP-STA pairs, shown in Fig.4.7. In the first step, each WD controller runs a simple frequency allocation algorithm to assign channels to its AP/BSs. In this experiment 2 orthogonal channels for 802.11g (1,11)

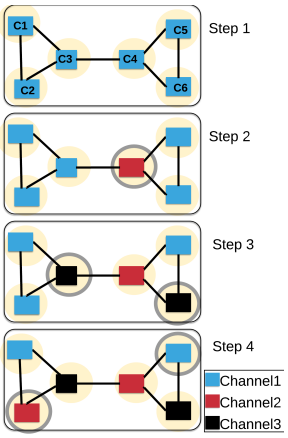

(a) WD connectivity topology, each circled WD is the one optimizing channel assignment at that step

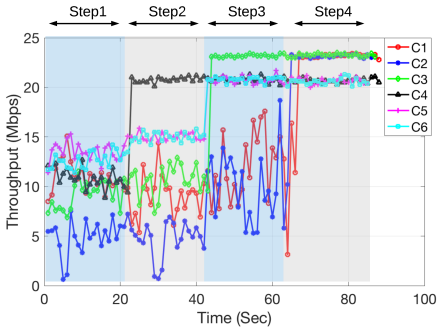

(b) Wi-Fi throughput.

Figure 4.8: Fully-distributed channel assignment for Wi-Fi WDs

are considered. For each WD, the channel assignment problem will result in frequency allocation shown in step 1 of Fig.4.9(a). Since the WD controllers are not exchanging information, they do not take into account the AP/BS in the edge regions.

The scenario depicted in step 1 of Fig.4.9(a) will cause significant performance degradation due to the Wi-Fi AP controlled by C3 and LTE BS controlled by C4 operating on the same channel. This is a result of Wi-Fi and LTE's operation in unlicensed band, which poses significant coexistence challenges for both radio access technologies [95].

The throughput results at step 1 and before information exchange of WDs is shown in Fig.4.9(b). The predicted performance degradation for C3 (AP at the edge) is a result of WD controllers' lack of information about the existence of a Wi-Fi AP and LTE BS operating on the same channel in their overlapping wireless coverage region. In step 2 after WD2 reruns the channel assignment algorithm given the information from WD1 the channel assignment will be as shown in step 2 of Fig. 4.9(a). The throughput results for step 2 are shown in Fig.4.9(b), confirming starvation has been avoided for AP controlled by C3.

Implementing Local Policy with Distributed Control

In this section we consider realization of local policy for a homogeneous Wi-Fi deployment. Similar to the setup in 4.4.4, each Wi-Fi AP will correspond to a wireless

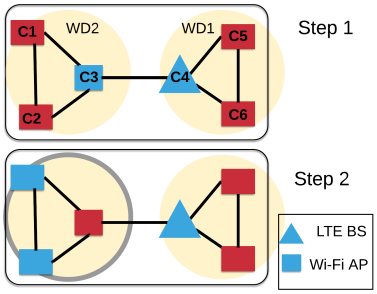

(a) WD connectivity topology, here there are 2 WDs, each controlling 3 AP/BSs

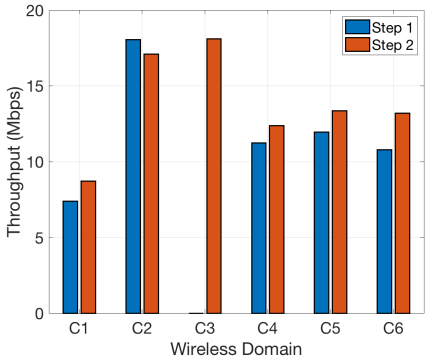

(b) Wi-Fi and LTE throughput

Figure 4.9: Distributed channel assignment for LTE/Wi-Fi WDs

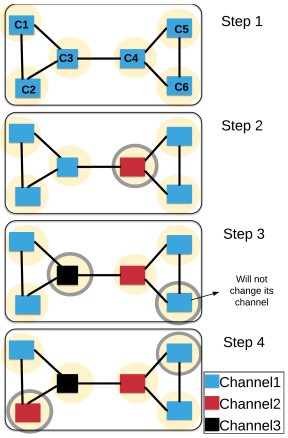

(a) WD connectivity topology, C3 and C4 have access to all the channels, while the rest of WDs only can operate on 2 channels.

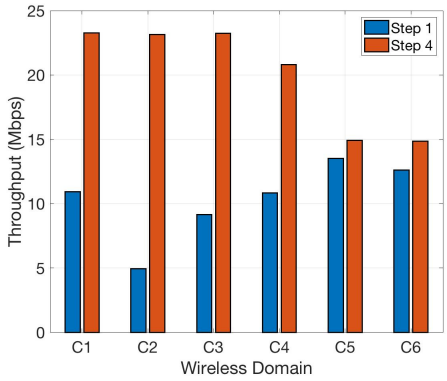

(b) Wi-Fi throughput

Figure 4.10: Local policy realization

domain. Here we consider a scenario common to "disaster provisioning" which might involve pre-empting spectrum for emergency use, for example, in order to establish an emergency Network Operation Center (NOC). In our baseline example, emergency notification services have priority over commercial networks for use of one of the shared unlicensed channels. Hence 2 of the WDs which are to be used by the emergency response network can operate on 3 channels, whereas the other 4 WDs can only access 2 channels. Fig. 4.10 depicts the channel assignment procedure for each step. As can be seen, these results show the feasibility of realizing fine-grained local policies using the distributed control plane in SMAP.

Logically Centralized Optimization (LCO):

We note here that a special case of the RNO algorithm is the scenario in which RadioMap information is broadcast to all WD controllers in the network graph using a flooding protocol similar to link state protocols used for network routing [127, 128]. Alternatively, the same functionality can be provided by a centralized cloud-based "spectrum broker" which is also a part of the SMAP architecture. Such an approach is more consistent with the trend towards software-defined control frameworks such as ONAP and may be a good option for systems with a single domain owner. Availability of full network and radio state makes it possible for each network node to construct the full topology and associated radio parameters for the whole system, thus enabling logically centralized optimization (called LCO) in which operating radio parameters for all the WDs are obtained by formulating a global optimization problem based on system performance metrics such as throughput and/or fairness. The feasibility and effectiveness of this approach has previously been demonstrated for heterogeneous WiFi/LTE deployments in [95].

4.4.5 Large-scale Evaluation

In this section we investigate the performance of the RNO algorithm discussed in Alg. 1 considering a real-world connectivity graph of Wi-Fi APs obtained from an open-access, crowd-sourced dataset "WIGLE" [118], shown in Fig. 4.5(b). In order to create the connectivity graph, we assume APs in $200m \times 200m$ areas to belong to one WD. However, if there exist more than 20 APs in the area we divide the area further not to aggregate more than 20 APs in one WD. These assumptions are dependent on the capabilities of the WD controller and preserving the locality of WDs.

The goal of the WD controllers is to assign channels to the Wi-Fi APs under their control to satisfy their total load. In the simulation, we quantify the load for each WD (L) by the total number of exclusive channels needed for transmission of the total traffic to all their APs. Two scenarios are then considered: 1) Each WD controller picks

channels for APs under its control without any coordination with other controllers. It ensures that within its domain no 2 APs are on the same channel, but does not have information regarding the neighboring APs at the edge of its domain. 2) Following the partial ordering algorithm in Alg. 1, each WD controller will avoid using the frequencies in use by their neighboring WDs. This can be considered as a fully-cooperative scenario, where for example all the WDs belong to the same entity.

Considering the high likelihood of APs in CSMA range of one another sharing a channel as the load increases, we need to compute the channel share each Wi-Fi AP effectively gets. To calculate the approximate channel share for each AP, a common approach is as follows [129]: for each channel, a contention graph of all co-channel APs is considered. For each contention graph, its Maximum Independent Sets (MIS) are found. MIS is defined as the sets with highest number of vertices, no two of which have an edge between them. The channel share for each node (AP) is then given by the ratio of number of MISs the node is a member of to total number of MISs [130]. In order to calculate the MIS for each graph, we used the NetworkX python package [131].

By varying the load from 1 to maximum number of channels available (20), we measure the percentage of total WDs which are able to serve all their load as shown in Fig. 4.11. As can be seen as the system load increases, the RNO algorithm enabled by SMAP's distributed control plane can achieve 20% better performance, compared to non-cooperative channel assignment by WDs.

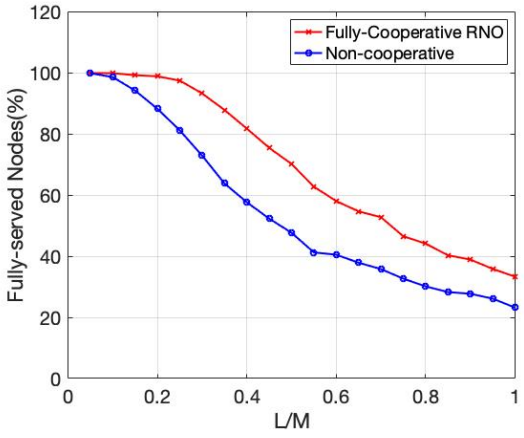

Figure 4.11: Percentage of WDs (out of 1572 as vertices of the real-world connectivity graph of SF Wi-Fi APs) fulfilling their load

Scalability Analysis

In order to evaluate the scalability of the RNO algorithm discussed in Alg. 1, we investigated the number of supersteps it takes for all the nodes in the graph to perform resource allocation once. As shown in the previous section, since the partial ordering ensures conflict-free resource allocation among neighboring nodes, one round of the RNO algorithm should result in better performance than non-cooperative scenarios. In the simulation we have generated arbitrary graphs, with their size (total number of nodes) increasing from 10 to 10000. The number of supersteps for completing one round of the RNO algorithm is plotted in Fig.4.12, considering different average node degrees ranging from 2 to 10 in steps of 2. As is shown, the number of supersteps required remains small and increases slowly (log relationship) with the size of the network.

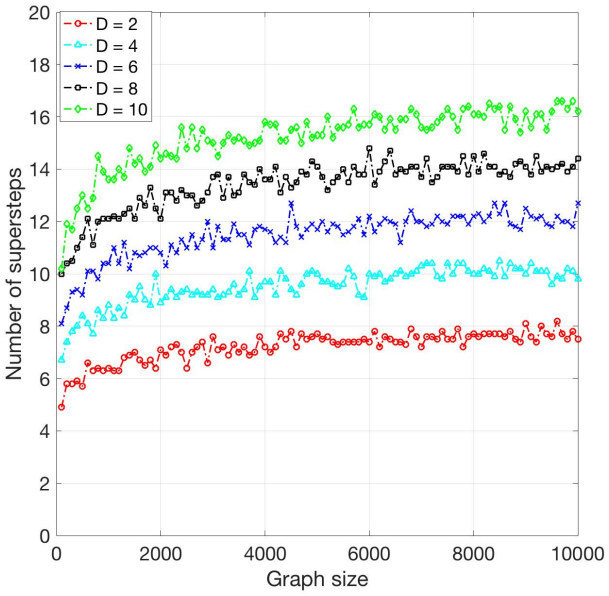

Figure 4.12: RNO Algorithm Convergence

4.5 Related Work

Since 2002, policymakers in the United States and elsewhere have recognized the importance of expanding options for dynamic spectrum sharing by shifting responsibility for spectrum management to market mechanisms [116]. This includes sharing among

commercial and government users, and increasingly, across heterogeneous networks, operating in the same spectrum but with different technologies and under different regulatory requirements [132]. Within the technical and policy community, significant work has addressed the challenges of promoting expanded sharing and in designing a roadmap for the research challenges that need to be addressed to advance this agenda [133, 134]. More recent work applying insights gained from the economics literature on the management of common pool resources highlights the value of adopting technical solutions that enable more flexible and adaptive mechanisms for managing spectrum [99]. The control plane architecture discussed herein represents a necessary first step toward creating the technical capabilities that are required to enable more flexible and adaptive spectrum governance that can span multiple regulatory frameworks (from licensed to unlicensed to multi-tier sharing), business models, and market needs.

Various dynamic spectrum management architectures and protocols have been proposed and investigated over the past few years. In general, two distinct approaches have been explored for spectrum management - centralized and distributed:

Centralized management: Earlier efforts towards achieving centralized coordination of spectrum have primarily been based on the concept of a *spectrum server*, responsible for allocating radio system parameters and controlling access at a regional scale. Several variants of the spectrum server approach have been proposed in the research literature [135–137], including schemes, such as DIMSUMnet [138], in which a regional "spectrum broker" provides centralized assignment of statistically multiplexed frequency resources across a given area. Dynamic Spectrum Access Protocol (DSAP) [139] introduces the concept of a centralized spectrum server for spectrum access and provides proof-of-concept validation of improved performance due to globally coordinated allocation of radio parameters for dense and local scenarios. More recently, a centralized *spectrum access system* (SAS) [16] has been proposed for the 3.5-3.7 GHz band being considered for shared use by three tiers of services (legacy, priority, and general)[140]. In [9] authors propose an end-to-end architecture for implementation of SAS.

Distributed coordination: The concept of a common spectrum coordination channel (CSCC) was proposed in [141] for distributed information exchange over separate control radio channel. Some recent papers on distributed control have focused on a single technology, like LTE [142–144] or Wi-Fi [17, 145, 146]. The authors in [147] introduce separation of network services from underlying physical infrastructure through a software defined control plane for heterogeneous networks. However, the main network services considered in that work are security and mobility management rather than spectrum. Other papers on this topic have addressed various aspects of wireless network management ranging from resource management, spectrum allocation and interference avoidance [148], load balancing, seamless mobility-handover, Quality-of-Service and traffic engineering [149, 150]. The SMAP architecture presented in this chapter is one of the first complete system architecture and policy contributions on the topic of fully distributed spectrum management. It is also the first work to show how local policy can be incorporated into distributed spectrum sharing.

4.6 Conclusion

This chapter has presented the policy and technology case for a distributed control plane that supports scalable and flexible spectrum coordination between wireless networks in a given region. The proposed SMAP architecture provides a generalized SLA interface for exchange of technical radio parameters to peer networks as well as for establishing policy and market mechanisms in a flexible way. Three classes of algorithms enabled at various hierarchical levels of SMAP are presented. We then present the feasibility and performance of deployment of SMAP's control plane on the ORBIT testbed for different scenarios including heterogeneous wireless technologies and incorporating policy to spectrum access. Through large-scale simulation, the spectrum efficiency gains using SMAP's distributed control plane is demonstrated. Finally, the scalability of a sample distributed algorithm with the growing size and connectivity level of the graph is shown.

Bibliography

[1] Cisco, "Cisco visual networking index: Global mobile data traffic forecast update, 2016,2021," white Paper, 2017.

[2] L. telcom AG, "When will exponential mobile growth stop?" 2017, white Paper.

[3] "Ericsson mobility report," www.ericsson.com/assets/local/mobility-report/documents/2018/ericsson-mobility-report-november-2018.pdf.

[4] 3GPP TS 38.201, "3rd generation partnership project; technical specification group radio access network; nr; physical layer; general description (release 15)," 2017.

[5] Cisco, "IEEE 802.11ax: The sixth generation of Wi-Fi," technical White Paper.

[6] Q. Peng, A. Walid, J. Hwang, and S. H. Low, "Multipath TCP: Analysis, design, and implementation," *IEEE/ACM ToN*, 2016.

[7] A. Langley, A. Riddoch, A. Wilk, A. Vicente, C. Krasic, D. Zhang, F. Yang, F. Kouranov, I. Swett, J. Iyengar *et al.*, "The QUIC transport protocol: Design and internet-scale deployment," in *Proceedings of the Conference of the ACM Special Interest Group on Data Communication*. ACM, 2017, pp. 183–196.

[8] F. M. Abinader, E. P. L. Almeida, F. S. Chaves, A. M. Cavalcante, R. D. Vieira, R. C. D. Paiva, A. M. Sobrinho, S. Choudhury, E. Tuomaala, K. Doppler, and V. A. Sousa, "Enabling the coexistence of lte and wi-fi in unlicensed bands," *IEEE Communications Magazine*, 2014.

[9] C. W. Kim, J. Ryoo, and M. M. Buddhikot, "Design and implementation of an end-to-end architecture for 3.5 GHz shared spectrum," in *2015 IEEE International Symposium on Dynamic Spectrum Access Networks (DySPAN)*, 2015.

[10] 3GPP TS 38.401, "NG-RAN; architecture description," 2018.

[11] G. Yuan, X. Zhang, W. Wang, and Y. Yang, "Carrier aggregation for LTE-advanced mobile communication systems," *IEEE Communications Magazine*, 2010.

[12] D. Lecompte and F. Gabin, "Evolved multimedia broadcast/multicast service (embms) in lte-advanced: overview and rel-11 enhancements," *IEEE Communications Magazine*, 2012.

[13] 3GPP TR 36.889 V13.0.0, "3rd Generation Partnership Project; Technical Specification Group Radio Access Network; Study on Licensed-Assisted Access to Unlicensed Spectrum; (Rel13)."

[14] Huawei Technology Co. Ltd, "U-LTE: Unlicensed spectrum utilization of lte," 2014, white paper.

[15] "MultiFire: LTE-like performance with Wi-Fi-like deployment simplicity." www.qualcomm.com/invention/5g/spectrum-sharing/multefire, 2019.

[16] SAS, "Google spectrum database," https://www.google.com/get/spectrumdatabase/.

[17] K.-K. Yap, M. Kobayashi, D. Underhill, S. Seetharaman, P. Kazemian, and N. McKeown, "The stanford openroads deployment," in *In Proc of the ACM WINTECH*, 2009.

[18] S. Mukherjee, A. Baid, I. Seskar, and D. Raychaudhuri, "Network-assisted multihoming for emerging heterogeneous wireless access scenarios," in *IEEE PIMRC*, 2014.

[19] K.-K. Yap, T.-Y. Huang, M. Kobayashi, Y. Yiakoumis, N. McKeown, S. Katti, and G. Parulkar, "Making use of all the networks around us: A case study in android," in *ACM CellNet*, 2012.

[20] "Google Project fi," https://fi.google.com.

[21] "Apple Sim," https://www.apple.com/ipad/apple-sim.

[22] "E-sim technology," https://www.engadget.com/2015/07/16/apple-samsung-e-sim.

[23] H. Balakrishnan, V. N. Padmanabhan, S. Seshan, and R. H. Katz, "A comparison of mechanisms for improving tcp performance over wireless links," *IEEE/ACM ToN*, 1997.

[24] D. Wischik, C. Raiciu, A. Greenhalgh, and M. Handley, "Design, implementation and evaluation of congestion control for multipath tcp," in *USENIX NSDI*, 2011.

[25] L. Li, K. Xu, T. Li, K. Zheng, C. Peng, D. Wang, X. Wang, M. Shen, and R. Mijumbi, "A measurement study on multi-path tcp with multiple cellular carriers on high speed rails," in *Proceedings of the 2018 Conference of the ACM Special Interest Group on Data Communication*, ser. SIGCOMM '18. New York, NY, USA: ACM, 2018, pp. 161–175.

[26] Z. Yuan, Q. Li, Y. Li, S. Lu, C. Peng, and G. Varghese, "Resolving policy conflicts in multi-carrier cellular access," in *Proceedings of the 24th Annual International Conference on Mobile Computing and Networking*. ACM, 2018, pp. 147–162.

[27] Y. Li, H. Deng, C. Peng, Z. Yuan, G.-H. Tu, J. Li, and S. Lu, "iCellular: Device-customized cellular network access on commodity smartphones," in *USENIX NSDI*, 2016.

[28] Y. Lim, Y. Chen, E. M. Nahum, D. Towsley, and K. Lee, "Cross-layer path management in multi-path transport protocol for mobile devices," in *IEEE INFOCOM*, 2014.

[29] S. Kandula, K. C.-J. Lin, T. Badirkhanli, and D. Katabi, "FatVAP: Aggregating AP Backhaul Capacity to Maximize Throughput," in *USENIX NSDI*, 2008.

[30] A. Ford, C. Raiciu, M. Handley, and O. Bonaventure, "TCP Extensions for Multipath Operation with Multiple Addresses," IETF RFC 6824, Oct. 2015.

[31] A. Venkataramani, J. Kurose, D. Raychaudhuri, and K. Nagaraja, "Mobilityfirst: A mobility-centric and trustworthy internet architecture," *SIGCOMM Comput. Commun. Rev.*, 2014.

[32] S. C. Nelson, G. Bhanage, and D. Raychaudhuri, "GSTAR: Generalized storage-aware routing for mobilityfirst in the future mobile internet," in *Proceedings of the Sixth International Workshop on MobiArch*, ser. MobiArch '11. New York, NY, USA: ACM, 2011, pp. 19–24.

[33] M. Li, D. Agrawal, D. Ganesan, and A. Venkataramani, "Block-switched networks: A new paradigm for wireless transport," in *Proceedings of the 6th USENIX Symposium on Networked Systems Design and Implementation*, ser. NSDI'09. Berkeley, CA, USA: USENIX Association, 2009, pp. 423–436.

[34] "3GPP specifications. ts 36.211 to 36.213, 2015."

[35] J. Gettys and K. Nichols, "Bufferbloat: Dark buffers in the internet," *Queue*, 2011.

[36] "ns-3," www.nsnam.org.

[37] N. Baldo, "The ns-3 lte module by the lena project."

[38] H. Tazaki, F. Uarbani, E. Mancini, M. Lacage, D. Camara, T. Turletti, and W. Dabbous, "Direct code execution: Revisiting library os architecture for reproducible network experiments," in *ACM CoNEXT*, 2013.

[39] "Linuxwireless ath9k," https://wireless.wiki.kernel.org/en/users/drivers/ath9k.

[40] "hostapd: IEEE 802.11 ap, ieee 802.1x/wpa/wpa2/eap/radius authenticator," http://w1.fi/hostapd/.

[41] "MultiPath TCP - Linux Kernel implementation," Accessed: 2018-01-21.

[42] F. Bronzino, K. Nagaraja, I. Seskar, and D. Raychaudhuri, "Network service abstractions for a mobility-centric future internet architecture," in *ACM MobiArch*, 2013.

[43] 3GPP TS 36.300 v14.0.3, "3rd generation partnership project; technical specification group radio access network; evolved universal terrestrial radio access (E-UTRA) and evolved universal terrestrial radio access network (E-UTRAN); overall description; stage 2 (rel14)."

[44] R. Chandra and P. Bahl, "Multinet: connecting to multiple ieee 802.11 networks using a single wireless card," in *IEEE INFOCOM*, 2004.

[45] A. Croitoru, D. Niculescu, and C. Raiciu, "Towards Wi-Fi mobility without fast handover," in *USENIX NSDI*, 2015.

[46] K. Chebrolu, B. Raman, and R. R. Rao, "A network layer approach to enable TCP over multiple interfaces," *Wirel. Netw.*, 2005.

[47] F. Lu, H. Du, A. Jain, G. M. Voelker, A. C. Snoeren, and A. Terzis, "CQIC: Revisiting cross-layer congestion control f or cellular networks," in *HotMobile*, 2015.

[48] X. Xie, X. Zhang, S. Kumar, and L. E. Li, "piStream: Physical layer informed adaptive video streaming over lte," in *ACM MobiCom*, 2015.

[49] R. Izard, A. Hodges, J. Liu, J. Martin, K.-C. Wang, and K. Xu, *An OpenFlow Testbed for the Evaluation of Vertical Handover Decision Algorithms in Heterogeneous Wireless Networks*, 2014.

[50] C.-L. Tsao and R. Sivakumar, "On effectively exploiting multiple wireless interfaces in mobile hosts," in *CoNEXT*, 2009.

[51] C. Raiciu, C. Paasch, S. Barre, A. Ford, M. Honda, F. Duchene, O. Bonaventure, and M. Handley, "How hard can it be? designing and implementing a deployable multipath tcp," in *USENIX NSDI*, 2012.

[52] S. Deng, R. Netravali, A. Sivaraman, and H. Balakrishnan, "WiFi, LTE, or both?: Measuring multi-homed wireless internet performance," in *Proceedings of the 2014 Conference on Internet Measurement Conference*, 2014.

[53] Y. Chen, "A measurement-based study of multipath tcp performance over wireless networks," in *Proceedings of the 2013 Conference on Internet Measurement Conference*, 2013.

[54] B. Sonkoly, F. Nemeth, L. Csikor, L. Gulyas, and A. Gulyas, "SDN based testbeds for evaluating and promoting multipath TCP," in *2014 IEEE International Conference on Communications (ICC)*, 2014.

[55] "Open-access research testbed for next-generation wireless networks (orbit)," http://www.orbit-lab.org/.

[56] 3GPP TS 36.300, "Evolved universal terrestrial radio access (E-UTRA) and evolved universal terrestrial radio access network (E-UTRAN); overall description; stage 2," 2017.

[57] J.-m. Lin, "Method of single-cell point-to-multipoint transmission," August 2016.

[58] Qualcomm Technologies Inc, "Accelerating the mobile ecosystem expansion in the 5G Era with LTE Advanced Pro," 2018.

[59] "Enhanced television services over 3gpp embms," www.3gpp.org/news-events/3gpp-news/1905-embms_r14.

[60] S. Mukherjee, F. Bronzino, S. Srinivasan, J. Chen, and D. Raychaudhuri, "Achieving scalable push multicast services using global name resolution," in *2016 IEEE Global Communications Conference (GLOBECOM)*, 2016.

[61] "Verizon, Telstra and EE launch LTE-Broadcast alliance," https://www.fiercewireless.com/tech/verizon-telstra-kt-and-ee-launch-lte-broadcast-alliance, LTE-B.

[62] J. Erman and K. Ramakrishnan, "Understanding the super-sized traffic of the super bowl," in *Proceedings of the 2013 Conference on Internet Measurement Conference*. ACM, 2013.

[63] "5g-xcast: Broadcast and multicats communication enablers for fifth-generation of wireless systems, horizon-2020," https://http://5g-xcast.eu/, 5Gxcast.

[64] L. Zhang, D. Estrin, J. Burke, V. Jacobson, J. Thornton, D. Smetters, B. Zhang, G. Tsudik, D. Massey, C. Papadopoulos *et al.*, "Named data networking (ndn) project," *Relatório Técnico NDN-0001, Xerox Palo Alto Research Center-PARC*, 2010.

[65] D. Raychaudhuri, K. Nagaraja, and A. Venkataramani, "Mobilityfirst: a robust and trustworthy mobility-centric architecture for the future internet," *ACM SIGMOBILE Mobile Computing and Communications Review*, 2012.

[66] F. Bronzino, S. Mukherjee, and D. Raychaudhuri, "The named-object abstraction for realizing advanced mobility services in the future internet," in *Proceedings of the Workshop on Mobility in the Evolving Internet Architecture*, 2017.

[67] J. Chen, H. Xu, Y. Zhang, and D. Raychaudhuri, "Graph-pubsub: An efficient pub/sub architecture with graph-based information relationship," in *Proceedings of the Fifth ACM/IEEE Workshop on Hot Topics in Web Systems and Technologies*, 2017.

[68] J. Huang, F. Qian, A. Gerber, Z. M. Mao, S. Sen, and O. Spatscheck, "A close examination of performance and power characteristics of 4G LTE networks," in *Proceedings of the 10th international conference on Mobile systems, applications, and services*. ACM, 2012, pp. 225–238.

[69] S. Sesia, M. Baker, and I. Toufik, *LTE-the UMTS long term evolution: from theory to practice*. John Wiley & Sons, 2011.

[70] G. T. 38.321, "Technical specification group radio access network; nr; medium access control (mac) protocol specification (release 15)," 2018.

[71] F. Capozzi, G. Piro, L. A. Grieco, G. Boggia, and P. Camarda, "Downlink packet scheduling in lte cellular networks: Key design issues and a survey," *IEEE Communications Surveys Tutorials*, vol. 15, no. 2, pp. 678–700, Second 2013.

[72] S. . Lee, S. Choudhury, A. Khoshnevis, S. Xu, and S. Lu, "Downlink mimo with frequency-domain packet scheduling for 3gpp lte," in *IEEE INFOCOM 2009*, April 2009, pp. 1269–1277.

[73] O. Grndalen, A. Zanella, K. Mahmood, M. Carpin, J. Rasool, and O. N. sterb, "Scheduling policies in time and frequency domains for lte downlink channel: A performance comparison," *IEEE Transactions on Vehicular Technology*, vol. 66, no. 4, pp. 3345–3360, April 2017.

[74] K. Sundaresan and S. Rangarajan, "Video multicasting with channel diversity in wireless ofdma networks," *IEEE Transactions on Mobile Computing*, vol. 13, no. 12, pp. 2919–2932, Dec 2014.

[75] Rohde & Schwarz, "LTE-Advanced pro introduction eMBB technology components in 3GPP release 13/14," white Paper.

[76] J. Chen, M. Chiang, J. Erman, G. Li, K. K. Ramakrishnan, and R. K. Sinha, "Fair and optimal resource allocation for lte multicast (embms): Group partitioning and dynamics," in *2015 IEEE Conference on Computer Communications (INFOCOM)*, 2015.

[77] R. Kwan, C. Leung, and J. Zhang, "Proportional fair multiuser scheduling in lte," *IEEE Signal Processing Letters*, vol. 16, no. 6, pp. 461–464, June 2009.

[78] A. Stolyar, "On the asymptotic optimality of the gradient scheduling algorithm for multi-user throughput allocation," *Operations Research*, vol. 53, 2005.

[79] Y. Huang, S. Li, Y. T. Hou, and W. Lou, "GPF: A GPU-based design to achieve 100 μs scheduling for 5G NR," in *Proceedings of the 24th Annual International Conference on Mobile Computing and Networking*, ser. MobiCom '18. New York, NY, USA: ACM, 2018, pp. 207–222.

[80] "Bell number," https://en.wikipedia.org/wiki/Bell_number.

[81] M. Kaneko, P. Popovski, and J. Dahl, "Proportional fairness in multi-carrier system with multi-slot frames: upper bound and user multiplexing algorithms,"

IEEE Transactions on Wireless Communications, vol. 7, no. 1, pp. 22–26, Jan 2008.

[82] ——, "Proportional fairness in multi-carrier system: upper bound and approximation algorithms," *IEEE Communications Letters*, vol. 10, no. 6, pp. 462–464, June 2006.

[83] 3GPP TS 38.214 version 15.2.0 Release 15, "5G; NR; physical layer procedures for data."

[84] A. Asadi, Q. Wang, and V. Mancuso, "A survey on device-to-device communication in cellular networks," *IEEE Communications Surveys Tutorials*, vol. 16, no. 4, pp. 1801–1819, Fourthquarter 2014.

[85] J. Chen, M. Arumaithurai, L. Jiao, X. Fu, and K. K. Ramakrishnan, "COPSS: An efficient content oriented publish/subscribe system," in *2011 ACM/IEEE Seventh Symposium on Architectures for Networking and Communications Systems*, 2011.

[86] O. Hahm, C. Adjih, E. Baccelli, T. Schmidt, , and M. Wählisch, "A case for time slotted channel hopping for icn in the iot," 2016.

[87] P. Kietzmann, C. Gündoğan, T. Schmidt, O. Hahm, and M. Wählisch, "The need for a name to mac address mapping in ndn: Towards quantifying the resource gain," in *Proceedings of the 4th ACM Conference on Information-Centric Networking*, ser. ICN '17, 2017.

[88] M. Li, D. Pei, X. Zhang, B. Zhang, and K. Xu, "NDN live video broadcasting over wireless LAN," in *2015 24th International Conference on Computer Communication and Networks (ICCCN)*, 2015.

[89] A. Guardado, Z. Ye, H. Guo, L. Liu, L. Xie, and A. Ito, "Ndnwifi: Named data networking enabled wifi in challenged communication environments," in *2016 IEEE Globecom Workshops (GC Wkshps)*, 2016.

[90] O. Ileri and N. B. Mandayam, "Dynamic spectrum access models: Toward an

engineering perspective in the spectrum debate," in *IEEE Communications Magazine*, 2008.

[91] Qualcomm Technologies Inc, "Making the best use of unlicensed spectrum for 1000x," 2015, white paper.

[92] Q. T. Inc, "Making 5G NR a reality," 2016, white paper.

[93] W. Lehr and L. W. McKnight, "Wireless internet access: 3G vs. WiFi?" in *Telecommunications Policy*, 2003.

[94] Z. Guan *et al.*, "CU-LTE: Spectrally-efficient and fair coexistencebetween LTE and Wi-Fi in unlicensed bands," in *IEEE INFOCOM*, 2016.

[95] S. Sagari, S. Baysting, D. Saha, I. Seskar, W. Trappe, and D. Raychaudhuri, "Coordinated dynamic spectrum management of LTE-U and Wi-Fi networks," in *IEEE DySPAN*, 2015.

[96] W. Lehr and N. Jesuale, "Public safety radios must pool spectrum," in *IEEE Communications Magazine*, 2009.

[97] M. Caesar and J. Rexford, "BGP routing policies in ISP networks," in *IEEE Network*, 2005.

[98] M. Schapira, Y. Zhu, and J. Rexford, "Putting BGP on the right path: A case for next-hop routing," in *ACM HotNets*, 2010.

[99] M. Weiss, W. Lehr, A. Acker, and M. Gomez, "Socio-technical considerations for spectrum access system (SAS) design," in *IEEE DySPAN,2015.*

[100] H. Zhou, R. Berry, M. L. Honig, and R. Vohra, "Complexity of allocation problems in spectrum markets with interference complementarities," in *IEEE J. Sel. Areas Commun*, 2013.

[101] R. Berry, M. L. Honig, and R. Vohra, "Spectrum markets: Motivation, challenges, implications," in *IEEE Commun. Mag.*, 2010.

[102] A. Baid, M. Schapira, I. Seskar, J. Rexford, and D. Raychaudhuri, "Network cooperation for client-AP association optimization," in *IEEE WiOpt*, 2012.

[103] W. Lehr and M. Oliver, "Small cells and the mobile broadband ecosystem," in *Euro ITS Conference*, 2014.

[104] T. Nguyen, H. Zhou, R. A. Berry, M. L. Honig, and R. Vohra, "The impact of additional unlicensed spectrum on wireless services competition," in *IEEE DySPAN*, 2011.

[105] J. Stine and C. Caicedo, "Enabling spectrum sharing via spectrum consumption models," *IEEE Journal on Selected Areas in Communications*, vol. PP, p. 1, 01 2015.

[106] M. M. Buddhikot, "Understanding dynamic spectrum access: Models,taxonomy and challenges," in *2007 2nd IEEE International Symposium on New Frontiers in Dynamic Spectrum Access Networks*, April 2007, pp. 649–663.

[107] M. B. H. Weiss, W. Lehr, M. Altamimi, and L. Cui, "Enforcement in dynamic spectrum access systems," *TRPC*, 2012.

[108] A. Dutta and M. Chiang, ""see something, say something" crowdsourced enforcement of spectrum policies," *IEEE Transactions on Wireless Communications*, vol. 15, no. 1, pp. 67–80, 2016.

[109] "Microsoft spectrum observatory," http://observatory.microsoftspectrum.com/.

[110] "Shared spectrum company," http://www.sharedspectrum.com/.

[111] R. Murty, R. Chandra, T. Moscibroda, and P. Bahl, "Senseless: A database-driven white spaces network," in *IEEE Transactions on Mobile Computing*, 2012.

[112] L. E. Li, Z. M. Mao, and J. Rexford, "Toward software-defined cellular networks," in *European Workshop on Software Defined Networking*, 2012.

[113] N. Feamster, J. Rexford, and E. Zegura, "The road to SDN," in *ACM Queue - Large-Scale Implementations*, 2013.

[114] A. Zubow, M. Döring, M. Chwalisz, and A. Wolisz, "A SDN approach to spectrum brokerage in infrastructure-based cognitive radio networks," in *IEEE DySpan*, 2015.

[115] "Presidential memorandum: Unleashing the wireless broadband revolution," http://www.whitehouse.gov/the-press-office/presidential-memorandum-unleashing-wireless-broadband-revolution.

[116] "FCC spectrum policy task force," Spectrum Policy Task Force Report, ET Docket, no. 03-237, 2002.

[117] "Presidents council of advisors on science and technology," http://www.whitehouse.gov/sites/default/files/microsites/ostp/pcast-spectrum-report-final-july-20-2012.pdf.

[118] WiGLE, "Wireless geographic logging engine," https://wigle.net.

[119] T. Jensen and B. Toft, *Graph coloring problems*. John Wiley & Sons, 2011, vol. 39.

[120] "An on-line graph coloring algorithm with sublinear performance ratio," *Discrete Mathematics*, vol. 75, no. 1, pp. 319 – 325, 1989.

[121] F. Kuhn and R. Wattenhofer, "On the complexity of distributed graph coloring," in *Proceedings of the Twenty-fifth Annual ACM Symposium on Principles of Distributed Computing*, ser. PODC '06. New York, NY, USA: ACM, 2006, pp. 7–15.

[122] D. Raychaudhuri, I. Seskar, M. Ott, S. Ganu, K. Ramachandran, H. Kremo, R. Siracusa, H. Liu, and M. Singh, "Overview of the orbit radio grid testbed for evaluation of next-generation wireless network protocols," in *IEEE WCNC*, 2005.

[123] "Hardware configuration of sandbox 4," http://www.orbit-lab.org/wiki/Hardware/bDomains/cSandboxes/dSB4#SB4, Accessed: 2018-01-21.

[124] P. Karimi, S. Mukherjee, J. Kolodziejski, I. Seskar, and D. Raychaudhuri, "Measurement based mobility emulation platform for next generation wireless networks," in *IEEE CNERT workshop colocated with INFOCOM*, 2018.

[125] "Ettus research, "usrp b200 and b210"," http://tinyurl.com/k7w6zh2.

[126] N. Nikaein, M. K. Marina, S. Manickam, A. Dawson, R. Knopp, and C. Bonnet, "Openairinterface: A flexible platform for 5g research," *SIGCOMM Comput. Commun. Rev.*, 2014.

[127] J. Moy, "OSPF version 2," Tech. Rep., 1997.

[128] P. Jacquet, "Optimized link state routing protocol (olsr)," 2003.

[129] S. C. Liew, C. H. Kai, H. C. Leung, and P. Wong, "Back-of-the-envelope computation of throughput distributions in csma wireless networks," *IEEE Transactions on Mobile Computing*, vol. 9, no. 9, pp. 1319–1331, Sept 2010.

[130] A. Baid, "Dynamic spectrum management architecture and algorithms for the future mobile internet," 2014, phD Thesis.

[131] "Networkx - software for complex networks," https://networkx.github.io.

[132] Executive Office of the President, President's Council of Advisors on Science and Technology (PCAST), "Report to the president realizing the full potential of government-held spectrum to spur economic growth," 2012.

[133] S. Bhattarai, J. J. Park, B. Gao, K. Bian, and W. Lehr, "An overview of dynamic spectrum sharing: Ongoing initiatives, challenges, and a roadmap for future research," in *IEEE Transactions on Cognitive Communications and Networking*, 2016.

[134] NITRD Wireless Spectrum R and D (WSRD) Senior Steering Group, "Promoting economic efficiency in spectrum use: the economic and policy research agenda," in *Group Workshop Report*, 2013.

[135] O. Ileri, D. Samardzija, T. Sizer, and N. B. Mandayam, "Demand responsive pricing and competitive spectrum allocation via a spectrum server," in *IEEE DySPAN*, 2005.

[136] IETF PAWS, "The IEEE 802.22 WRAN standard and its interface to the white space database: Requirements for PAWS," working Group Meeting.

[137] R. Murty, R. Chandra, T. Moscibroda, and P. Bahl, "Senseless: A database-driven white spaces network," *IEEE Transactions on Mobile Computing*, 2012.

[138] M. M. Buddhikot, P. Kolodzy, S. Miller, K. Ryan, and J. Evans, "DIMSUMnet: new directions in wireless networking using coordinated dynamic spectrum," in *IEEE WoWMoM*, 2005.

[139] V. Brik, E. Rozner, S. Banerjee, and P. Bahl, "DSAP: a protocol for coordinated spectrum access," in *IEEE DySPAN*, 2005.

[140] X. Ying, M. M. Buddhikot, and S. Roy, "SAS-assisted coexistence-aware dynamic channel assignment in CBRS band," *IEEE Transactions on Wireless Communications*, vol. 17, no. 9, pp. 6307–6320, Sep. 2018.

[141] X. Jing and D. Raychaudhuri, "Spectrum co-existence of IEEE 802.11b and 802.16a networks using reactive and proactive etiquette policies," *Mobile Networks and Applications*, 2006.

[142] X. Jin, L. E. Li, L. Vanbever, and J. Rexford, "SoftCell: Scalable and flexible cellular core network architecture," in *ACM CoNEXT*, 2013.

[143] A. Basta, W. Kellerer, M. Hoffmann, H. J. Morper, and K. Hoffmann, "Applying NFV and SDN to LTE mobile core gateways, the functions placement problem," in *All Things Cellular Workshop: Operations, Applications, Challenges*, 2014.

[144] M. Moradi, W. Wu, L. E. Li, and Z. M. Mao, "SoftMoW: Recursive and reconfigurable cellular WAN architecture," ser. ACM CoNEXT 2014.

[145] L. Suresh, J. Schulz-Zander, R. Merz, A. Feldmann, and T. Vazao, "Towards programmable enterprise WLANs with Odin," in *ACM HotSDN Workshop*, 2012.

[146] A. Patro and S. Banerjee, "COAP: A software-defined approach for home WLAN management through an open API," in *ACM MobiArch*, 2014.

[147] K.-K. Yap, R. Sherwood, M. Kobayashi, T.-Y. Huang, M. Chan, N. Handigol, N. McKeown, and G. Parulkar, "Blueprint for introducing innovation into wireless mobile networks," in *ACM SIGCOMM Workshop on Virtualized Infrastructure Systems and Architectures*, ser. VISA, 2010.

[148] A. Zubow, M. Döring, M. Chwalisz, and A. Wolisz, "A SDN approach to spectrum brokerage in infrastructure-based cognitive radio networks," in *IEEE DySPAN*, 2015.

[149] L. E. Li, Z. M. Mao, and J. Rexford, "Toward software-defined cellular networks," ser. EWSDN. IEEE Computer Society, 2012.

[150] A. Gudipati, D. Perry, L. E. Li, and S. Katti, "SoftRAN: Software defined radio access network," in *ACM HotSDN*, 2013.

[151] R. Beuran, J. Nakata, T. Okada, L. T. Nguyen, Y. Tan, and Y. Shinoda, "A multi-purpose wireless network emulator: QOMET," in *AINA workshops*, 2008.

[152] P. Zheng and L. M. Ni, "EMWIN:: Emulating a mobile wireless network using a wired network," in *ACM WOWMOM*, 2002.

[153] P. Mahadevan, A. Rodriguez, D. Becker, and A. Vahdat, "MobiNet: A scalable emulation infrastructure for ad hoc and wireless networks," *SIGMOBILE Mob. Comput. Commun. Rev.*, 2006.

[154] Y. Zhang and W. Li, "An integrated environment for testing mobile ad-hoc networks," in *ACM MobiHoc*, 2002.

[155] D. Raychaudhuri, I. Seskar, M. Ott, S. Ganu, K. Ramachandran, H. Kremo, R. Siracusa, H. Liu, and M. Singh, "Overview of the orbit radio grid testbed for evaluation of next-generation wireless network protocols," in *IEEE WCNC 2005*.

[156] G. Huang *et al.*, "Metis-ii," *Deliverable D7.3 Final 5G visualization*, 2017.

[157] "JFW industries, Inc. manufacturer of RF components and automated RF test systems," http://www.jfwindustries.com, Accessed: 2018-01-21.

[158] T. Rakotoarivelo, M. Ott, G. Jourjon, and I. Seskar, "OMF: a control and management framework for networking testbeds," *ACM SIGOPS Operating Systems Review*, 2010.

[159] "Information System on Graph Classes and their Inclusions," http://www.graphclasses.org/smallgraphs.html, Accessed: 2018-01-21.

[160] K. Winstein, A. Sivaraman, and H. Balakrishnan, "Stochastic forecasts achieve high throughput and low delay over cellular networks," in *USENIX NSDI*, 2013.

[161] "G-NetWorld," Accessed: 2018-01-21.

[162] "The world's largest Open Database of Cell Towers," Accessed: 2018-01-21.

[163] "CellID Finder," Accessed: 2018-01-21.

Chapter 5

Appendix A: Wireless Emulation Platform

In order for future Internet protocols to meet the requirements of advanced mobility services, they should be designed with mobility considerations for various signal propagation scenarios, i.e. various wireless technologies operating in different frequency bands, diverse mobility patterns in different environments ranging from vehicular mobility to pedestrian in urban and suburban scenarios. In this appendix we describe "EmuWNet", an Emulation framework for Wireless Networks, using real-world signal propagation measurements in a controlled testbed environment. This framework enabled us to evaluate the performance of novel Internet protocols in a controlled environment for various mobility scenarios and perform fair comparisons with existing protocols for the same emulated mobility scenarios. We have used EmuWNet in chapter 2 to evaluate mobility and multihoming protocols proposed.

EmuWNet has been designed with the following features for mobile wireless experimentation: (i) repeatability of the experiments, (ii) reconfigurability and programmability of the nodes, (iii) automation and remote management, and, (iv) realism in different layers of the protocol stack. There have been multiple projects aimed at emulating wireless scenarios through different strategies, mostly using wired networks. One class of emulator frameworks used a hybrid approach of running real protocols on top of simulated physical layer[151]. Emulators like [152] use virtualization of multiple machines with different wired connectivity configurations to emulate wireless environment. Similarly, in [153, 154] the authors proposed frameworks to emulate 802.11 ad-hoc networks. Unlike these frameworks, EmuWNet is designed on the ORBIT testbed [155] which is an open-access wireless testbed with fully programmable nodes and software defined radios (SDRs). It takes as input real-world or simulation-based signal strength

measurements[156] for a characteristic end-host, maps these measurements to operation range of wireless links based on the technology aimed to use (such as Wi-Fi, LTE) and programs the attenuation of wireless links in a dynamic manner to emulate mobility. Being fully programmable with SDRs, EmuWNet can be utilized to evaluate any existing or proposed protocols.

5.1 System Architecture

EmuWNet is an emulation framework built on top of the ORBIT testbed. In this section we present the hardware and software capabilities of it.

5.1.1 Hardware

EmuWNet runs on a sandbox [123] on ORBIT with RF controllable attenuators. It consists of 9 ORBIT nodes (general purpose computers) in RF shielded boxes. Each of the nodes is located inside RF enclosure providing 80 dB of RF isolation. All of the nodes have Intel Wi-Fi/WiMAX cards. In addition to these wireless interfaces, four of the nodes have Ettus USRP B205mini-i SDRs [125] to experiment with programmable RF physical layer, while three others have commercial USB LTE client adapters to permit LTE based experiments. Two NEC WiMAX basestations and two Airspan LTE basestations are deployed in the sandbox for WiMAX and LTE experiments. All of the nodes are also equipped with Atheros AR928X wireless network adapters (2.4/5 GHz)[39] to perform Wi-Fi based experiments. The RF connections of the enclosures housing the nodes as well as the antenna connections of the LTE and WiMAX base stations are all connected to the RF transceiver test system, as shown in Fig. 5.1, which is composed of an array of RF switches and two attenuator matrices. The tight control of attenuation between each pair of nodes is enabled by the JWF attenuator matrix [157] and a custom attenuator matrix. The JWF test system ("RF Matrix 1" in Fig. 5.1) allows for 0 to 63 dB of attenuation between each pair of nodes. The custom 5 port attenuator matrix (RF Matrix 2 in Fig. 5.1) is based around a series of digital step attenuators controlled via an Ethernet connected Raspberry Pi. Two

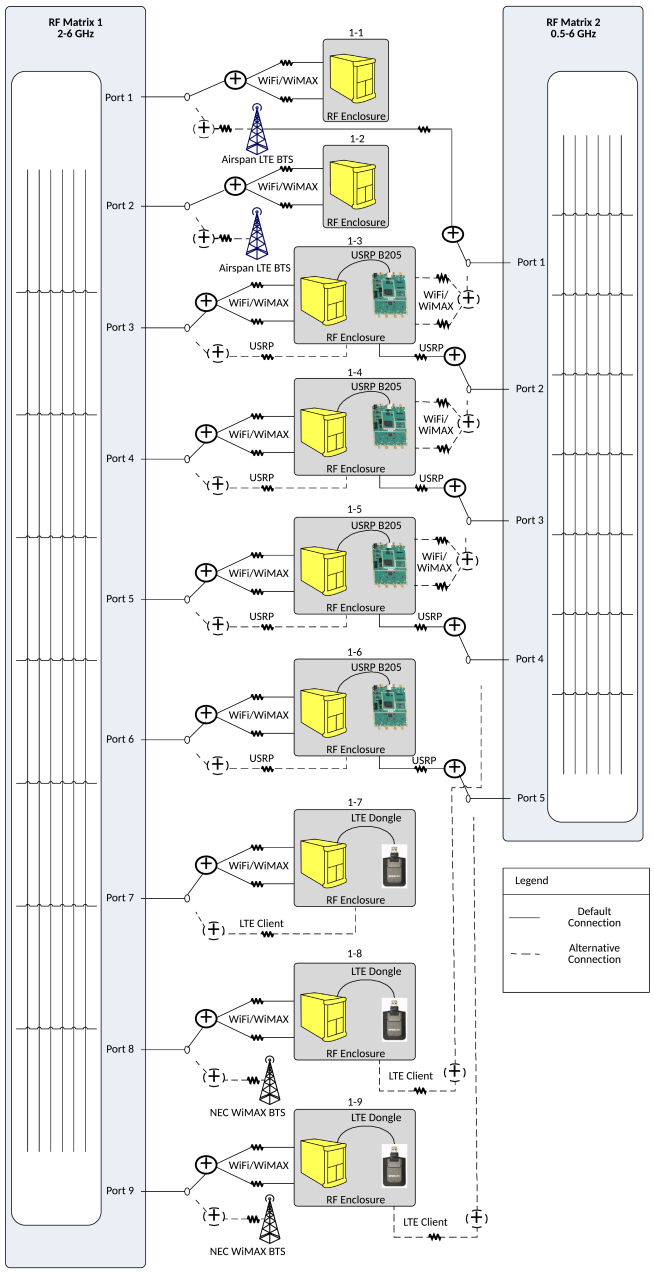

Figure 5.1: Overview of the sandbox with RF attenuation matrices in ORBIT

attenuators in series are installed per port pair giving 0 to 63.5 dB of attenuation range. Therefore, depending on the experimenter requirements, the sandbox can be setup with two independent topologies of 5 or 9 nodes consisting multiple LTE or WiMAX basestaions, Wi-Fi APs and one or more clients. This makes it suitable for controlled tests of handoffs, interfering devices, and multi-homing across different access technologies. There is an additional tenth node which is unshielded and has no radios.

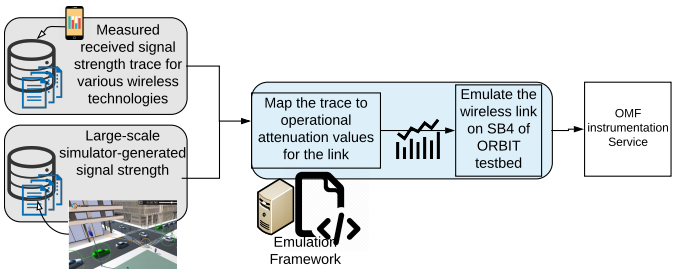

Figure 5.2: Overview of the emulation framework on ORBIT

It can be utilized for network services such as LTE mobility management (MME), a webserver, a network cache or a network router. Fig. 5.1 provides and overview of the overall sandbox hardware setup.

5.1.2 Software

The ORBIT management framework (OMF) instrumentation service [158] provides user control of the RF interconnect topology and individual link attenuations in the sandbox. Through a simple REST API, a user can change the system's parameters at will. At the simplest level, the service provides the ability for certain nodes to be replaced with WiMAX or LTE basestations and permits the user to set the attenuation values (0 to 63dB) between port pairs on the JFW attenuator matrix. Actual attenuations between devices are greater due to specifics of the system architecture. Interconnect topologies can be defined by setting unconnected link attenuations to their maximum possible value (63dB). A subset of the ISGCI Smallgraphs [159] topologies is preloaded into the system.

More complex control of the attenuator matrix is also possible through the OMF instrumentation service. For example, the attenuations of multiple port pairs can be synchronously set with a single call to the service. This allows for a user's experiment script to more accurately emulate mobility of clients between basestations. Additionally, the service permits attenuations to be scheduled with respect to UNIX epoch time to facilitate synchronization between the experiment and changes in link attenuation. Given the limitation of 1dB resolution in the attenuator matrix, this method combined with NTP time synchronization between devices is sufficient for most experiments. EmuWNet is built on top of these described capabilities of the OMF instrumentation

service to allow for "replay" of discrete time based traces. At a fundamental level, EmuWNet automatically steps through a given set of time indexed port pair attenuator values. This automatic replay can be scheduled to begin just like the individual attenuator setting commands described earlier to facilitate synchronous execution of the experiment. Alone, this capability is no different than what a user's experiment script can achieve. However, the framework is expanded to accept different user provided datasets to produce the required time indexed attenuator traces. For example, EmuWNet can generate a mapping table to translate a user provided RSSI trace (e.g. cellular RSSI data collected in the field or via realistic simulations) into a time indexed attenuation trace that the service can then replay. Taking this a step further, a mobility trace with a set of known basestation coordinates can be used to calculate RSSI values that the mapping module can then translate into a dataset usable by the service. This simplifies running the experiments, since trace data processing can be offloaded to the service and allows for repeatable experiments using not only real world data, but also purely simulation-generated data, as well as any combination thereof. Fig. 5.2 shows the system design of the framework.

5.2 Wireless Link Emulation

In order to design realistic emulation of real-world mobility in a testbed setup, we first looked into sample measurements and collected fine-grained wireless connectivity data using two smartphones. The details of these measurements are described in chapter 2. These measurements provide us with insights on different schemes to emulate real-world wireless links. In Sec. 5.2.1, we discuss how various measurement categories can be replayed based on possible mappings. Some examples of these possible mappings are depicted using our sample measurements.

5.2.1 Real-World Trace Emulation

• **RSSI-based Emulation:** According to the architecture of our system and framework explained previously, the most straight-forward way of replaying traces is having access

to signal strength (RSSI) measurements. It should be taken into account that due to different receiver sensitivity (which is governed by noise floor for different devices) and different technologies, the raw signal strength data cannot be directly injected into the emulation environment. In order to address this issue, the measurements were mapped to the operating range of our system based on the technology used.

• **Download Rate-based Emulation:** One of the most common ways to emulate real-world wireless systems is to replay download traces obtained from periodic retrieval of constant-sized objects through the wireless medium. Compared with RSSI-based emulation, download rate-based emulation takes into account additional information about the system, for example, the load on the system (number of concurrent UEs being served by a base station, the MAC scheduling at the base station in a cellular network), in-network latency (caused by huge buffers deployed at the LTE base stations, core network conditions and congestion at each routing hop, etc.), interaction of the application layer with wireless channel conditions, etc.

There are various ways to use the download rate traces in an emulation environment. In [160], packet arrival times are used to inject delays in the emulator to replicate cellular network conditions. Since our emulation environment is based on setting attenuation levels, we are interested to investigate the relationship between download rate and signal strength. To do so, we parametrize the correlation between download test rates and RSSI for our measurements, by calculating the Pearson's product-moment coefficient for them. The closer the correlation coefficient is to 1, greater is the linear dependence between the two variables. One example of highly correlated measurement (with a correlation coefficient of 0.72) for a commercial cellular network is depicted in Fig. 5.3.[1]

Not all the RSSI-bitrate measurements we conducted show this level of correlation. As a matter of fact, the average correlation coefficient for each of the cellular networks over all of the traces is 0.36. Considering all the aforementioned factors that have an impact on the value of download bitrate, only when those factors are at rest we can see the download bitrate to be a function of RSSI. For example, the measurements shown

[1]In the RSSI plot, for consistency purposes only the RSSI measurements denoting LTE technology have been shown. It can be seen that the download rate vastly decreases when the connectivity downgrades from LTE to a different technology (discontinuity in the RSSI plot at 3000 seconds)

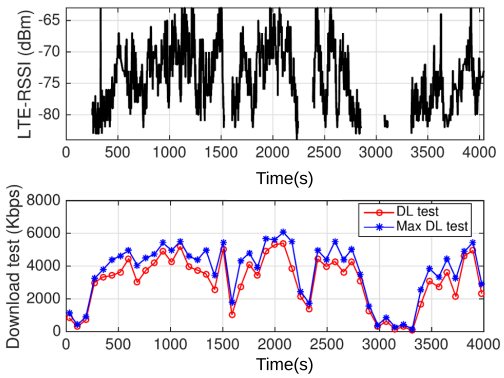

Figure 5.3: Example of a highly correlated RSSI and download test bitrate

in Fig. 5.3 have been recorded during off-peak time[2]. In order to investigate the role of other parameters involved in mapping between download bitrate and RSSI (which will be ultimately fed to our system to replay the trace), we plotted the correlation coefficient between RSSI and measured download test bitrates, as a function of time of day and average speed of the vehicle in Fig. 5.4. As can be seen, the correlation is highest for off-peak times and higher average vehicle speed (which is an indication of less traffic on the road and less load on the cellular network), and lowest for rush hour times with traffic on the road. Similar analysis can be done to extract statistical information regarding the mapping of download bitrates to RSSI measurements based on parameters at hand (ranging from the most basic ones like time of day, or traffic on the road, to fine-grained information from the base stations or the network).

• **Location/Distance-based Emulation:** Another type of trace that can be replayed in our system is the mobility (location) trace of a user. There exist databases [161] of signal quality for different cellular carriers. By specifying the route of the user the signal strength information can be extracted and then after mapping the data to the operating range of our system, the mobility trace can be replayed. In our set of measurements, we investigated the variance of RSSI values for different times, but constant locations on a route for a commercial cellular network. The route is nearly 14 miles, as shown in Fig. 2.4, and the subset of traces considered is 13. We averaged out all the measurements in a trace, in steps of 0.1 mile and then computed the mean and standard

[2]The average speed of the car driven while making the measurements shows no effect of traffic, which corresponds to a lightly-loaded system.

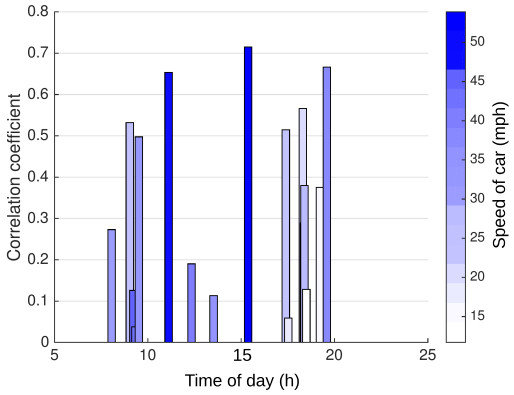

Figure 5.4: Correlation Coefficient between RSSI and download test bitrate. The color of each bar denotes the average speed of the vehicle (mph), which can be an indicator of traffic along the route, hence the load on the system

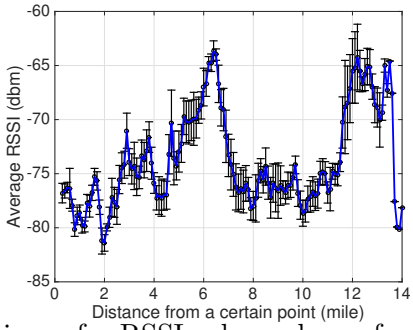

Figure 5.5: Mean and Variance for RSSI values, shown for specific locations on a route.

deviation across the 13 traces for each 0.1 mile interval. The result is shown in Fig. 5.5. The average of standard deviation is 1.41 and as can be seen, the RSSI variance is around 4-5 dBm for each 0.1 mile step. This confirms some level of correlation between RSSI values for specific locations and the possibility of replaying mobility traces in our system.

If databases for mapping specific locations to corresponding signal strength is not available, there exist also the opportunity to conduct distance-based emulations. By knowing the route of the user and obtaining base station distribution from available databases [162, 163], one can apply mappings to translate the distance values to signal attenuation values (following mainstream path-loss and fading models). These attenuation values can be injected to our system, to replay the mobility trace of a user.

Chapter 6

Appendix B: Mathematical Proofs for Chapter. 3

Proof of Proposition 1. Prob.1 is concave and its Lagrangian is as follows:

$$\begin{aligned} L(\{y_n\},\{x_{m,k}\},\lambda) = &-\sum_{n=1}^{N} log(d_n y_n) - \sum_{m=1}^{M}\sum_{k=1}^{K_m(t)} |G_{m,k}(t)| log(x_{m,k} c_{m,k}) \\ &+ \lambda(\sum_{n=1}^{N} y_n + \sum_{m=1}^{M}\sum_{k=1}^{K_m} x_{m,k} - N_B) \end{aligned} \tag{6.1}$$

Taking $\frac{\partial L}{\partial y_n}$ and setting it to 0, $\forall n$ yields to

$$y_n = \frac{1}{\lambda} \tag{6.2}$$

Taking $\frac{\partial L}{\partial x_{m,k}}$ and setting it to 0, $\forall m,k$ yields to

$$x_{m,k} = \frac{|G_{m,k}|}{\lambda} \tag{6.3}$$

As a result $\lambda > 0$, so from complementary slackness we will have:

$$\sum_{n=1}^{N} y_n + \sum_{m=1}^{M}\sum_{k=1}^{K_m} x_{m,k} - N_B = 0 \tag{6.4}$$

This combined with Eq.6.2 and 6.3 will yield the optimal values for y_n^* and $x_{m,k}^*$. □

Proof of Theorem 1. In order to show we should always place the UEs with the same MCS values in the same group, we should prove that the PF utility of 1 group is higher than any arbitrary grouping of UEs with the same MCS. Considering N total UEs, and K arbitrary groups each with N_k members (so that $\sum_{k=1}^{K} N_k = N$), we will prove:

$$Nlog(NxM) \geq \sum_{k=1}^{K} N_k log(N_k xM) \tag{6.5}$$

in which M is MCS which is the same for all the UEs and x is a normalization factor related to the number of RBs assigned. Basically if total of Nx RBs are assigned to all the UEs considered, if the UEs are grouped each will get $N_k x$ portion of the RBs. The proof of 6.5 is conducted using induction as follows:

$$\text{Inductive hypothesis:} \qquad Nlog(NxM) \geq \sum_{k=1}^{K} N_k log(N_k xM) \tag{6.6}$$

$$\text{Inductive step:} \qquad (N+1)log((N+1)xM) \geq \sum_{k=1}^{K'} N'_k log(N'_k xM) \tag{6.7}$$

To prove 6.7, we should consider two cases: 1) $K' = K$, which means that the new UE is added to one of the existing groups, 2) $K' = K + 1$, which means that the new UE will form a new group with 1 member.

1. $K' = K$: Without loss of generality we can assume that the new UE is added to the K_{th} group. So we can rewrite 6.7 as:

$$(N+1)log((N+1)xM) \geq \sum_{k=1}^{K-1} N_k log(N_k xM) + (N_K+1)log((N_K+1)xM) \tag{6.8}$$

Eq. 6.8 can be proved by contradiction, considering that the following will contradict the inductive hypothesis:

$$(N+1)log((N+1)xM) < \sum_{k=1}^{K-1} N_k log(N_k xM) + (N_K+1)log((N_K+1)xM) \tag{6.9}$$

Rewriting 6.9 will result in:

$$(N+1)log((N+1)xM) - log(\frac{(N_K+1)^{N_K+1}}{N_K^{N_K}} xM) < \sum_{k=1}^{K} N_k log(N_k xM) \tag{6.10}$$

Eq.6.11 is proved in lemma.6.1, which states that the LHS of 6.10 is larger than

LHS of the inductive hypothesis(Eq. 6.6), by transitive property Eq. 6.6 is contradicted, hence proving Eq. 6.7 holds.

$$log(\frac{(N+1)^{N+1}}{N^N}xM) > log(\frac{(N_K+1)^{N_K+1}}{N_K^{N_K}}xM) \tag{6.11}$$

2. $K' = K + 1$: In this case the new UE will form a 1-member group. Hence Eq. 6.7 can be rewritten as:

$$(N+1)log((N+1)xM) \geq \sum_{k=1}^{K} N_k log(N_k xM) + log(xM) \tag{6.12}$$

Subtracting 2 sides of Eq. 6.6 from 2 sides of Eq.6.12 will result in the following inequality which is always true (since $\frac{(N+1)^{N+!}}{N^N} > 1$).

$$log(\frac{(N+1)^{N+!}}{N^N}) > 0 \tag{6.13}$$

□

Lemma 6.1.

$$log(\frac{(N+1)^{N+1}}{N^N}xM) > log(\frac{(N_K+1)^{N_K+1}}{N_K^{N_K}}xM) \tag{6.14}$$

proof: Since the function $f(x) = \frac{(x+1)^{x+1}}{x^x}$ *is a monolithically increasing function (since* $\frac{\partial f}{\partial x} = \frac{(x+1)^{x+1} ln(\frac{x+1}{x})}{x^x}$ *is always positive), for* $N > N_K$*, we have* $f(N) > f(N_K)$*. Multiplying the 2 sides by* xM *and taking the log will prove Eq. 6.14*